Investigations of the Potential of Synthetic Phospholipids as Membrane Mimics: Interactions with Amphiphilic and Polyphilic Block Copolymers

Dissertation

zur Erlangung des Doktorgrades der Naturwissenschaften

(Dr. rer. nat.)

der

Naturwissenschaftlichen Fakultät II
Chemie, Physik und Mathematik

der Martin-Luther-Universität Halle-Wittenberg

vorgelegt von

Herrn M.Sc. Syed Waqar Hussain Shah
geb. am 28.02.1972 in Rawalpindi (Pakistan)

Gutachter:

1.   Prof. Dr. Alfred Blume
2.   Prof. Dr. Jörg Kressler
3.   Prof. Dr. Thomas Wolff

Tag der Verteidigung: 04. May 2016

Which is it, of the favors of your Lord that ye deny?

(Al-Quran 55:13)

To my parents and family

Acknowledgement

More than a shoulder to cry, hand to hold.

What thou hast bestowed is simply beyond,

that words could tell n' silence would fold.

Doing doctorate is similar to sailing in an ocean, where one is exposed to many benign as well as unfavorable circumstances. Failures occur beyond one's expectations and significant distances are covered without facing much resistance. It is not easy to delineate the ways in which one's life is beautified by someone's presence, because of uncountable tiny contributions, such as a few words, a smile, a gesture, a touch, a sparkle in an eye and even silence.

Leonardo da Vinci said[1], *"...people of accomplishment rarely sat back and let things happen to them. They went out and happened to things"*. For me, it all began with the award of scholarship for attending the *Martin-Luther University, Halle-Wittenberg* for doctoral study under the `Faculty Development Program`of the Higher Education Commission, Pakistan. This was aimed at strengthening the *Hazara University, Mansehra* (*Pakistan)* through upgradation of its faculties. Such initiative by HEC and Hazara University is highly appreciable.

I would not have been triumphant without persistent aiding by family, and help and support of others and it is pertinent to acknowledge them all.

Words are not enough to express my gratitude for Prof. Alfred Blume for accepting me into his group and enabling me to finish this task under his erudite guidance. His remarkable contributions to the *lipid science* have always been an inspiration for an early-stage researcher like me. He has been a guiding light that kept me on my course throughout my travel in the mist of uncertainties. The problems which appeared much bigger initially, shrunk in his presence that carried a hue of his friendly gestures and

---

[1] www.michaelhartzell.com/quotes-to-Inspire/bid/66576/Leonardo-Da-Vinci-Quotes

assuring discussions. His trust in my abilities and continuous encouragement motivated me to take daring strides and explore multiple dimensions. The time spent in his group will always be among the golden chapters of my life.

The provision of the block copolymers synthesized in the group of Prof. Jorg Kressler or acquired through his cooperation with Prof. Holger Frey is gratefully acknowledged. Their former group members Zheng Li, Samuel Oppong Kyeremanteng and Sophie Müller who assembled these macromolecules also deserve word of thanks.

I am indebted to Prof. Jorg Kressler and Prof. Dariush Hinderberger for allocation of lab space for attempting the synthesis of halogenated phospholipids and for scientific and social discussions.

Thanks are due to Dr. Annette Meister for Cryo-EM investigations and Prof. Kirsten Bacia for enticing discussions during *FOR1145* meetings regarding future research prospects.

I am also thankful to Andreas Lonitz and Heike Schimm for technical support. I owe a lot to Tilo Wieczorek. I could not have solved many of my problems without his assistance.

I wish to record special appreciation for group members including Sebastian Finger, Dr. Christian Schwieger, Andre Hadicke, Dr. Bob Dan Lechner, Dr. Andreas Kerth and Dr. Peggy Scholtesyk for making it easier to learn different techniques and methods through sharing their experiences and giving valuable suggestions. I can never repay Sebastian Finger for succor provided in low moments, especially when my beloved mother passed away.

Dr. Nadica Maltar Strmečki of the Ruđer Bošković Institute, Zagreb (Croatia) and Dr. Simon Drescher of the Institute of Pharmacy, MLU deserve admiration for camaraderie, understanding and advices.

Finally, I am grateful to Dr. Nasir Mahmood, Dr. Anas Mujhtaba, Muhammad Humayun Bilal, Muhammad Harris Samiullah, Thi Minh Hai Nguyen, Mark Jbeily, Daniel Heinz, Dr.

x

Content

Abbreviations and Symbols

(Introduction)

PEO	Poly(ethylene oxide)
PPO	Poly(propylene oxide)
PGMA	poly(glycerol-monomethacrylate)
GUV	Giant unilamellar vesicles
SLB	Supported lipid membranes
AFM	Atomic force microscopy
MD	Molecular dynamics
2D	Two dimensional
3D	Three dimensional
L_c	Sub gel phase
$L_{\beta}{'}$	Lamellar gel phase
$P_{\beta}{'}$	Rippled gel phase
L_{α}	Liquid crystalline phase
$L_{\beta}I$	Interdigitated gel phase
KSCN	Potassium thiocyanate
sn	Stereospecific number
F-DMPC	1-myristoyl-2-(14-fluoromyristoyl)-sn-glycero-3-phosphocholine
DPPC	1,2-dipalmitoyl-sn-glycero-3-phosphocholine
DPPG	1,2-dipalmitoyl-sn-glycero-3-phosphoglycerol (sodium salt)
F-DPPC	1-palmitoyl-2-(16-fluoro palmitoyl)-sn-glycero-3-phosphocholine
DHPC	1,2-di-O-hexadecyl-sn-glycero-3-phosphocholine
EDPPC	1,2-dipalmitoyl-sn-glycero-3-ethylphosphocholine (chloride salt)
HSA	Human serum albumin
DNA	Deoxyribonucleic acid
GP	$PGMA_{20}\text{-}PPO_{34}\text{-}PGMA_{20}$
FGP	$F_9\text{-}PGMA_{20}\text{-}PPO_{34}\text{-}PGMA_{20}\text{-}F_9$
GF40	$PGMA_{40}\text{-}F_9$
GF14	$PGMA_{14}\text{-}F_9$
EF44	$PEO_{44}\text{-}F_9$
PFG78	$PPO_{42}\text{-}PGMA_{78}\text{-}F_{10}\text{-}PGMA_{78}\text{-}PPO_{42}$
CPGR	$CHO\text{-}PEG_{30}\text{-}hb\text{-}PG_{17}\text{-}RHO$
RH-DHPE	1,2-dipalmitoyl-sn-glycero-3-phosphoethanolamine- N-(lissamine rhodamine B sulfonyl) (triethyammonium salt)
DHPE/DPPE	1,2-dipalmitoyl-sn-glycero-3-phosphoethanolamine
DMPE	1,2-dimyristoyl-sn-glycero-3-phosphoethanolamine
NBD-12HPC	2-(12-(7-nitrobenz-2-oxa-1,3-diazol-4-yl)amino)dodecanoyl-1-hexadecanoyl-sn-glycero-3-phosphocholine
NBD-DPPE/NBD-PE	1,2-dipalmitoyl-sn-glycero-3-phosphoethanolamine-N-(7-nitro-2,1,3-benzosadiazol-4-yl) (triethyammonium salt)

(Theory, Techniques and Methods)

π	Lateral or surface pressure
T	Temperature

σ_o	Surface tension in the absence of lipid
σ_1	Surface tension in the presence of lipid
χ	Compressibility
A	Area
k	Boltzmann's constant
π_c	Critical pressure
A_c	Critical area (or area corresponding to critical pressure)
LE	Liquid expanded
LC	Liquid condensed
X_1	Bulk concentration of monomeric surfactant
γ	Surface tension
cmc	Critical micelle concentration
Γ	Surface coverage
π_{ini}	Initial spreading pressures
π_{max}	Maximum surface pressure approached after polymer injection
π_e	Exclusion pressure/Maximal insertion pressure
λ_1	Absorption wavelength
λ_2	Emission wavelength
CCD	Charge-coupled device
DSC	Differential scanning calorimetry
H	Enthalpy of a system
H_o	Arbitrary constant for enthalpy at $T = 0$
ΔH_{trans}	Enthalpy of phase transition
C_p	Heat capacity at constant pressure
$C_{p(diff)}$	Measured heat capacity
$C_{p(baseline)}$	Interpolated heat capacity without transition
ΔS_{trans}	Transition entropy
T_m	Main phase transition temperature

(Additional Terms used in Chapters 4 – 8)

FM	Fluorescence microscopy
BAM	Brewster angle microscopy
TEM	Transmission electron microscopy
DODA	Dioctadecylamine
Cho/CHO	Cholesterol
PEG	Poly(ethylene glycol)
PG	Polyglycerol
T_p	Pre-transition temperature
T_a	transition temperature for additional transition in EDPPC
F-DPPG	1-palmitoyl-2-(16-fluoro palmitoyl)-phosphatidylglycerol
RNA	Ribonucleic acid
EDOPC	1,2-dioleoyl-sn-glycero-3-ethylphosphocholine
TLC	Thin layer chromatography
TOC	Total organic carbon
DMPG	1,2-dimyristoyl-sn-glycero-3-phosphoglycerol (sodium salt)

_____

1 INTRODUCTION

1.1 Biomembranes, Membrane Mimics and Polymer-membrane Interactions

Biological membranes are built up by a bilayer of lipids and solid proteins. The proteins are either embedded or peripheral or bound.[1] The understanding of properties of membranes and the role of their components have evolved over time since the presentation of the *fluid mosaic model.*[2-6] A simplified fluid-mosaic model is shown in Fig. 1.1.
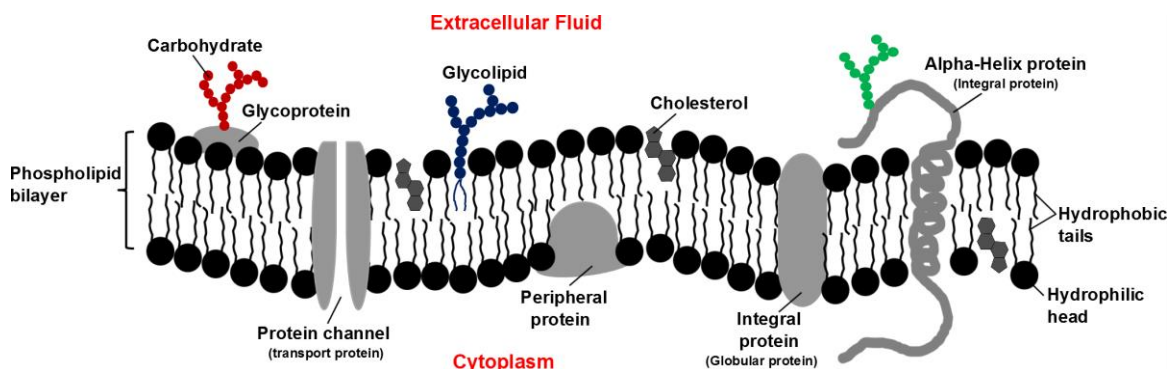
Figure 1.1: Simplified fluid-mosaic model of biomembranes.

The biological membranes are composed of a variety of different molecules, with chemical functionalities on the surface of the membrane. The fate of a molecule located in the extracellular fluid will therefore depend on its chemical structure and the functional groups on the membrane surface. The *Meyer-Overton rule,* which remains valid for over a century (despite some exceptions), defines the permeability of a molecule in terms of its lipid solubility, which is chiefly governed by the additive's hydrophobicity.[7] On the other hand, it is now well established that the transport of most of the excipients through cell membranes is aided by proteins. The membrane lipids organize into microdomains (called lipid rafts), which differ in binding ability and control over permeation from the bulk phospholipids.[8] Direct observations of domain formation can provide a better insight into membrane heterogeneities.[9,10] Frequently, simplified systems have been evaluated for their suitability as membrane models.[11-14] They range from a highly simplified single component system based on one particular lipid to the one possessing a complex mixture of several lipids and proteins[15]. Alterations in lipid

_____

structure supplement knowledge on the behavior of biomembranes and shed light on the relevance of synthetic or artificial lipids.[16,17] The qualifications of synthetic lipids to mimic cells membranes have recently been tested and promising results achieved.[18–20] For instance, a self-reproducing oligotriazole catalyst continuously produces triazole phospholipids and leads to a lipid membrane capable of indefinite self-generation depending upon the availability of its chemical precursors.[20] 1,3-phospholipids containing amide linkers instead of ester form the lenticular vesicles, which only release their cargo after mechanical stimulation.[21] The investigations of synthetic or modified lipids can also provide information on processes such as interdigitation (see section 1.3.3 for details of interdigitated lamellar phases), interactions of drugs with membranes etc., and promote their effective delivery at the site of action.[16,21,22] The lipid behavior alone can serve as a marker for certain abnormalities such as cancer.[23]

Macromolecules depending upon their architecture assemble into diverse morphologies.[24–29] The amphiphilic diblock copolymers based on polystyrene and poly(acrylic acid) blocks attain several types of self-assembly regimes in aqueous solutions. They include spherical micelles, rods, lamellae, vesicles and hexagonally packed hollow hoops.[24] The macromolecules comprising PGMA as one of the terminal blocks in ABC polymers, assemble into double or triple helices.[25] The triblock copolymers of ABC type with an intermediate perfluorinated block produce micelles with defined fluorous region.[30] They are effective delivery systems for hydrophobic and fluorophilic therapeutic agents. It is also possible to produce the planar biomimetic membranes comprising of amphiphilic block copolymers.[26] In addition, the block copolymers can be tailored to demonstrate biological activity themself or specifically deliver biocides because they can imitate liposomes.[31,32]

There are several scenarios for the interactions between polymers and biomembranes. Block copolymer can induce ephemeral poration of biomembranes.[33] On contrary, others can seal impaired membranes and prevent apoptosis.[34] Hybrid materials for specialized functions can be genetrated using living cells and polymers, which display completely different properties from their precursors.[35] The replacement of PEO units in triblock PEO_n-PPO_m-PEO_n by PGMA causes greater disruption in model membranes.[36] In

fact, it is possible to overcome the limitations associated with the use of Poloxamers through introduction of a different block.[28,37]

Halogenation increases permeability of drugs through fluid biomembranes and comparable impacts are achieved through chlorination and trifluoromethylation.[38] Similar effects have been observed in macromolecules, where perfluoroalkylation led to peculiar properties.[39,40] The presence of an additional perfluorinated segment imparts stability to fluorous emulsions.[41] The amphiphiles and polymers containing perfluorinated units are polyphilic and exhibit distinct aggregation tendencies.[30,40,42,43] To fully harness their potential in pharmacy and other related areas, it is vital to completely understand their self-assembly regimes and modes of interactions with biological membranes.[44,45] The fluorophilic chains prefer lipid phases over aqueous environment and influence the retention of polymers in phospholipid monolayers and bilayers.[39,46] Despite of what is known already, the area remains widely unexplored. The interactions between macromolecules and phospholipids vary with change in the structure of membrane lipids and provide greater understanding of polymer's behavior in biological compartments.[46–49]

1.2   Membrane Models

The membranes that enclose cells or organelles are composite in nature[50] and to study their interactions with substances such as drugs, excipients and other substances of biological significance, much simpler systems are employed. They mainly include lipid monolayers, liposomes, and supported lipid membranes.[11,51,52]

1.2.1 Lipid Monolayers

The organization of insoluble amphiphilic molecules at the air/water interface produces a monomolecular layer, where the hydrophilic groups are immersed in water and the hydrophobic hydrocarbon chains are directed in air.[53–55] This monomolecular layer resembles half of the lipid bilayer, that is, only one of the leaflets of biomembranes. This basic model lacks complexity associated with the real membranes.[2] Nevertheless, it can provide plenty of information about the origin of interactions occurring between biomembranes and ligands.[56] The composition of monolayers can be varied and

conditions such as temperature, pressure, subphase type, stress etc. can be changed to achieve closeness to naturally occurring phenomena or a system under consideration.[57] In addition to air/water interface, the alignment of phospholipids at n-heptane/water interface has also served as biomimetic model membrane.[58,59] An arrangement of phospholipid monolayer at an air/water interface is shown in Fig. 1.2.
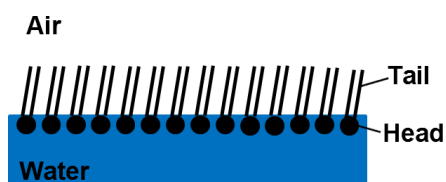
Figure 1.2: A condensed phospholipid monolayer at air/water interface.

1.2.2 Lipid Vesicles/Liposomes

Lipid molecules aggregate in aqueous solution to form spherical vesicles, which are composed of lipid bilayers. These vesicles, commonly known as liposomes vary in size, generally between 0.025 µm to 2.5 µm.[60] The smaller unilamellar vesicles consist of a single bilayer, whereas the multilamellar vesicles contain more than one lipid bilayer, and represent an onion like structure. They can be produced through extrusion or sonication of the dilute lamellar dispersions.[11]
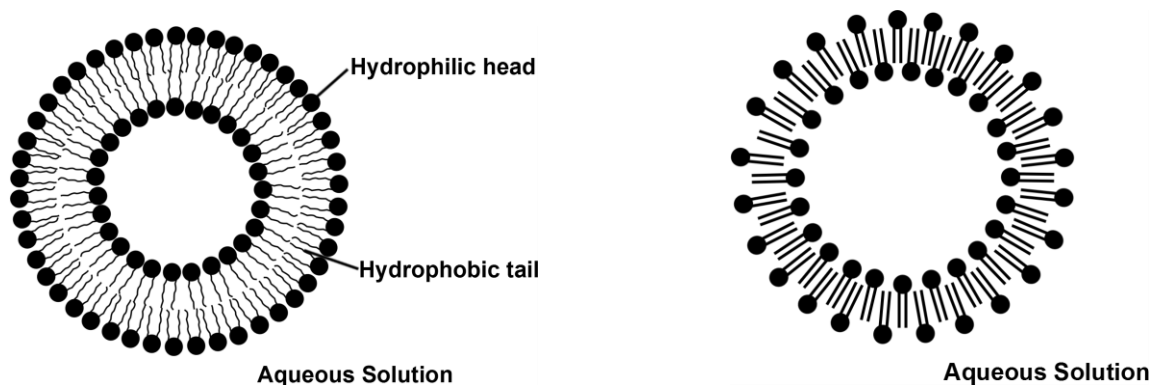
Figure 1.3: a) A phospholipid vesicle (left); and b) an interdigitated liposome (right).

Giant unilamellar vesicles up to the size of 100 µm can be generated through electroformation.[61] The effectiveness of GUVs as cell models has recently been reviewed.[62] The properties of vesicles are dependent on method of preparation.[60] Despite of all the advantages offered by utilization of GUVs for mimicking cell membranes, it is virtually impossible to reconstitute the actual membrane with precision. Fig. 1.3 shows the vesicles comprising of the lipid bilayers. Under special

conditions, the lipid monolayers in the two leaflets of a bilayer can interpenetrate, giving rise to liposomes comprising of an interdigitated layer.

1.2.3 Supported Lipid Membranes[63]

Lipid as a monolayer or a bilayer can be assembled on solid surface such as mica or silica. The transfer of lipid monolayers onto the solid supports from air/water interface is known as Langmuir-Blodgett transfer (Fig. 1.4a).
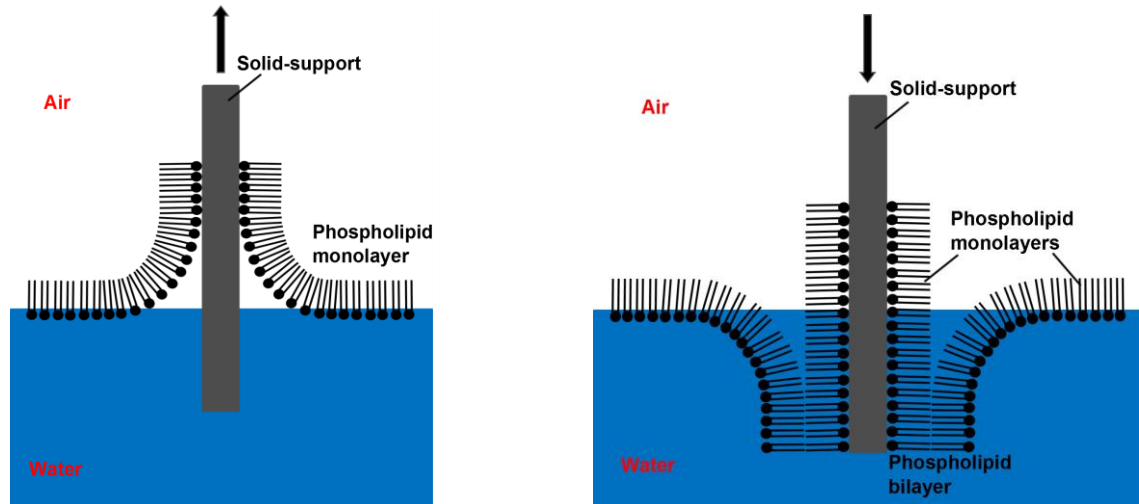
Figure 1.4: a) Langmuir-Blodgett Deposition (left); b) Langmuir-Schaefer Transfer (right).

Adhesion of lipids to the surface gives an arrangement where the hydrophilic heads are attached to the surface, whereas hydrocarbon tails are directed into air. The subsequent transfer of the second monolayer, the Langmuir-Schaefer deposition, produces a bilayer onto the surface (Fig. 1.4b).
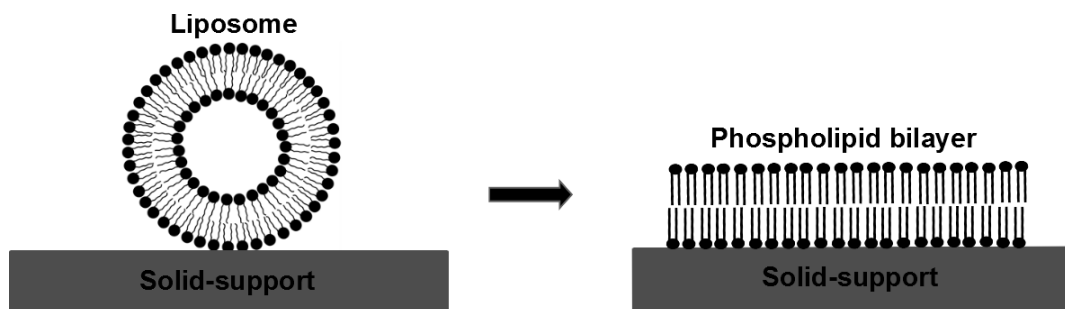
Figure 1.5: Rupture of liposome on solid-support to produce phopspholipid bilayer.

Another way of fabricating SLBs is through adsorption of liposomes onto the surface, which causes deformation, flattening and rupture of liposomes to produce membrane patches (Fig. 1.5).

_____

The Solid supported membranes not only provide greater control over composition and assembly, but also allow investigations at nanometric level using techniques like Atomic Force Microscopy (AFM).[64]

1.3 Phase Transitions in Lipid Monolayers and Bilayers

1.3.1 Phase Transitions in Lipid Monolayers

The mechanical compression of amphipathic lipid molecules, or amphiphilic macromolecules produces phase transitions in monolayers at the air/water interface.[65,66] These phases exhibit distinct translational and orientational order, which becomes apparent in the π-A isotherms. This phenomenon is summarized in **Fig. 1.6.**
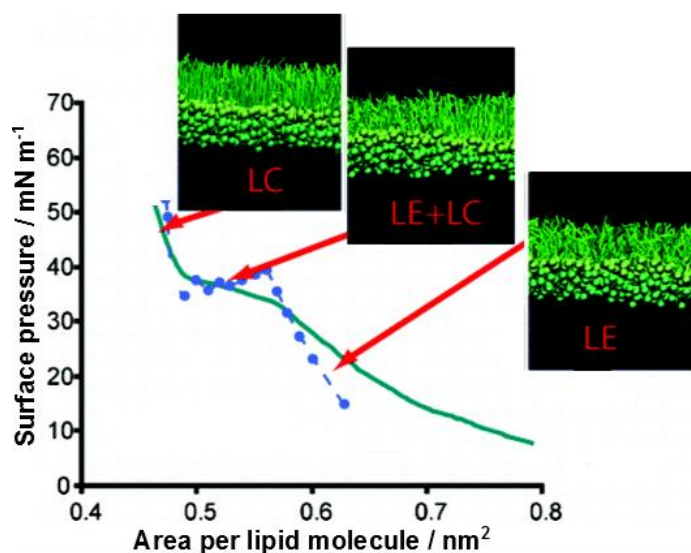
Figure 1.6: Molecular dynamic images of different phases in DPPC monolayers (green line is experimental π-A isotherm recorded at 37°C , whereas blue line represents the MD plot obtained at 27°C). Adapted from[66]

The lateral pressure, π, varies with change in area per molecule. At larger surface areas, π is practically zero, and the molecules are widely apart in 2D-gas phase. The gas phase does not persist above 1 mN m^{-1}. The compression brings molecules closer and the gas analogous phase transforms to the liquid expanded (LE) phase. The alkyl chains are conformationally disordered at this stage. Generally, but not always, the transition from LE to LC phase is represented by a kink and subsequent flattening of the isotherm. This transition is of first order and the expanded and condensed phases co-exist throughout the plateau. At the end of plateau, the surface pressure increases rapidly with small

_____

changes in area. In the condensed phase, the compressibility is markedly reduced[67] and the chains attain *all trans* conformations, and are tilted with respect to the surface normal in the case of saturated phosphatidylcholines.[68,69] The tilt angle decreases with increase in lipid density. The compression of the monolayer beyond the stability limit causes a collapse[70], which is a type of 2D- to 3D transition.[71] The 2D crystals have finite correlation lengths.[72] Upon so-called solidification, the arrangement of chains shift from oblique to hexagonal lattice. It is possible to correlate transitions in monolayers to thermotropic states in corresponding bilayers.[73]

1.3.2 Phase Transitions in Lipid Bilayers

In aqueous solution/dispersions the lipid molecules display a variety of lyotropic phases, namely micellar, lamellar and hexagonal phases.[74,75] Lamellar phases consist in most cases of bilayers and show thermotropic polymorphism depending upon structure of lipid.[76] The manifestation of phases is also dependent on degree of hydration, pressure and environment.[77,78] Excessive data is available on the thermotropic phase behavior of lipids.[79] Lipids forming non bilayer phases impart distinct features to membranes and enable to them to adapt to variation in membrane's environment.[75]
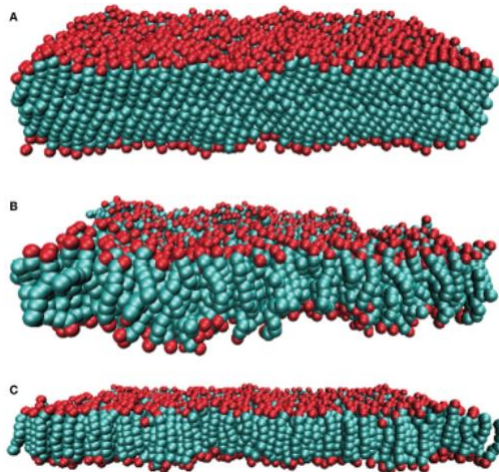
Figure 1.7: Coarse grained modeling of phospholipids: A) gel phase; B) fluid phase; and C) interdigitated gel phase (Heads are shown in a larger red bead and tails comprising of six beads in blue color).[80]

Phosphatidylcholines possessing saturated chains exhibit four different phases.[81,82] At low temperature, a quasi-crystalline subgel phase (L_c) is formed which converts to tilted lamellar gel phase (L_β'). Further heating leads to an intermediate rippled gel phase (P_β')

which transforms at higher temperature to a lamellar liquid crystalline phase (L_α). The transition from L_c to L_β' is called subtransition, while the transitions from L_β' to P_β' and P_β' to L_α are referred to as pre- and main transitions, respectively. The chains are packed in regular hexagonal lattice in the L_β' phase, which is distorted in the case of P_β'. The chains attain all trans conformations at low temperatures and significant proportion transform to gauche in the disordered fluid phase. Under special circumstances, the gel phase in phospatidylcholines is interdigitated.[83–87](see Fig. 1.7 for coarse grain models of gel, fluid and interdigitated phases in phospholipid bilayers and Fig. 1.8 for detailed description of different lipid phases).

1.3.3 Interdigitated Lamellar Phases

The interdigitated membranes are rigid *i.e.,* they occur only as gel phases with ordered chains.[88] Their surface hydrophobicity and electrostatic properties are different from bilayers.[89] The interdigitation should occur in a way to avoid the exposure of hydrocarbon chains to water (Fig. 1.7C). In fact, existence of an interdigitated gel phase ($L_\beta I$) represents a delicate balance of hydrophobic, electrostatic and interfacial forces.[89,90] Smith and Dea[91] have compiled DSC investigations on interdigitation in phospholipids. In PCs with ester linkage of the chains, $L_\beta I$ can be induced by a chemical additive, mainly an alcohol.[92] Other chemical inducers include anesthetics, drugs, organic solvents and salts (e.g. KSCN).[91] Application of pressure also fosters interdigitation in membranes.[93] Certain lipids undergo spontaneous interdigitation in the gel phase without the addition of an effectuator. In fact, the reasons for this distinct behavior exist in the structures of lipids. In phosphatidylcholines, these structural variations are: a) switching of the link between glycerol and alkyl chain from ester to ether[94]; b) substitution of one of the hydrogen atoms at *sn*-2 alkyl chain terminal by a fluorine atom[95]; c) interchanging the positions of *sn*-2 acyl chain and 3-phosphocholine moiety[87]; and d) esterification of phosphate group to produce a cationic lipid.[96] In addition, 1,3-diaminophospholipids also under go interdigitation at low temperatures.[86] It is noteworthy that the presence of 16 carbons atoms in a chain leads to interdigitation after all the above-mentioned modifications. The shortening or lenghtening of alkyl chains may or may not result in similar thermotrophic phase behavior. The monofluorinated derivative of 1,2-dimyristoyl-3-phosphatidylcholine (that is, F-DMPC),

_____

for instance, exists in normal bilayer gel phase.[97] Phospatidylcholine possessing alkyl chains of two different lengths show partial interdigitation in the gel phase.[16]
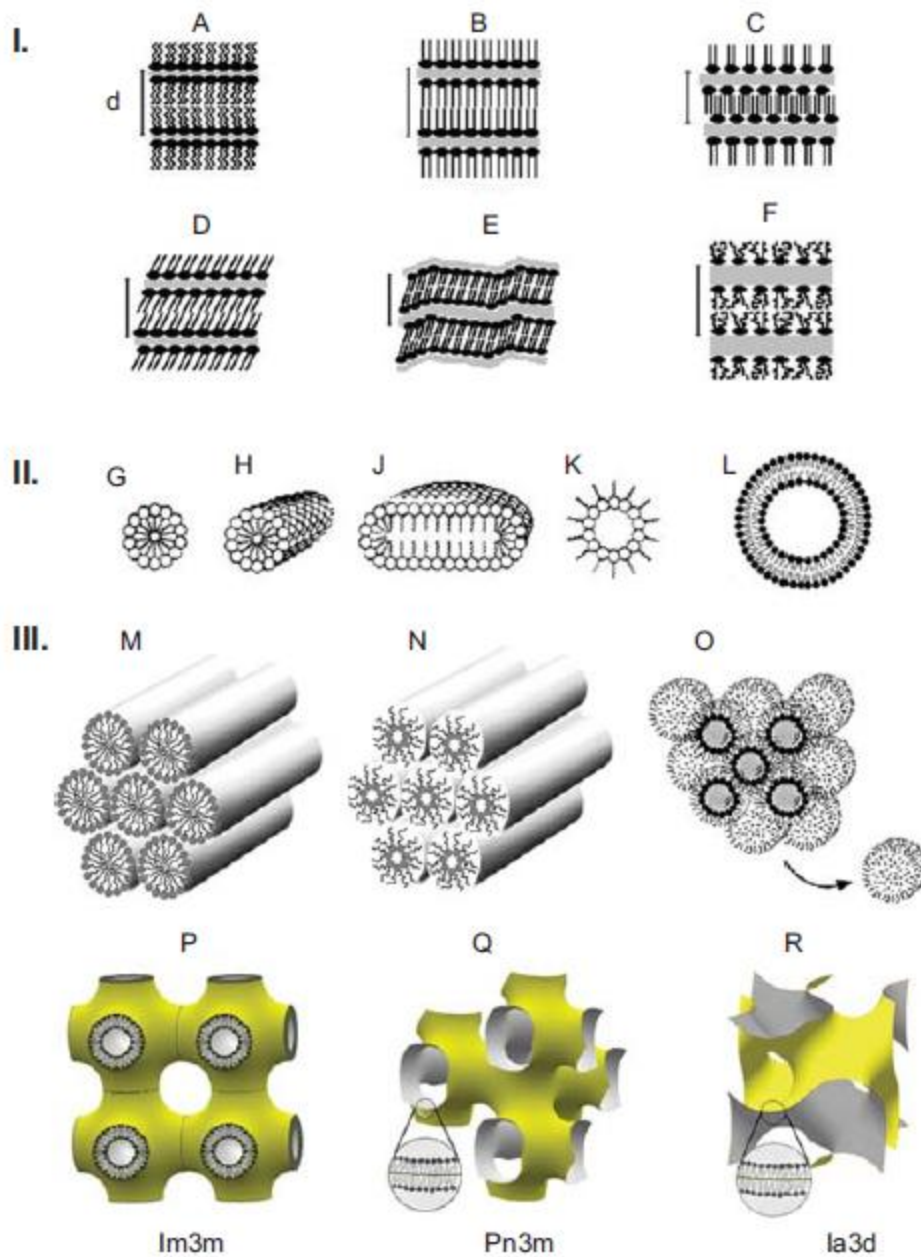
Figure 1.8: Different lipid phases.[98] I. Lamellar phases: (a) sub-gel; (B) gel (C) interdigitated gel; (D) gel, titled chains; (E) rippled gel ; (F) liquid crystalline; II. Micellar aggregates: (G) spherical micelles; (H) cylindrical micelles (tubules); (J) disks; (K) inverted micelles; (L) liposome; III. Non lamellar liquid crystalline phases of various topology: (M) hexagonal phases; (N) inverted hexagonal phase; (O) inverted micellar cubic phase; (P) bilayer cubic phase Lm3m; (Q) bilayer cubic phase Pn3m; (R) bilayer cubic phase La3d.

1.4   Motivation/Aim of Work

The membranes that enclose cells and cellular compartments act as a selectively permeable barrier and thus control the diffusion and intracellular transport of chemical entities. They are composed of a complex mixture of lipids and proteins. Plasma membranes contain more than 50% lipid. The distribution of lipids in the outer and inner leaflets of a membrane is different and responsible for regulating a variety of functions. Lipids have been amongst the most explored molecules for over a century.[99] Van Meer *et al*[100] have reviewed the essential aspects of membrane lipids, regarding their biological significance. Phosphatidylcholines are one of the four major types of lipids present in the mammalian plasma membrane. DPPC (1,2-dipalmitoyl-*sn*-glycero-3-phosphocholine) is found predominantly in the outer-leaflets of erythrocyte membranes and bilayer vesicles of DPPC are without a doubt one of the most rigorously explored membrane models[13]. Modifications in lipids have been utilized for different purposes.[86,97,101–110]

Amphiphilic and polyphilic block copolymers have significance for pharmacy and medicine.[33,111–115] The functionalization of living cells with polymeric nanofilms generate so-called *cyborg cells* for novel applications in bioelectronics and bioengineering.[35] The architecture of block copolymers modulate their interactions with simplified membrane mimics.[36,39,116,117] The block copolymers containing fluorophilic moieties demonstrate peculiar properties.[30,44] Besides polymer constitution, the outcome of the interactions of these polymers with model membranes is dependent also on the lipid structure.[46] The aim of the present work is to investigate the response of amphiphilic and polyphilic block copolymers towards specifically tailored membrane models. For this purpose, three derivatives of DPPC are employed. F-DPPC bears a single fluorine atom at *sn*-2 chain terminus, so it can be considered as a tail modified lipid. In DHPC, the head group is connected to dialkyl chains through an ether linkage instead of an ester linkage (as in DPPC). EDPPC is a cationic derivative of DPPC, because the oxygen of phosphate in this lipid is esterified with an ethyl group. These lipids show a common trait, that is, they all adopt interdigitated motif in the gel phase.

_____

The lipid selection has a biological relevance. Phase transitions in DHPC and EDPPC display main phase transition temperatures in the vicinity of those reported for DPPC. DHPC acts similar to DPPC under high pressures, which is vital for applications related to development of hybrid cell membranes capable of resisting high pressures. Watschinger and Werner[118] have reviewed the orphan enzymes involved in the metabolism of ether lipids. The main phase transition temperature of F-DPPC is 10 degrees above that of DPPC. This trait of F-DPPC is relevant to the applications involving the coexistence of the interdigitated and normal bilayer gel phases. The liposomes consisting of the partially interdigitated bilayers have a higher permeability compared to the non-interdigitated liposomes, because the permeation of molecules at the interfaces between interdigitated and non-interdigitated phases is facilitated.[119,120] No data is available so far on the fate of F-DPPC in biological systems. EDPPC, despite its cationic nature is biocompatible (*i.e.,* degradable by the *phospholipases*). Therefore, it can impart distinctive properties as a component of the artificial membranes.

The thermotropic phase transitions in the binary mixtures of F-DPPC, EDPPC and DHPC have been examined recently,[121–124] but an analysis of their behavior in the presence of amphiphilic and polyphilic block polymers is still lacking. Though, the present study includes the exploration of interdigitated phases in lipid/polymer mixtures, the monolayers of pure lipids and binding of polymers to lipid monolayers remain our emphasis, simply to evaluate the potential of these modified lipids as membrane models. Similar to bilayer studies, these lipids have rarely been scrutinized as monolayers at air/water interfaces.[125–128] Evaluation will be performed utilizing block copolymers with diverse architecture. The interactions of these polymers with DPPC and other lipids have been focused lately.[39,46,117]

2 THE MODEL SYSTEM

In this thesis model membrane systems based on modified phospholipids are used, which deviate from membrane lipids in organization, binding capacity (due to presence of specific functionality) and permeability owing to the interdigitation in the gel phase.[119] Such selection offers a benefit of understanding the response of molecules/macromolecules to chemical and organizational heterogeneities in membranes. Simultaneously, the effect of macromolecules on the properties of membrane can be monitored.[129,130]

The lipids used for the model membranes are based on derivatives of 1,2-dipalmitoyl-*sn*-glycero-3-phosphocholine (DPPC), but possess modified hydrocarbon chains, headgroup and a different linkage of the alkyl chains. Their behavior in the presence of block copolymers with diverse architectures were studied.

2.1 The Lipids

The three derivatives of DPPC tested as membrane models are shown in Fig. 2.1. The replacement of the *palmitoyl* group at *sn*-2 position of DPPC by a *16-fluoropalmitoyl* moiety yields F-DPPC. The terminus containing a C-F dipole develops an affinity for polar environment and causes spontaneous interdigitation in the gel phase.[95] The length of alkyl chains is important because F-DMPC (1-myristoyl-2-(14-fluoromyristoyl)-*sn*-glycero-3-phosphocholine) shows a normal bilayer gel phase.[97] The interdigitated gel phase differs in penetrability than a normal bilayer gel phase.[131] Monofluorinated phosphatidylcholines possessing fluorine atom at different positions in the alkyl chain can be utilized to probe membrane topology utilizing techniques such as FTIR and ^{19}F-NMR.[132,133] Studies on F-DPPC monolayers are rare and only two investigations have been published so far, one on its mixtures with DPPC[125] and other on the properties of monolayers in the presence of human serum albumin (HSA).[126]

The esterification of phosphate group in DPPC by ethanol eliminates the negative charge at the phosphate and thus leads to a cationic head. The gel state of EDPPC is also interdigitated, and the reason for interdigitation in this case is the conflict between the

areas occupied by alkyl chains and the head group.[96] The interdigitation in cationic lipids is not as sensitive to alkyl chain length as that observed for monofluorinated phosphatidylcholine[134]. Recently, the phase transitions in the binary mixtures between EDPPC and F-DPPC have been investigated.[124] EDPPC forms complexes with DNA and RNA similar to other cationic lipids used in gene transfection[135]. The lipid performance is also enhanced, when used in combination with other lipids[136,137] or in the presence of cholesterol.[138,135] The DNA release from lipoplex is essential for gene expression.[139] The cationic monolayers of lipids other than EDPPC have been studied for DNA interactions using the Brewster angle microscopy.[140,141] However, EDPPC monolayers have never been examined so far nor interactions with block copolymers reported (only a thesis is available on EDPPC monolayers[142]).

(DPPC) 1,2-dipalmitoyl-*sn*-glycero-3-phosphocholine

(F-DPPC) 1-palmitoyl-2-(16-fluoropalmitoyl)-*sn*-glycero-3-phosphocholine

(DHPC) 1,2-di-*O*-hexadecyl-*sn*-glycero-3-phosphocholine

(EDPPC) 1,2-dipalmitoyl-*sn*-glycero-3-ethylphosphocholine (chloride salt)
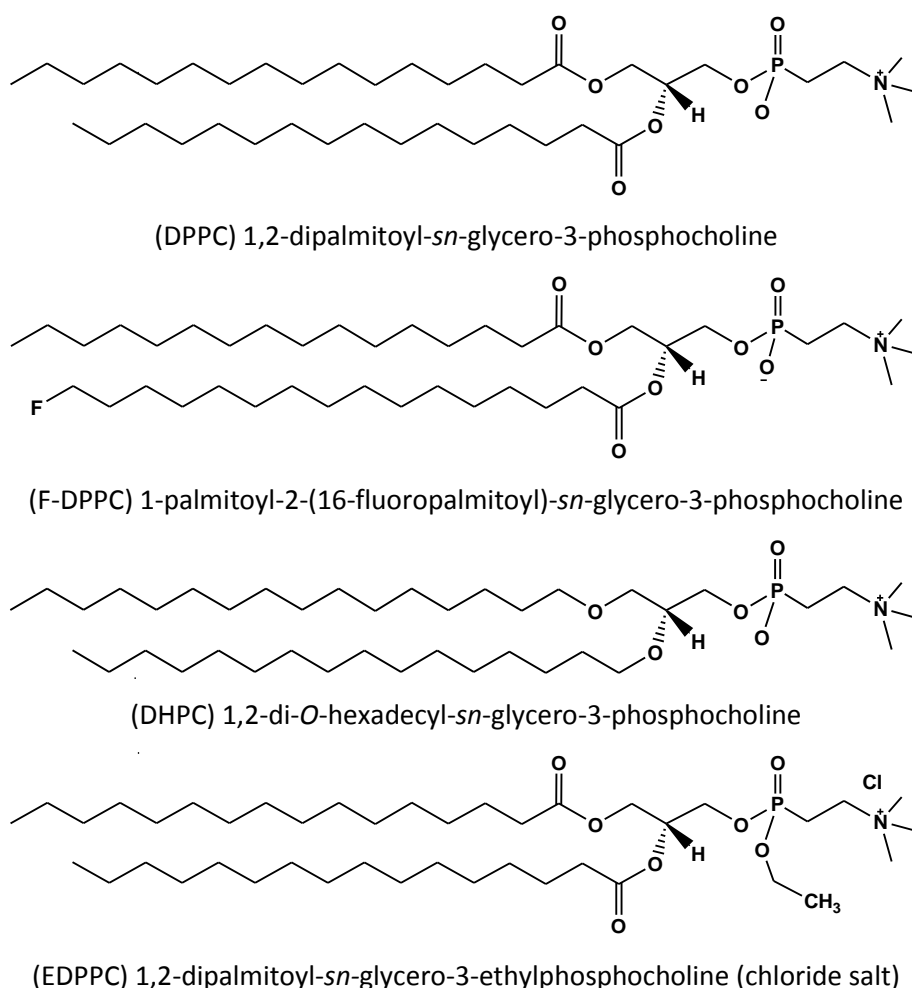
Figure 2.1: Phosphatidylcholines used in present study.

Another phospholipid forming an interdigitated gel phase is DHPC. Unlike DPPC, the alkyl chains of DHPC (1,2-di-*O*-hexadecyl-sn-glycero-3-phosphocholine) are linked to 1 and 2 positions of glycerol via an ether linkage. Ether lipids are found in cell membranes of

_____

archaea and deep-sea organisms.[143] Ether lipids are unique in a sense that they form an interdigitated gel phase which then transforms first into a rippled gel phase and then into the liquid crystalline phase.[144] This lipid is more densely packed compared to DPPC. The absence of carbonyls also reduces interactions with interfacial water. The phase transitions in aqueous dispersions of DHPC have been widely investigated.[94,144–147] Its monolayers at air/water interface were also inspected, but to much lower extent.[127,148] This ether analogue of DPPC undergoes spontaneous interdigitation without application of pressure[149] or presence of a chemical additive.[92,89] The linkage dependent behavior of antimicrobial peptide shows stronger binding with ether lipid.[109]

2.2 Categorization of Block Copolymers

The block copolymers employed in the present study can be categorized as amphiphilic and polyphilic or triphilic. They also differ in the type, length and sequence of blocks. Some of these polymers can be recognized as a part or component of another polymer. Such structural diversity allows several comparisons, and hence the polymers are sorted on the basis of the purpose they serve. The interactions of these polymers with DPPC have recently been studied.[39,46,117]

2.2.1 Presence/Absence of Perfluoroalkyl Moieties

The amphiphilic ABA triblock copolymers used here consist of a hydrophobic PPO block flanked by PGMA blocks. These block copolymers with variable block lengths have been synthesized in the group of *Prof. Jorg Kressler* and their properties were studied in bulk solution as well as at the air/water interface and after adsorption to phospholipid monolayers[28]. One of these macromolecules referred to as `GP' is included in the present study. This telechelic polymer upon end capping with perfluoroalkyl chains gives polyphilic `FGP'.[150] In these polymers, the hydrophobic PPO block is sufficiently long to span whole thickness of phospholipid bilayers. Fig. 2.2 shows the chemical structure of GP and FGP.

Schwieger *et al*[46] have examined the role of perfluoroalkylation towards membrane insertion capability of these polymers. Perfluoroalkanes are inflexible and the chains adopt a helical structure due to steric hindrance[151].
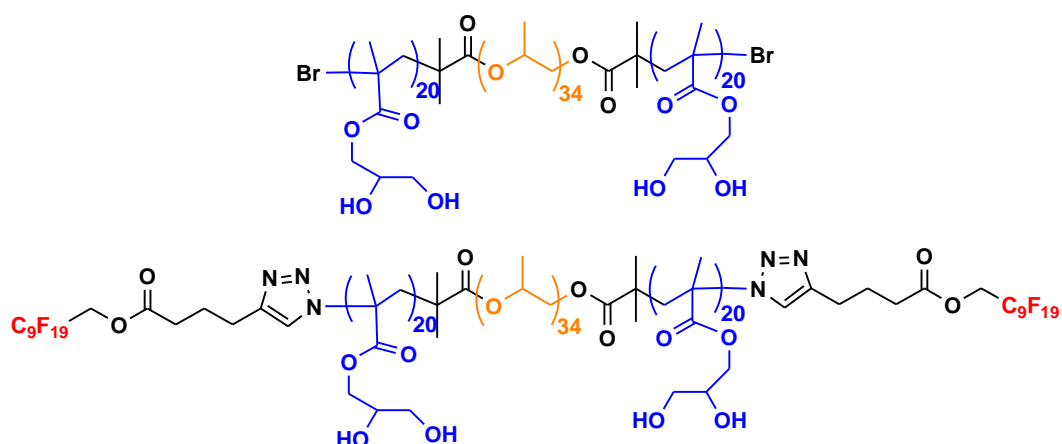
Figure 2.2: Telechelic block copolymer *GP* and triphilic block copolymer *FGP*.

2.2.2 Length and Type of Hydrophilic Block

In FGP, the hydrophobic PPO block and perfluorinated C_9F_{19} chains compete for insertion into monolayers/bilayers. To further investigate the role of perfluorinated segment alone, semitelechelic polymers consisting of a PGMA hydrophilic block end capped by F9 (i.e., C_9F_{19}) were selected.[152] In GF14 and GF40, the length of PGMA block is 14 and 40 units, respectively. GF14 is very similar to one of the two $PGMA_{20}$-F_9 blocks existing on both sides of the PPO block in FGP. GF40 has total hydrophilicity comparable to FGP, but contains only one perfluorinated alkyl chain.
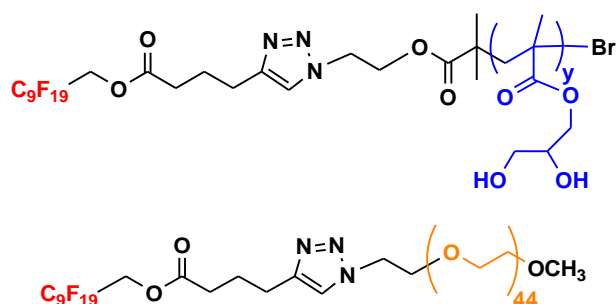
Figure 2.3: Semitelechelic block copolymers *GF40*, *GF14* and *EF44* (y = 40 & 14).

During an investigation on their recognition of DPPC chirality, it has been identified that the lengthening of the PGMA block also enhances surface activity of these polymers.[39] To see if the hydrophilic block contributes to the effects produced by perfluorinated chains or the type of hydrophilic block effects the penetration of perfluorinated chains, another polymer EF44 was also studied. Here hydrophilic block consists of PEO, instead

_____

of PGMA, and the degree of polymerization of ~ 44 is comparable to that of PGMA in GF40[152]. These polymers are shown in Fig. 2.3.

2.2.3 Change in Block Sequence

Perfluorocarbon segments in FGP and semitelechelic polymers have a free end, which can insert into lipid mono- and bilayers with ease. A pentablock copolymer with constrained fluorophilic moiety and a different block sequence was synthesized to see whether the block sequence has any influence on the interaction with lipids.[153] PFG78 differs from FGP not only, in the sequence but also, in the block lengths of PGMA and PPO blocks. PFG78 contains much larger hydrophilic and hydrophobic blocks and it is expected to cause appreciable perturbations in model membranes. The chemical structure of PFG78 is given in Fig. 2.4.
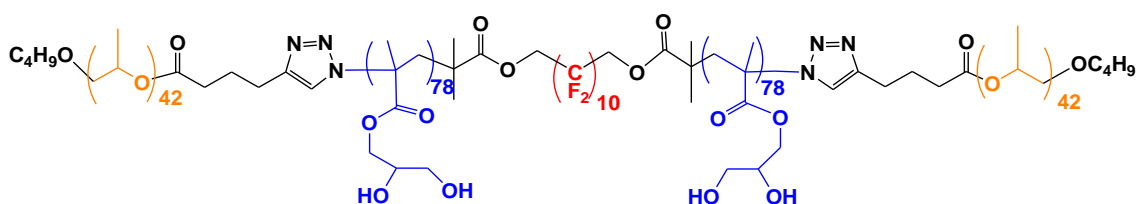
Figure 2.4: Polyphilic block copolymer with constrained perfluoroalkyl moiety, *PFG78.*

2.2.4 Attachment of a Cholesterol Moiety to a Diblock Copolymer

Cholesterol is water insoluble and fits perfectly into lipid membranes owing to its predominantly hydrophobic character.[154] Cholesterol has inhibitory effects on interdigitation in DHPC[147] and F-DPPC.[127]
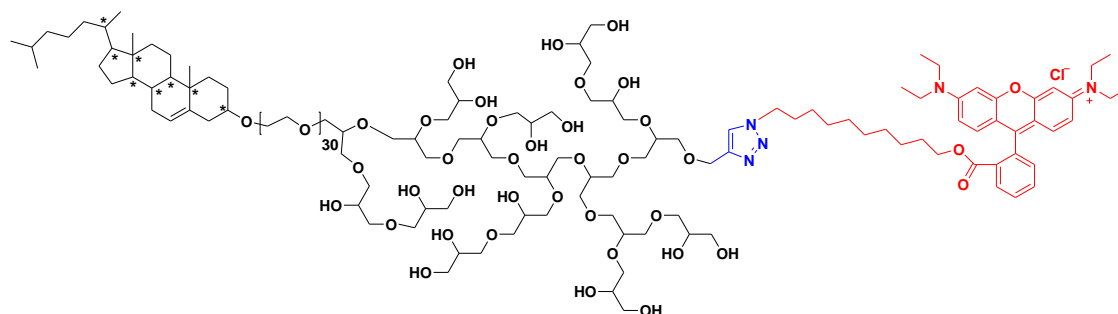
Figure 2.5: Amphiphilic rhodamine labelled block copolymer with cholesterol anchor, *CPGR*.

The attachment of cholesterol to a hydrophilic block copolymer allows its anchoring into lipid membranes and monolayers.[117,156] The synthesis of this water soluble polymer and its interactions with DPPC have recently been reported.[117] The present work describes how the presence of a cholesterol moiety modulates the interaction of this diblock copolymer with F-DPPC monolayers and bilayers. Simultaneously, the impact of the substitution of 3-OH in the cholesterol on the lipid phase transition will be monitored. The chemical structure of CPGR is shown in Fig. 2.5.

2.3 Fluorescently Labeled Lipids[157,158]

In order to visualize the domain formation in lipid monolayers or their co-spread mixtures with polymers, three different fluorescently labeled lipids were utilized. Two probes were head labeled and one contained the fluorophore at one of the hydrocarbon tails. RH-DHPE and NBD-12HPC remain in the expanded state at air/water interface, whereas NBD-DPPE under goes condensation due to small size of fluorophore and is expected to partition between LE and LC phases in a lipid monolayer.

2.3.1 RH-DHPE

This head labeled lipid, 1,2-dipalmitoyl-*sn*-glycero-3-phosphoethanolamine- N-(lissamine rhodamine B sulfonyl) (triethylammonium salt) contains rhodamine moiety attached with the nitrogen atom of DHPE. The extinction and emission maxima of this label are 560 nm and 583 nm, respectively. The structure of this label is given below
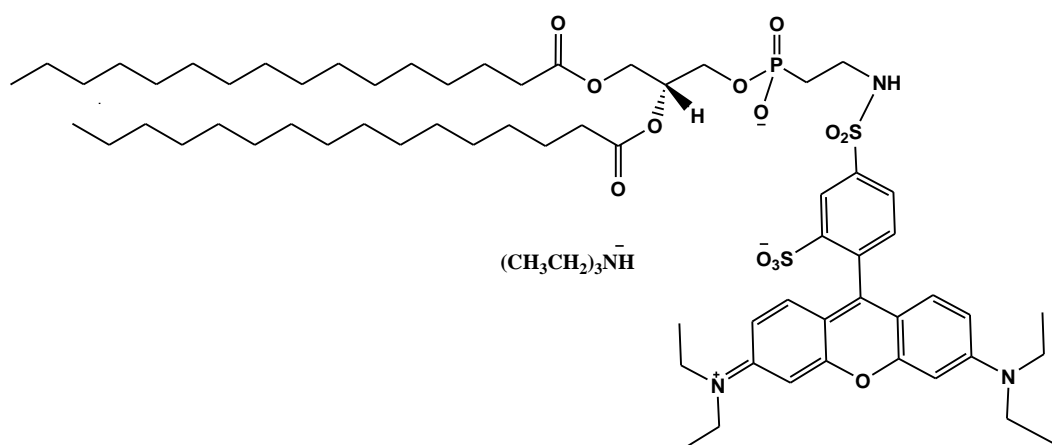
Figure 2.6: Fluorescent probe *RH-DHPE*

_____

2.3.2 NBD-DPPE

1,2-dipalmitoyl-*sn*-glycero-3-phosphoethanolamine-N-(7-nitro-2,1,3-benzosadiazol-4-yl)
(triethylammonium salt) has extinction and emission maxima at at 470 nm and 538 nm,
respectively.

Figure 2.7: Fluorescent probe *NBD-DPPE*

2.3.3 NBD-12HPC

NBD-12HPC (2-(12-(7-nitrobenz-2-oxa-1,3-diazol-4-yl)amino)dodecanoyl-1-hexadecanoyl
-*sn*-glycero-3-phosphocholine) bears fluorophore at *sn*-2 chain terminal. It has extinction
and emission maxima at 470 nm and 538 nm, respectively. The structure is shown
below.
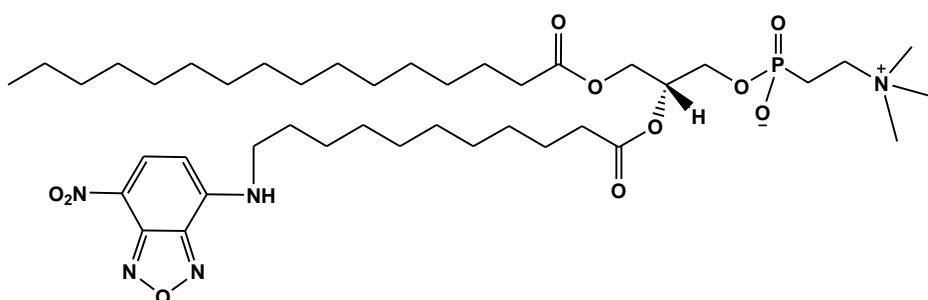
Figure 2.8: Fluorescent probe *NBD-12HPC*

_____

3 THEORY, TECHNIQUES AND METHODS

3.1 Langmuir Monolayers

3.1.1 Theory

Insoluble amphiphiles spread at an air/water interface form monolayers termed as "Langmuir monolayers". Upon compression , that is, with the reduction in area A, the lateral pressure π increases[159], where π is defined as

$$\pi = \sigma_o - \sigma_1 \tag{1}$$

with σ_o and σ_1 being the surface tension in the absence and presence of a lipid monolayer, respectively.
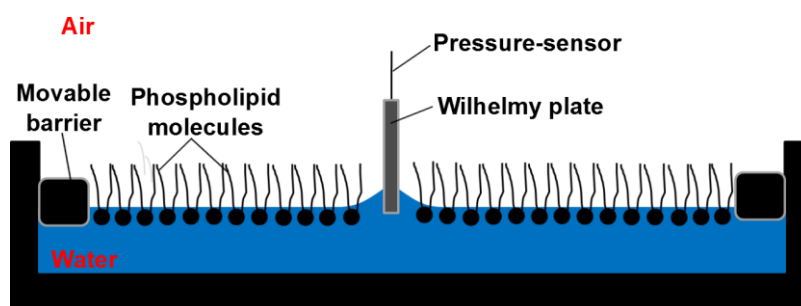
Figure 3.1: Langmuir trough for recording of pressure-area isotherms of lipid monolayer.

Recording compression or π-A isotherms allows the calculation of compressibility χ of monolayers at fixed T by employing the relationship[160,161]

$$\chi = -\frac{1}{A}\left(\frac{\partial A}{\partial \pi}\right)_T \tag{2}$$

A very dilute monolayer behaves like a gas in a cylinder, and can be represented by a *van der Waals* equation of state in two dimensions.[162]

$$\left(\pi + \frac{a}{A^2}\right)(A - b) = kT \tag{3}$$

where π is again the surface tension (or pressure), A is the area, and a and b are constants[163].

The presence of different phases on the surface can be correlated to the arrangement of lipid molecules. At a critical pressure π_c (and a corresponding area A_c), a phase transition takes place, initiating aggregation of molecules into a condensed phase. The condensation of lipids is visible in the pressure-area isotherm as a change in slope (or an alteration in compressibility[67]).

_____

3.1.2 Experimental

Pressure-area isotherms were recorded on a film balance, consisting of a trough with maximal area 536 cm^2, two moveable barriers and Wilhelmy plate as pressure sensor (Riegler and Kirstein GmbH, Berlin, Germany). An image of Langmuir trough is given in Fig. 3.1. The trough was thoroughly cleaned using Hellmanex solution and deionized water before each experimental run. The trough was filled with ultrapure water and calibration was performed for the pressure sensor using the surface tensions of water and air, i.e., 72 mN m^{-1} and 0 mN m^{-1}, respectively. The sub-phase was 100 mM aqueous NaCl for the cationic lipid EDPPC and its mixtures with polymers.

Pure lipids, polymers, or their mixtures in desired ratios were prepared in chloroform or chloroform/methanol (9:1 or 2:1). These mixtures were spread at air/water interface using microsyringe (Hamilton Bonaduz AG, Bonaduz, Switzerland). A time of 15 minutes was allowed for evaporation of solvent, before initiating the compression of the monolayer. The rates of compression varied between 0.5 to 4.0 Å^2 molec^{-1} min^{-1}. The temperature of sub-phase was maintained at 20 ± 0.1 °C using an external circulating water bath (Thermostat F3, Karlsruhe, Germany). In all the cases the pressure-area isotherms were reproducible with a difference of about 1-2 Å^2 molecu^{-1}.

3.2 Gibbs Monolayers

3.2.1 Theory

The adsorption of soluble amphiphiles to an air/water interface produces Gibbs monolayers[164]. The Gibbs equation connects the surface coverage Γ to the surface pressure π and the bulk concentration of a monomeric surfactant X_1 by:[162]

$$\Gamma = -\frac{1}{kT}\left(\frac{\partial \pi}{\partial logX_1}\right)_T \qquad (4)$$

With enhanced adsorption of surfactant with increasing X_1, the surface tension γ drops. For surfactants showing a critical micellization concentration (cmc), γ stays almost constant above the *cmc*.

Moroi *et al*[165,166] pointed-out deviations from the Gibbs model and provided evidences that the adsorbed films were not located at air/solution interface unlike insoluble monolayers.

When the air/water interface is covered by Langmuir monolayers of lipids and water soluble amphiphiles are injected into the sub-phase, these will be able to insert into the monolayers, depending on the initial surface coverage and the surface activity of the amphiphile and their interactions with the lipid. Fig. 3.2 shows this phenomenon.
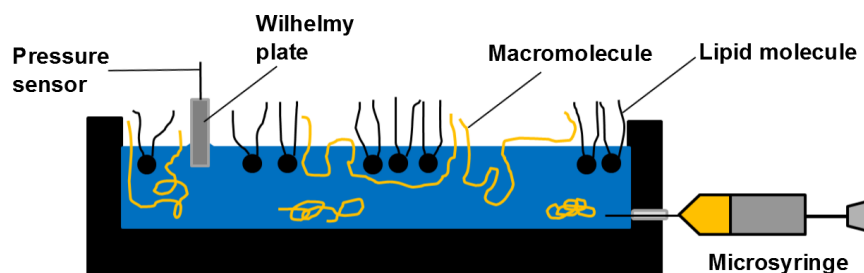
Figure 3.2: Adsorption of polymer injected into the subphase to lipid monolayer at certain initial spreading pressure.

A possibility of comparison between pressure-area isotherms for Langmuir monolayers to pressure-time isotherms of Gibbs monolayers was proposed.[167] The evaluation of the adsorption of macromolecules injected into the sub-phase underneath lipid monolayer in different physical states is therefore also possible to test their interactions.

The surface pressure exhibited by the lipid monolayer, called the initial spreading pressure (π_{ini}) changes after polymer's injection, until it reaches certain constant value (π_{max}). Plotting the change in surface pressure $(\Delta\pi = \pi_{max} - \pi_{ini})$ vs. π_{ini} and extrapolation to $\Delta\pi = 0$, gives exclusion pressure (π_e). At π_{ini} values above π_e, the macromolecule is excluded from the lipid monolayer. The exclusion pressure, π_e also termed as maximal insertion pressure (MIP) is regarded as an important parameter to describe the membrane permeability of macromolecules.

3.2.2 Experimental

To monitor the adsorption of polymers to pre-existing lipid films maintained at particular initial pressures, a system based on two homemade circular troughs (with an individual diameter of 6 cm and depth of 0.3 cm) were used. Each trough was equipped with a

_____

Wilhelmy plate as pressure sensor (Riegler and Kirstein GmbH, Berlin, Germany) for recording of surface-pressures. The whole system was enclosed in a plastic hood to ensure optimal environment for error free recordings. Before an experimental run, the troughs were thoroughly cleaned with Hellmanex solution and deionized water, filled with ultrapure water or 100 mM aqueous NaCl and pressure-sensor was calibrated using the surface tensions of water and air as standards. The sub-phase was kept at 20 ± 0.1 °C using an external water thermostat (Thermostat F3, Karlsruhe, Germany). A monomolecular layer of lipid at certain initial surface-pressure was produced at air/water interface from lipid solution prepared in chloroform. A microsyringe from Hamilton Bonaduz AG, Bonaduz, Switzerland was utilized for this purpose. After allowing enough time for solvent evaporation and homogeneities, certain volume of aqueous polymer solution was injected underneath the monolayer, to attain the desirable strength of polymer in the sub-phase (i.e., 100-400 nM). A small spherical magnetic stirrer in the subphase enabled the controlled diffusion of added macromolecule. The surface-pressure *vs*. time data was processed using Origin 8.0 (Origin Lab Corporation).

3.3   Epifluorescence Microscopy

3.3.1 Theory

Fig. 3.3 shows the Jablonski energy diagram for adsorption and emission (fluorescence) of light in fluorescent molecules.
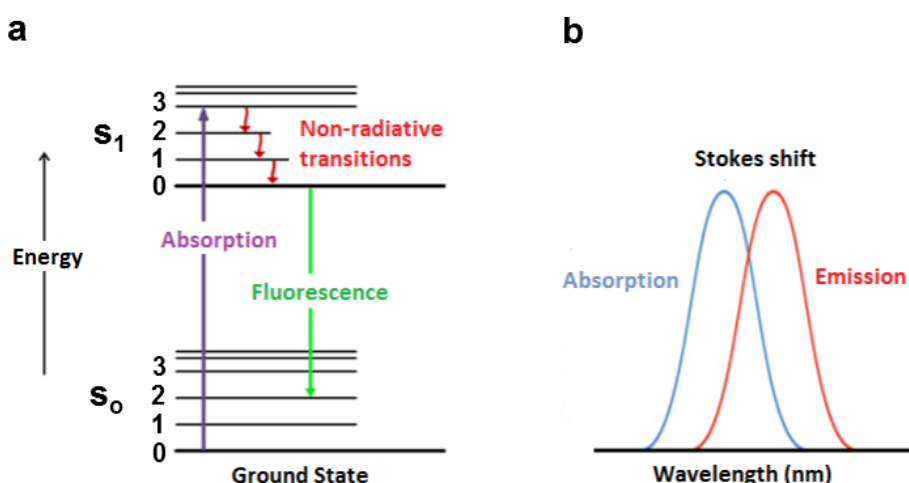
Figure 3.3: a) Jablonski diagram for absorption and emission of photon; and b) Stokes Shift (adapted from Wikipedia).

Fluorescence occurs when molecules absorb light at a particular wavelength (λ_1) and afterwards emit light of longer wavelength (λ_2). The difference ($\lambda_2 - \lambda_1$) is called Stokes Shift[168]. The phenomenon of fluorescence is based on three events, which take place on different time scales. Initially, the molecule is excited by an incident photon on a time scale of femtoseconds. This is followed by non-radiative vibrational relaxation, which happens in picoseconds. Finally, the molecule returns to the ground state after emitting a longer wavelength photon. This much slower process occurs in nanoseconds, depending upon the average time that a fluorescing molecule spends in excited state before returning to the ground state. The time before emitting a photon is known as fluorescence lifetime.[169]
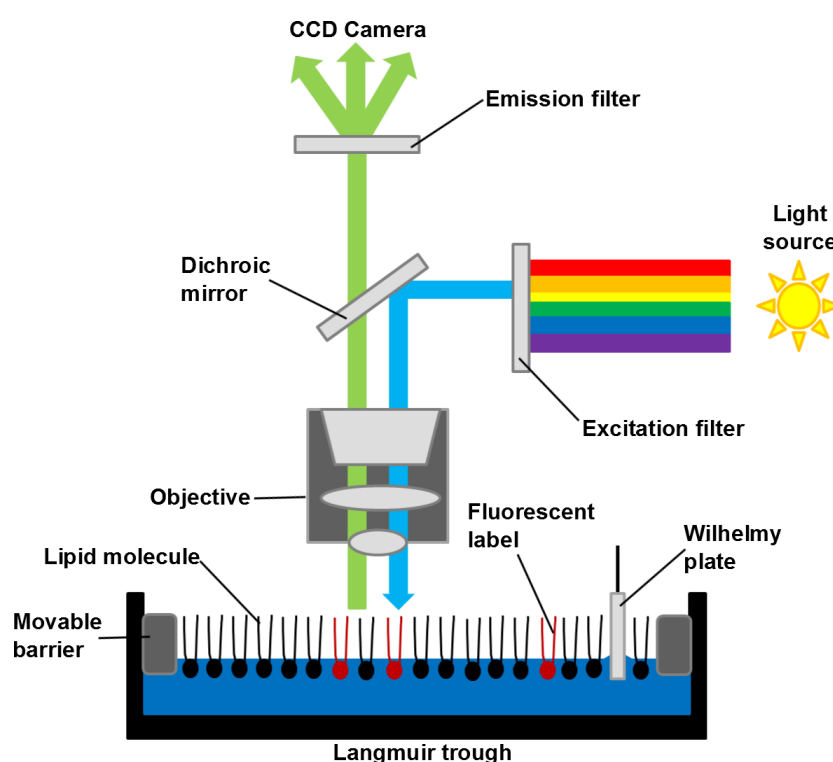
Figure 3.4: Epifluorescence microscopy imaging of a lipid monolayer at air/water interface (adapted from www.thermofisher.com).

For the LE-LC transition observed in the lipid monolayers, it was for a long time unclear whether this transition is of first order or second order. In the case of first order transition, a coexistence of LC and LE domains should be present during the compression in the range of the plateau region. In order to track phase transition, the visualization tool of epifluorescence microscopy[170–172] was employed using fluorescent

probe incorporated into the monolayers, alongside the recording of isotherms. In a simple setup, an epifluorescence microscope with a CCD camera is mounted over the Langmuir trough (Fig. 3.4).

The lipid monolayer including the low percentage of dye is created at the air/water interface and snap shots of the film under observation are taken at desired molecular areas or surface pressures. Weis[173] reviewed the phase transitions in phospholipid monolayer and linked the domain formation to competition between long-range electrostatic forces and short-range attractive interactions. The determination of gas-fluid and fluid-solid transitions and fluid-fluid miscibility is also possible.

Depending upon the type of fluorescently labeled lipid, the dye molecules partitions into either the LE or the LC phase. The more common case is that the probe is uniformly distributed in the fluid phase, so the whole region appears bright under the microscope. Upon condensation, the probe is excluded from the LC domains and dark regions are visible. In the case of NBD-DPPE, the probe partitions preferentially into the LC domains though some of the dye molecules are still present in the LE phase. The shapes of domains are indicative of molecular chirality and tilt.[174] Changes in shape provide insight into insertion of block copolymers into lipid monolayers.[175]

3.3.2 Experimental

Monolayers were visualized using an Axio Scope A1 Vario epifluorescence microscope from Carl Zeiss Microimaging, Jena, Germany. The components of microscope included in the set-up were: i) a 100 W mercury arc lamp (HXP 120 C); ii) an objective (LD EC Epiplan-NEOFLUAR 50x); iii) a filter *cum* beam spliter (Filter Set 81HE) and iv) a highly sensitive EMCCD camera (ImageEM C9100-13, Hamamatsu, Herrsching, Germany). A trough with moveable barriers having maximal area 264 cm^2 and pressure sensor based on Wilhelmy plate (Riegler and Kirstein GmbH, Berlin, Germany) was mounted on an adjustable stage from Märzhäuser, Wetzlar, Germany to allow movements along x, y and z-dimensions using a MAC5000 system (Ludl Electronic Products, Hawthorne, NY, USA). The trough was enclosed in a homemade Plexiglas chamber to ensure stable, homogeneous and dust-free environment. The measurements were performed at 20°C

and temperature was kept within ± 0.1 °C by utilizing an external water circulating thermostat described above. The whole system was supported by a vibration-damped optical table from Newport, Darmstadt, Germany. A desired amount of fluorescent label (0.01 mol% RH-DHPE or 0.5-1.0 mol% NBD-12HPC or NBD-DPPE) was added to the freshly prepared lipid, polymer or lipid/polymer mixtures in chloroform or chloroform/methanol mixtures (9:1 or 2:1). A monolayer was formed at the air/water interface on the pre-cleaned trough containing ultrapure water and appropriately calibrated surface pressure indicator. The subphase was 100 mM aqueous NaCl for cationic lipid EDPPC and its mixtures with polymers. The spreading was done by using a microsyringe from Hamilton Bonaduz AG, Bonaduz, Switzerland. The monomolecular film was compressed at different rates (0.5 to 4.0 Å^2 molec^{-1} min^{-1}) utilizing the moveable barriers, after sufficient time was allowed for solvent evaporation and attainment of homogeneities. The images were recorded at the desired areas and surface pressures. The Axiovision software (Carl Zeiss Microimaging, Jena, Germany) was employed for imaging and data analysis.

3.4 Differential Scanning Calorimetry

3.4.1 Theory

Calorimetry is widely applicable in biological and biomedical sciences and associated disciplines.[176] Differential scanning calorimetry (DSC) is one of the most powerful techniques for investigating thermally induced transitions in lipids[81] and thermodynamic stability and molecular recognition in membranes[177,178] and conformational changes in macromolecules.[179]

The enthalpy H of a system at constant pressure as a function of temperature is given by

$$H = \int_0^T C_P \, dT + H_o \qquad (5)$$

With H_o being an arbitrary constant for the enthalpy at $T = 0$ and C_p being the heat capacity.

If a system undergoes a phase transition from state *A* to *B* in a certain temperature range, the enthalpy and entropy of the phase transition from one state to another are given by:[180]

$$\Delta H_{trans} = \int_{T_1}^{T_2} \left(C_{p(diff)} - C_{p(baseline)} \right) dT \qquad (6)$$

$$\Delta S_{trans} = \frac{\Delta H_{trans}}{T_{trans}} \qquad (7)$$

with T_1 and T_2 being the onset and end temperatures of the transition. $C_{p(diff)}$ the measured heat capacity, and $C_{p(baseline)}$ being the interpolated heat capacity without transition. T_m is the midpoint of the transition.
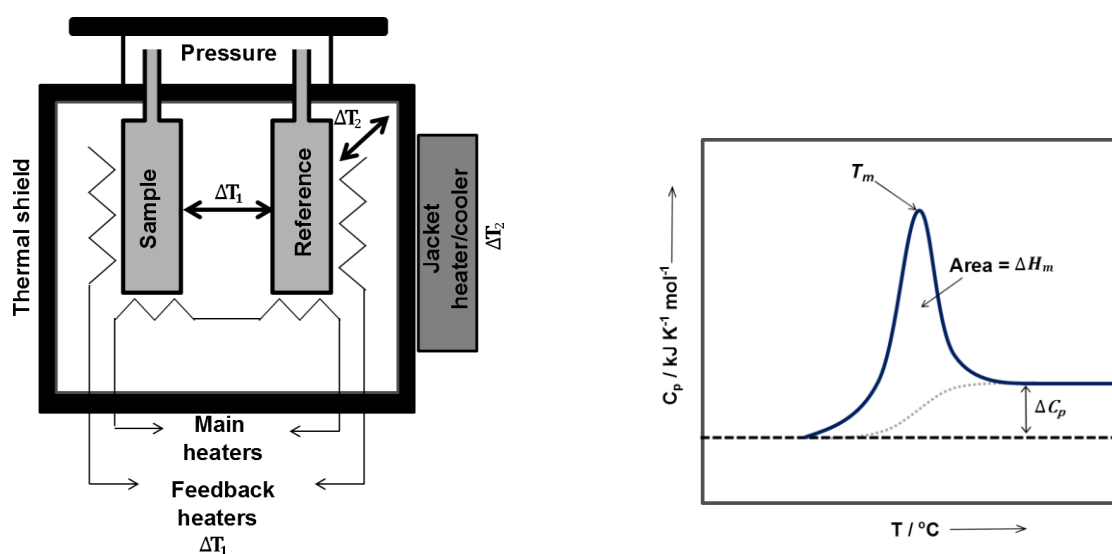
Figure 3.5: a) Scheme of a differential scanning microcalorimeter (left); and b) A typical DSC thermogram (right) (adapted from[180])

A feedback mechanism in a differential scanning calorimeter (shown in Fig. 3.5) removes the temperature difference between reference and sample cells and alters the temperature in two cells at certain desired, fixed rate[181]. Furthermore, the heat flow from one compartment to another, as well as to the environment is prevented. The integral of a DSC curve from base line gives the enthalpy of transition. The maximum in C_P represents the transition temperature T_m.[182]

DSC has successfully been employed for investigations into the behavior of pure lipids, lipid mixtures and lipid/polymer mixtures.[47,81,91,183,184]

_____

3.4.2 Experimental

The recording of thermograms for aqueous dispersions of pure lipids or their mixtures (with polymers) was accomplished with Microcal VP-DSC from MicroCal Inc., Northhampton, USA. The aqueous samples of pure lipids were prepared in ultrapure water or 100 mM aqueous NaCl to give a lipid concentration of 1 mM. Before addition to the sample-cell of the calorimeter, they were heated above their respected phase transition temperatures and either vortexed or sonicated (or extruded); and degassed after gradual cooling to room temperature. The lipid/polymer mixtures were prepared in two different ways. One, they were premixed in chloroform/methanol (2:1) and dried under N_2 stream and kept under vacuum at 25°C overnight for the removal of residual solvent. The dried samples were later hydrated (with water or 100 mM aqueous sodium chloride), sonicated in an ultrasonication bath above the phase transition temperature and degassed at room temperature, prior to DSC analysis. Other, the polymer solution was prepared separately in water and then added (in a desired proportion) to unilamellar lipid vesicles formed through extrusion of aqueous lipid dispersions. The extrusion was carried out with a Lipofast-Extruder (Avastin) using a 100 nm polycarbonate membrane. In every case, the lipid concentration was maintained at 1 mM. The scan rates varied between 10-60 degrees per hour. A time resolution of 4s/data points was employed. Depending upon the nature of lipid, the reference was either water or 100 mM aqueous sodium chloride.

_____

4 INVESTIGATIONS OF MONOFLUORINATED LIPID F-DPPC

F-DPPC (1-hexadecanoyl-2-(16-fluorohexadecanoyl)-*sn*-glycero-3-phosphocholine) is a synthetic derivative of L-DPPC where the fatty acid at *sn-2* position contains a single fluorine atom at the terminus. The presence of a polar C-F bond leads to change in lipid bilayer behavior. Therefore, F-DPPC is known to form interdigitated gel phase.[95] Several investigations have been done on the effect of phospholipids[121,123,124], calcium[131] and lanthanum[185] ions and cholesterol[155] on the gel phase of this lipid. The gel phase remains partially interdigitated under area constraints.[186] The interdigitation in F-DPPC reveals a delicate balance of forces between lipids molecules in a bilayer because F-DMPC, a F-DPPC homolog having fourteen carbon atoms in each chain, does not produce an interdigitated gel phase.[97] In contrast, there are are hardly any studies done on the monolayer behavior of F-DPPC, probably because the presence of single fluorine atom is not expected to alter the monolayer behavior, where the possibility of interdigitation does not exist. The only available reports are about F-DPPC monolayers studied as co-spread mixtures with L-DPPC[125] and human serum albumin.[126] To the best of our knowledge, the interactions of monofluorinated DPPC with synthetic polymers have never been investigated.
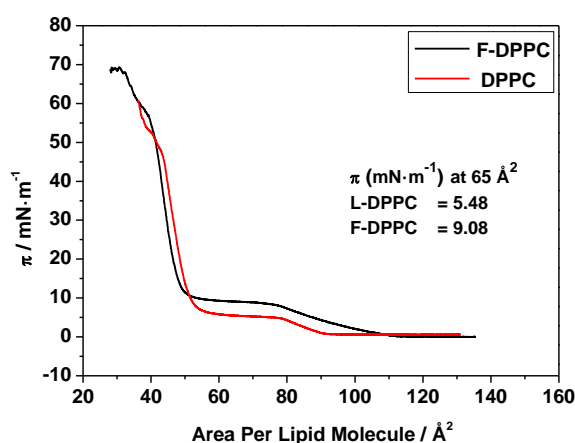

Figure 4.1: Compression isotherms for L-DPPC and F-DPPC monolayers on aqueous subphase.

4.1 Monolayer Studies

F-DPPC monolayers at the air/water interface in the liquid expanded phase correspond to only half the fluid bilayer phase. The interdigitation in bulk phases is driven by the affinity of polar C-F bond to localize close to the aqueous or polar environment, but this

_____

should occur in such a way that the hydrocarbon chains are not exposed to water. Based on the propensity of fluorine atom for the interfacial region, a distinguishable monolayer behavior is also possible. The π-A isotherms for F-DPPC and DPPC monolayers at the air/water interface at shown in Fig. 4.1**.** The LE-LC transition begins at higher surface pressure for F-DPPC monolayers compared to those of DPPC. In the studies done earlier using BAM, F-DPPC monolayers exhibited ovoid type condensed domains.[125,126] These domains are different from *bean* or *cardioid* type domains observed with DPPC.

4.1.1 Pure Lipid

FM-Images in the Presence of Different Fluorescent Labels

FM-images of F-DPPC in the presence of different fluorescently labeled lipids are shown in Fig. 4.2. The onset of the LE-LC transition at the beginning of the plateau and conversion of some lipid to the condensed phase causes expulsion of the labeled lipids (NBD-12HPC and RH-DHPE), because both fluorescent labels remain only in the liquid expanded phases, RH-DHPE due to presence of the large rhodamine moiety attached to the lipid head and NBD-12HPC due to presence of the NBD dye at one of the hydrocarbon chain termini. The elimination of fluorescent probes from condensed domains of lipids makes these domains to appear as dark regions. The LC domains have fractal growth patterns, and initially observed distorted beans evolve into seaweed like 2D-aggregates. The fractal growth patterns are exhibited by the lipid monolayers which have untitled alkyl chains (e.g. DMPE). Preliminary IRRAS investigations indicate that the alkyl chains in the LC phase of F-DPPC monolayers are tilted at an angle of 30° to the surface normal. This tilt angle is similar to that recorded for DPPC monolayers. The elongation of domain boundaries and demonstration of branched LC domains is possible due to enlargement of the LE-LC interface.[187] If fluorine atom in F-DPPC is localized near the air/water interface in the LE phase, then the widening of interface between LE and LC phase is conceivable. This behavior will be explained further in the proceeding section on kinetic effects observed in F-DPPC monolayers. In the case of third label NBD-DPPE, the NBD moiety is attached to the head and due to the smaller size of the NBD label, this labeled lipid stays in the LC phase of the monolayers of F-DPPC and gives rise to white instead of black domains in LE/LC coexisting region. The domains become more organized with NBD-DPPE, probably due to existence of the negatively charged

_____

phosphate group in the label, which alters interactions with the head groups of F-DPPC. The greyish core of these domains is either due to self-quenching of NBD or due to elimination of the probe from solid domains.[158] NBD-DPPE in L-DPPC shows similar behavior and the curling directions become visible as greyish cores (Fig. 4.3).
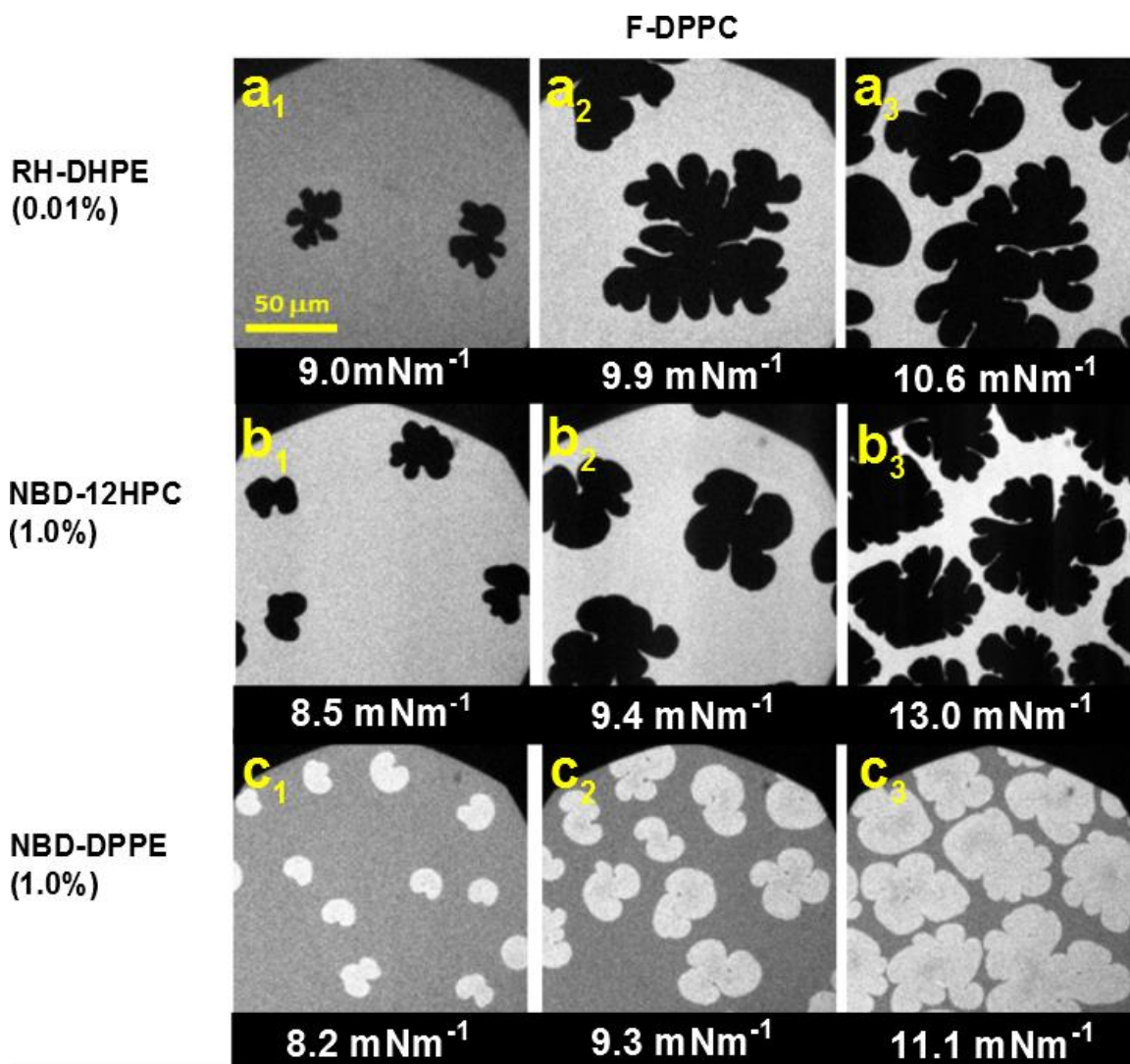
Figure 4.2: Epifluorescence microscopy images of F-DPPC in the presence of different fluorescent labels a) RH-DHPE; b) NBD-12HPC; c) NBD-DPPE.

The grey areas are more prominent in the case of DPPC, reflecting a denser packing compared to F-DPPC. The shapes of F-DPPC and DPPC isotherms virtually remain unchanged upon probe addition. The shapes of LC domains in DPPC monolayers are slightly altered with NBD-DPPE and there is a tendency to exhibit propeller shapes with elongated blades. Still, the shapes of these domains are highly comparable to those observed for L-DPPC in the presence of RH-DHPE (Fig. 4.9b). Thus, it can be safely

assumed that the probe at the used low concentration is not affecting the lipid behavior even when it penetrates the condensed domains.
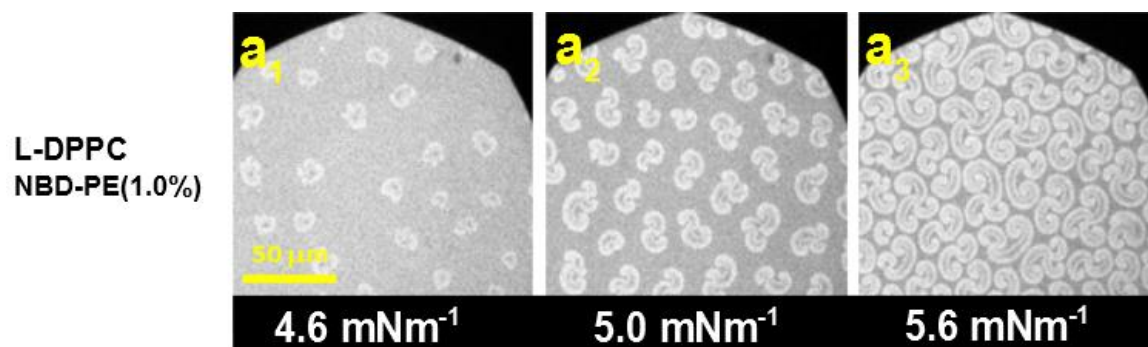
Figure 4.3: FM-images for L-DPPC in the presence of NBD-DPPE on aqueous subphase.

On 0.15M NaCl subphase, the dye is partitioned differently between the LE and LC lipid phases (Fig. 4.4). Here, black LC domains with greyish border are seen initially. Upon compression, the roughening of domain boundaries occurs, and accumulation of probe at the edges is noticed. A closer analysis of these domains reveals a gamut of dye distribution. The interactions between anionic phosphate group in NBD-DPPE and head group of F-DPPC are reduced due to screening of charges and can be considered responsible for different dye distribution in LC domains on 0.1M NaCl subphase.
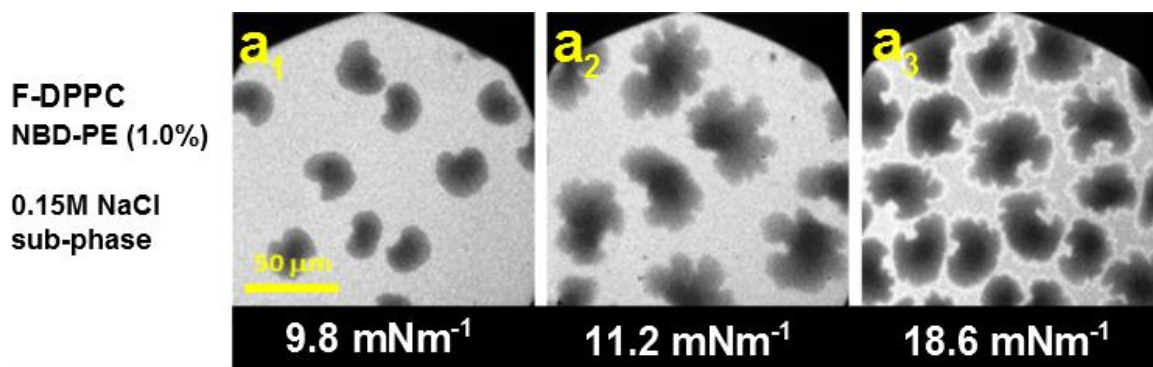
Figure 4.4: FM-images for F-DPPC in the presence of DPPE-NBD on 100 mM NaCl subphase.

Kinetic Effect Observed by Epifluorescence Microscopy of F-DPPC Monolayers

It is apparent from Fig. 4.2 that F-DPPC produces distorted bean like LC domains, which develop through fractal growth. Vanderlick and Möhwald[188] discussed the variety of modes relevant for shape transitions in monolayers, especially under the impact of externally applied fields. According to them, the circular shape represents the zeroth mode, whereas all the other shapes represent the higher modes. The fractal growth has

_____

been related to diffusion limited aggregation.[189] Brewster Angle Microscopy, where a dye probe is absent reveals that non-equilibrium domain shapes may be caused by crystallinity of the condensed phase, for which chain length, chain tilt and head group type are responsible.[190] Higher monolayer compression rates can also lead to dendritic or fractal domain shapes.[191,192] The tips of fractal fingers lack defined orientation in the LC domains.

In order to highlight the factors responsible for seaweed type 2D-aggregates in F-DPPC monolayers, the kinetics effects on the lipid monolayers were monitored and the evolution of LC domain shapes under different compression speeds and after pressure-jumps were studied. Fig. 4.5 shows π-A isotherms for F-DPPC monolayer recorded at different compression rates. In one of such measurements, the monolayer was compressed to the surface pressure of 9.0 mN m^{-1} and allowed to stand for 20 h. Later, the compression was continued with the same speed of 4.0 Å^2 min^{-1} molec^{-1}. The surface pressure changed less steeply with decrease in area per lipid molecule in this case, indicating the loss of some lipid to the subphase.
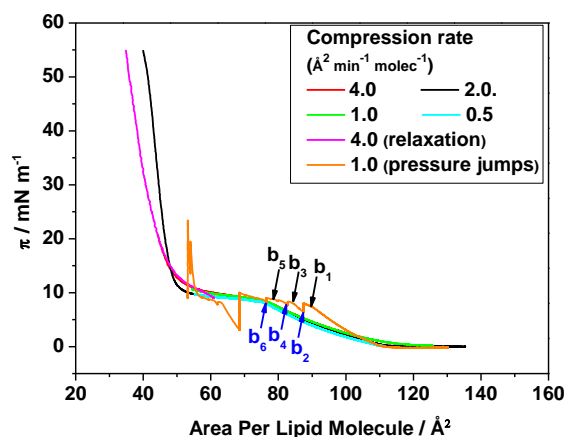
Figure 4.5: Compression isotherms of F-DPPC recorded at different speeds of compression, after relaxation and pressure jumps.

The first pressure jump was applied just before the onset of the LE-LC transition, which resulted in a sudden increase in the surface pressure. The subsequent jerks covered the whole LE-LC coexistence region during which the area per lipid decreased abruptly after each jump and consequently the surface pressure was raised. The monolayer was allowed to relax and reach equilibrium before the application of next pressure (or area) jerks during which a drop in π-value was seen. In Fig. 4.5, the onset of pressure jumps

are indicated by black arrows, which are followed by the relaxation represented by the blue arrows.

The evolution of LC domains of F-DPPC under different compression speed, after relaxation and application of pressure jumps is presented in Figs. 4.6 & 4.7, respectively. When compression speed is increased, the splitting of fractal fingers occurs. A decrease in the compression rate reduces the distortion of bean shaped LC domains. However, they remain disorganized even when the monolayer is compressed with a speed of 0.5 Å^2 min^{-1} molec^{-1}. This clearly indicates that F-DPPC monolayer is more prone to kinetic effects compared to that of DPPC. Again, this is probably due to elongation of the LE/LC interface resulting from the localization of fluorinated chain terminus close to the water surface in F-DPPC monolayers. Initially formed non-equilibrium shapes relax to more organized shapes, once compression is stopped.[191] DPPC monolayers compressed at the speed of 2.0 Å^2 min^{-1} molec^{-1} produces bean like condensed islands, which evolve into propeller shaped domains later (see Fig. 4.6). The domain shapes observed in F-DPPC monolayers, show that the electrostatic forces dominate during compression, and the monolayer does not actually reach equilibrium, even when the compression rates are low.

The fractal domains attain bean or propeller like morphologies when compression is halted (Fig. 4.7a). When the monomolecular film is compressed again after they have relaxed to bean like shapes, the beans develop *cilia* or hair like outgrowth, and do not actually turn into seaweed like structures probably because of the limited area available for their growth. Similar patterns were observed previously for dioctadecylamine (DODA) monolayers.[193] Out-of-equilibrium processes have significant biological implications[194], especially in adaptability and selectivity.

To investigate further the fractal domain growth, the lipid monolayer was allowed to be compressed at a speed of 1.0 Å^2 min^{-1} molec^{-1} initially and then a pressure jump was applied. However, this small jerk caused only a small change in the area *i.e.,* 0.3 Å^2, the surface pressure dropped significantly and the domains disappeared. At this point, the compression was stopped and the monolayer was allowed to relax until equilibrium

cardioid-type domains were visible. Black and blue arrows in Fig. 4.7 represent a part of this phenomenon and the corresponding FM-images are gathered in Fig. 4.9b.
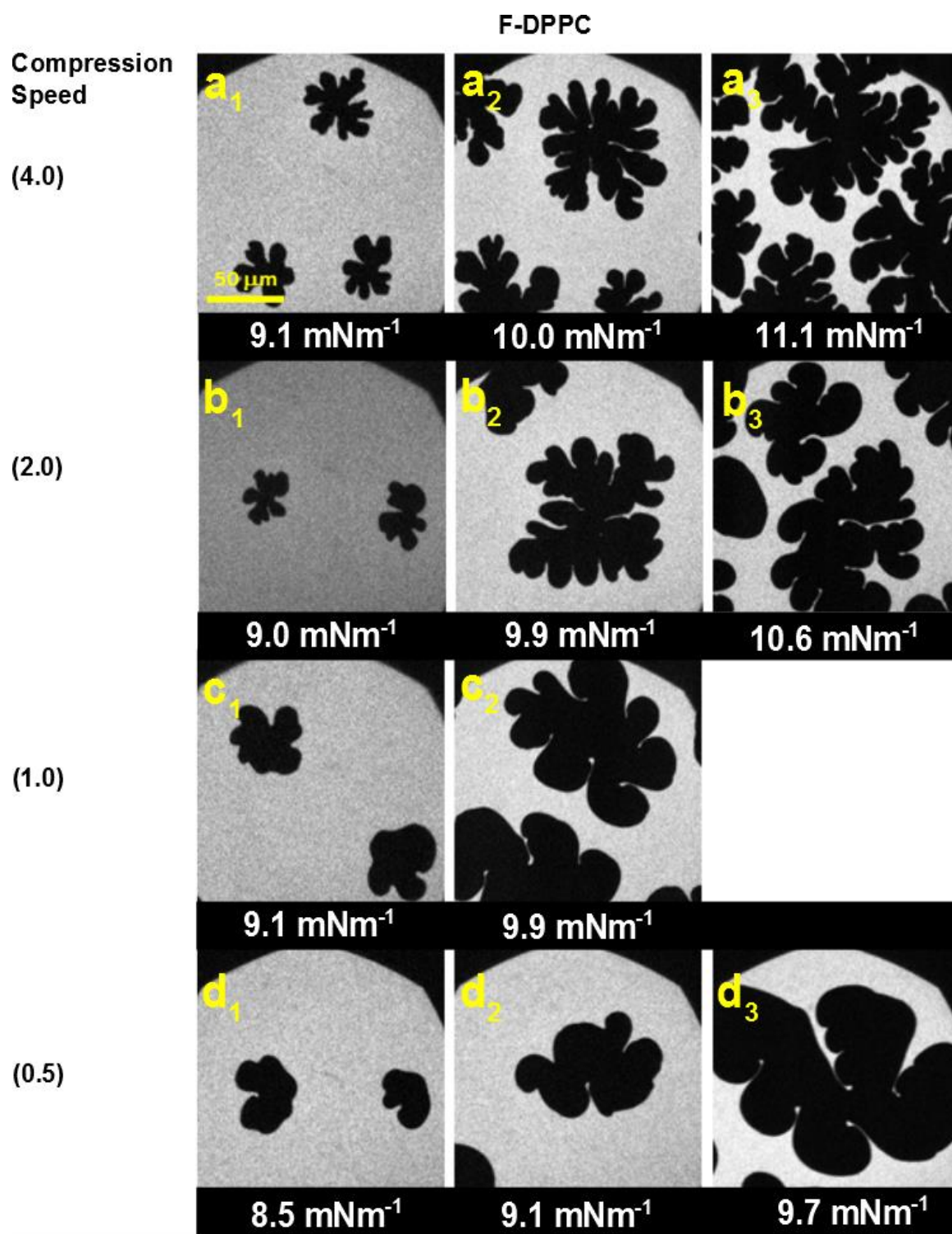
Figure 4.6: Evolution of LC-domains of F-DPPC monolayers containing 0.01% RH-DHPE under different compression rates (in $Å^2 min^{-1} molec^{-1}$).

The pressure jump at 65 Å^2 molec^{-1} produced greatest decrease in surface pressure once the compression was stopped and the surface pressure dropped from 9.9 mN m^{-1} to 3.2 mN m^{-1}. The higher values of surface pressures representing the LE-LC coexistence were regained after subsequent pressure jumps without allowing the monolayer to relax, until it collapsed at the surface pressure of 23 mN m^{-1}.
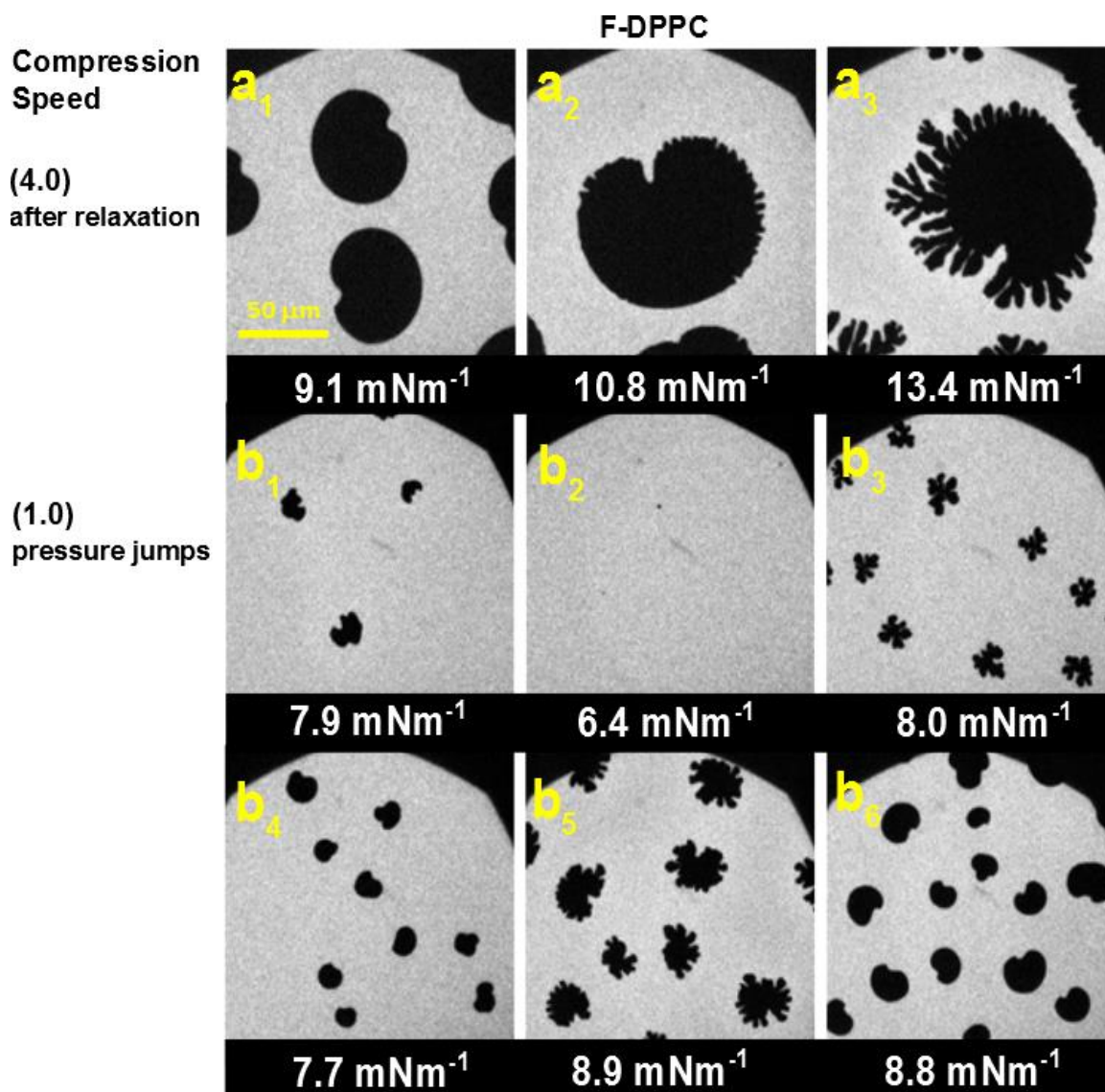
Figure 4.7: Kinetics effects on LC-domains of F-DPPC monolayers containing 0.01% RH-DHPE. a) compression at 4.0 Å^2 min^{-1} molec^{-1} after relaxation for 20 h; and b) Pressure jumps followed by relaxation (indicated by arrows in Fig. 4.5)

Considering monolayer as a thin solid sheet on fluid, these jolts lead to wrinkle formation or buckling[195,196], especially at collapse pressures.[197] Such instability does not occur through enhancement of compression speed only, which can only destabilize the domain boundaries and lead to disorganized fractal growth of 2D-condensed phase.

_____

Pressure-Area Isotherms of Pure Lipids and their Mixtures
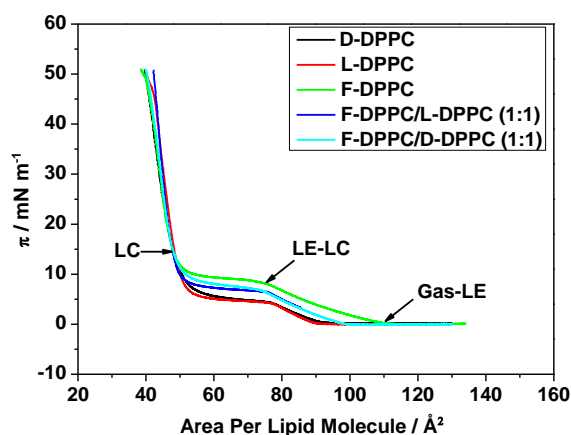
Figure 4.8: Compression isotherms for L-DPPC, D-DPPC, F-DPPC and their 1:1 mixtures (The coexistence or presence of different phases is indicated by arrows)

The π-A isotherms of pure lipids L-DPPC, D-DPPC, F-DPPC and their equimolar mixtures are shown in Fig. 4.8. In all the cases, the limiting areas average at $\sim$ 51 Å^2 molec^{-1}, which agree with the reported values.[125]

Table 4.1: Characteristics data regarding phase transitions in L-DPPC, F-DPPC and L-DPPC/F-DPPC (1:1) (The onset of different phases is indicated by arrows in Fig. 4.8)

Lipid/Lipid mixtures	Phase transitions in lipid monolayers			
	Gas to LE	LE to LC		LC phase
	Area per Lipid Molecule / Å^2	Area per Lipid Molecule / Å^2	Pressure / mN m^{-1}	Area per Lipid Molecule / Å^2
L-DPPC	92.6	77.01	4.2	51.8
F-DPPC	110.6	75.3	8.1	50.8
L-DPPC/F-DPPC(1:1)	99.3	75.9	6.4	49.9

The onset of the gas-LE phase transition in the lipid monolayers takes place at higher area in the case of F-DPPC (110 Å^2 molec^{-1}) compared to that in DPPC. This means that the interaction between chains start earlier than DPPC. This is understandable[198], considering the existence of polar C-F bond close to the water surface in the expanded monolayer. DPPC lacks this additional dipole and its chains are more likely to avoid contact with the subphase underneath. The weakening of cohesive forces resulting from substitution of hydrogen at *sn-2* terminus by the bigger fluorine atom, could also lead to occupation of higher area per molecule.[125] The coexistence region appears as a plateau

_____

similar to the one found for DPPC, but at relatively higher surface pressures (~ 8.1 mN m^{-1} compared to 4.4 mN m^{-1}) than DPPC.
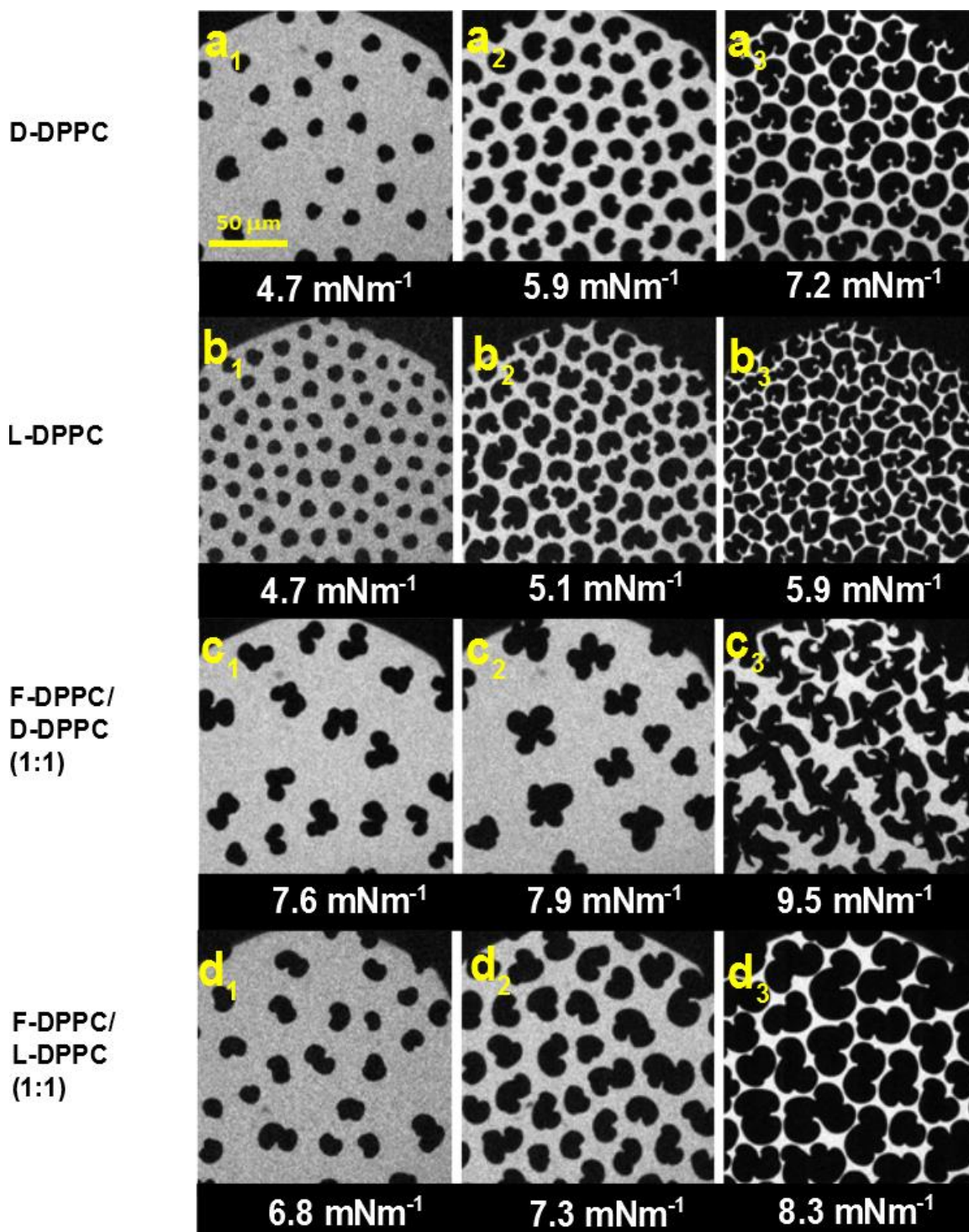
Figure 4.9: LC-domains of homochiral DPPC and their mixtures with F-DPPC visualized by using 0.01% RH-DHPE.

The conversion of the LE to LC phase for 1:1 mixtures of fluorinated and unfluorinated lipids begins at ~ 6.4 mN m^{-1} that represents an average of the surface pressures of the pure systems. Both DPPC enantiomers behave in a similar fashion, besides slightly higher surface pressures recorded at the end of the coexisting region for D-DPPC. The effect is also visible in the mixtures, where an equimolar mixture between F-DPPC and D-DPPC is a *quasi-racemate*. The results are summarized in Table 4.1.

Effect of Phospholipid Chirality on LC-Domains of Lipid Mixtures

The condensed domains visualized by epifluorescence microscopy of DPPC, F-DPPC and their 1:1 mixtures are shown in Fig. 4.9. The curling direction of propellers is reflective of the lipid chirality and indicates the orientation of tilted chains.[174,199,200] The domains attain the shapes of kidney beans in an equimolar mixture of DPPC enantiomers.[39] In the mixtures with lower proportions of L-DPPC, the behavior is dominated by F-DPPC and irregular shaped domains were observed in 10:1 and 5:1 mixtures of the two lipids (not shown). Spanner shaped domains are observed in equimolar mixture of D- and L-DPPC studied earlier by BAM are representative of the chiral phase separation originating from the electrostatic interaction of normal spontaneous polarization with electric quadrupole density.[201] The similar effect was observed for the racemic mixture of D-DPPC and L-FDPPC, where initially twinned domains[202] attained butterfly like geometries that finally evolved into more complex multi-lobed 2D-structures (Fig. 4.9c).

4.1.2 Interactions of Amphiphilic and Polyphilic Polymers with F-DPPC Monolayers

Effect of Perfluoroalkylation: GP vs. FGP

Block copolymers (depending upon the type and organization of blocks) can assemble into several types of aggregates and hence show a diversity in terms of applications.[24,25,32,116,203] The block copolymers containing perfluorinated moieties are polyphilic owing to these additional segments, which are neither hydrophilic nor lipophilic.[30] Hence they impart certain interesting properties to the polymers.[30,31,39,44,45] The hemifluorinated dibranch polymers form stable fluorous emulsions because they are capable of fully inhibiting Oswald Ripening.[41] In order to harness the fluorophilicity

of these polymers in medicine and pharmacy, it is important to understand the interaction of these polymers with biological membranes or their simplified mimics.[46]

Time-dependent Adsorption of Polymers to Preformed Lipid Monolayers

The monolayer-bilayer equivalence pressure is about 30 mN m^{-1}. The polymers capable of penetrating into the monolayers with π-values above 30 mN m^{-1} can actually insert into the cell membranes – a significantly important phenomenon if polymers act as a sealant, or a carrier of drugs, or as an agent for gene transfection. Additionally, they could form channels or pores and cause cell leakage, or could induce *apoptosis*, leading to cell death.[111] There is plethora of studies available on the role of block copolymers in biomimetic chemistry.[111,112,114,115] The ABA triblock copolymers consisting of PEO-PPO-PEO blocks, commonly known as Poloxamers or Pluronics produce toxic degradation products on sonication[37], and provide a basis for structural modifications for applications in pharmacy or industry.[36,44,45,116,204] End capping of the amphiphilic triblock copolymers with perfluorinated moieties[40] changes the interactions with phospholipid bilayers[46], or monolayers.[205] Time-dependent adsorption of polymer from the subphase allows the determination of exclusion pressure (π_e) or maximal insertion pressure (MIP). The monolayers being simplified models, merely give partial information about the interactions with membranes, which are a complex mixture of lipids and proteins.

The adsorption of amphiphilic polymer molecules injected into the subphase to lipid monolayers is most likely caused by the presence of hydrophobic blocks. At low surface pressure, when lipid surface concentration is low, polymers suffer less hindrance in reaching the surface. The interaction of PGMA units with charged lipid head groups enhances the capability of these polymers to penetrate the monolayers. The hydrogen bonding between lipid head groups and PGMA units reduces the headgroup repulsions. Beside this, the PPO block swims upwards to the surface and occupies the space between the lipid molecules. The adsorption of the polymer pushes the expanded lipid molecules into more densely packed condensed phase. Fig. 4.10 shows the adsorption kinetics after polymer injection into the subphase and a plot to determine the maximal insertion or exclusion pressure. All the experiments were allowed to run for sufficient

time, until the surface pressure stayed constant. When polymers were injected underneath the bare air/water interface, the maximum surface pressure exhibited by GP and FGP were 13 mN m^{-1} and 24 mN m^{-1}, respectively. Hence, FGP has higher surface activity compared to GP that lacks fluorophilic end capping. At low F-DPPC concentration when it is in the LE phase, the surface is partly covered with lipid molecules and poses a hindrance to polymers reaching the surface, especially when fluorinated terminal of the fatty acid chain loops towards the interface. This leads to a reduction in $\Delta\pi$ values. The polymer concentration in the subphase, that is, 200 nM, is far below the critical aggregation concentration.[40] For π_{ini} < 8.1 mN m^{-1}, the extent to which F-DPPC molecules are pushed from expanded to condensed phase is directly dependent on polymer content on the surface.
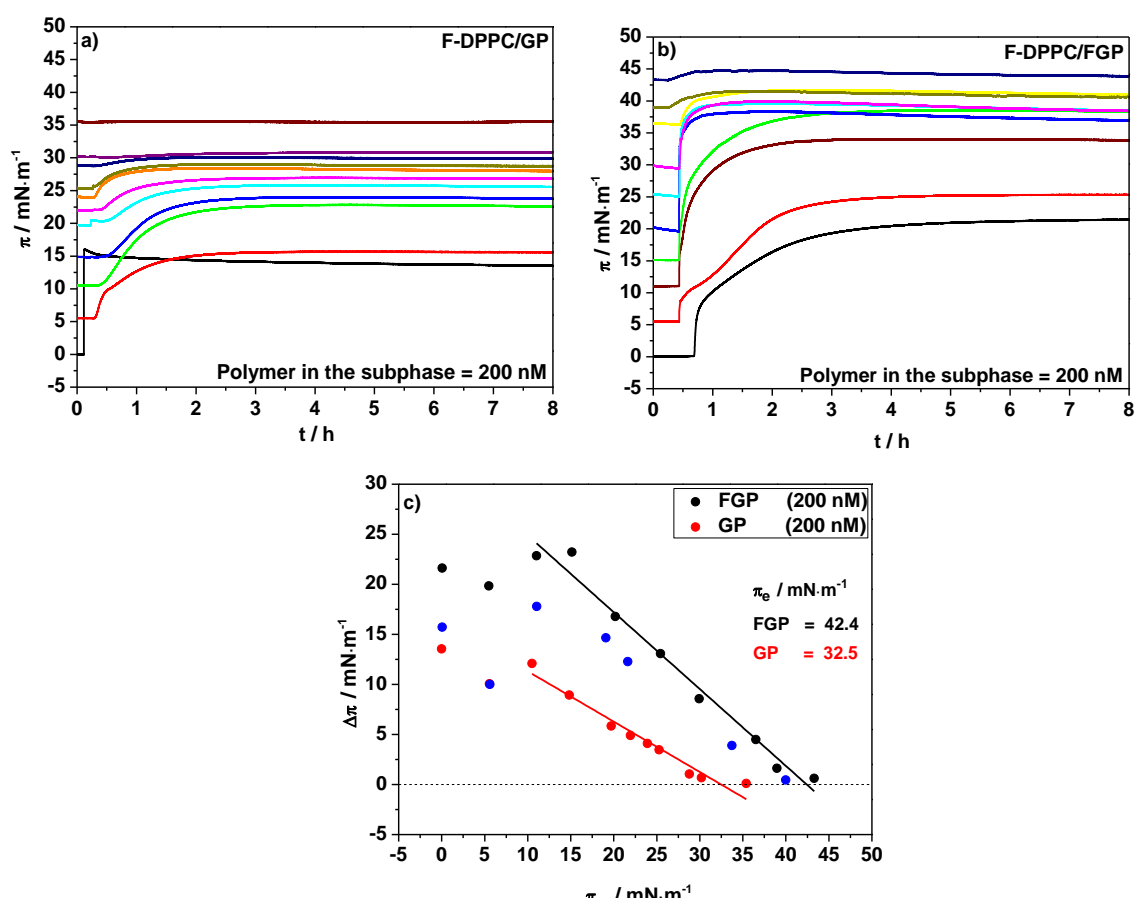
Figure 4.10: Time-dependent adsorption of polymers to F-DPPC monolayers spread at different initial pressures a) 200 nM GP; b) 200 nM FGP; c) Plot of $\Delta\pi$ vs. π_{ini} for FGP and GP (The blue circles show the adsorption of 100 nM FGP from the subphase).

At higher initial surface pressure, more and more lipid exists in the condensed phase and limits the polymer insertion. For π_{ini} > 30 mM m^{-1}, no polymer insertion occurred for GP and the surface pressure virtually remains unchanged after polymer injection. For FGP,

_____

however, the polymer is excluded from F-DPPC monolayers at a much higher surface pressure ($\sim$ 43 mN m^{-1}). For a reduced polymer concentration (100 nM) in the subphase, the maximal insertion pressure of FGP ($\sim$ 40 mN m^{-1}) is similar to that of DPPC.[205] Thus, the presence of the fluorine atom in F-DPPC does not alter significantly the interactions with the polymers. The anchoring of perfluorinated chains and their affinity for air, allows them to prevail and persist in the lipid monolayers at surface pressures greater than 30 mM m^{-1}. In conclusion, perfluoroalkylation supplements polymer's ability to stay in the lipid phase up to the higher π-values than the unfluorinated analog.

Compression Isotherms and Epifluorescence Microscopy

The π-A isotherms of the co-spread mixtures of lipid and polymers show an increase in area per lipid molecule with the increase in polymer content for both GP and FGP (Fig. 4.11 & Table 4.2).
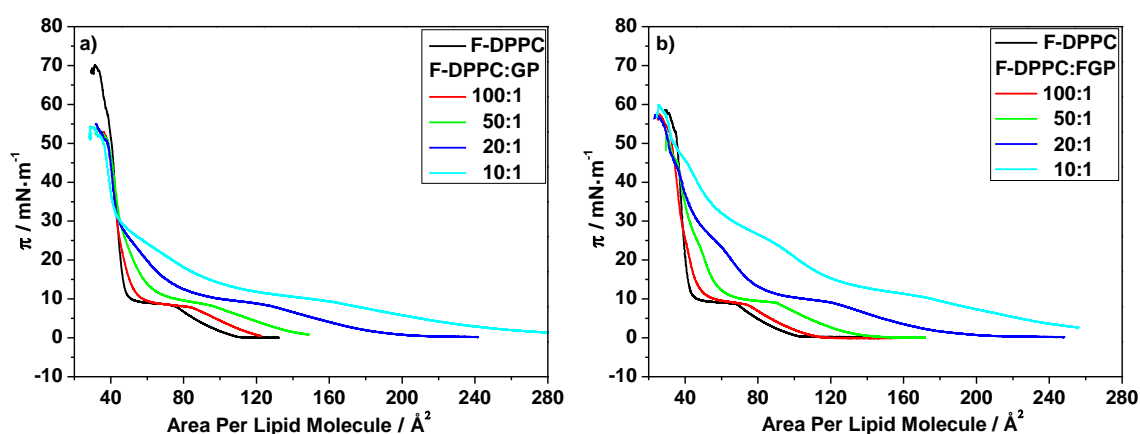
Figure 4.11: Compression isotherms for a) F-DPPC/GP; and b)F-DPPC/FGP mixtures.

The LE/LC coexisting region moves to higher areas (per lipid molecule) as well as the higher pressures, revealing that the lipid enters into LC phase at higher surface pressures under the influence of the polymer. For only 1% polymer, the area per lipid is greater in the presence of GP than FGP at low lateral pressures of the monolayers, when the lipid is in the LE phase only. The impact is reversed for higher polymer content or higher surface pressures. This indicates attainment of different regimes by FGP and GP on the surface. GP can adopt a fully stretched pancake arrangement on the water surface, but for FGP, the F9 chains are directed in air, away from polar subphase, disallowing FGP to expanse the available surface due to greater looping of PGMA chains into water.

_____

There is a second transition visible for FGP at $\pi > 25$ mNm^{-1} due to exclusion of the PPO part of FGP, which is followed by full polymer exclusion at pressure of 42.5 mN m^{-1}. This polymer transition does not exist for GP, which is excluded just above 30 mN m^{-1}. This suggests that end capping impedes the immediate polymer exclusion, a trait not shown by the hydrophobic PPO block alone. This will be discussed in the proceeding section on semitelechelic polymers GF40 and GF14. The exclusion pressure obtained from compression isotherms are similar to those arrived at from the adsorption studies.

Table 4.2: Shift in areas available per lipid molecule(ΔA) in a monolayer after FGP and GP addition recorded at different surface pressures.

Lipid/ polymer ratio (moles)	ΔA / Å^2 molec^{-1} (F-DPPC) at various surface pressures (π)							
	4 mN m^{-1}		9 mN m^{-1}		15 mN m^{-1}		25 mN m^{-1}	
	F-DPPC/ GP	F-DPPC/ FGP	F-DPPC/ GP	F-DPPC/ FGP	F-DPPC/ GP	F-DPPC/ FGP	F-DPPC/ GP	F-DPPC/ FGP
100:1	12.6	7.9	4.2	0.9	3.5	3.9	0.6	1.1
50:1	32.0	29.5	27.3	28.5	11.4	13.5	3.9	7.4
20:1	71.3	73.0	58.0	60.0	23.8	33.0	6.8	17.4
10:1	133.5	152.4	104.2	122.3	47.2	80.2	13.3	47.4

FM images recorded for F-DPPC/FGP and F-DPPC/GP systems look almost alike (Fig. 4.12). The fractal domains grow into larger aggregates in 100:1 and 50:1 mixtures. For mixtures containing greater amounts of polymer, more organized bean shaped domains are formed. Small amounts of polymers inhibit the growth of lipid 2D crystals hence faceting or branching is augmented. With further polymer addition, domain thinning occurs, because a significant part of the surface area is covered by polymer, and lipid molecules are segregated into discrete regions. In addition, with increase in polymer content in the mixture, the polymer diffusion away from the boundaries of the domains is also reduced. Polymers at low surface pressure are lying nearly flat on the surface of water in a well-known pancake regime. Upon compression, the hydrophilic units loop into water, giving rise to mushroom and brush morphologies. During this process, the lipid molecules are pushed together to nucleate. The polymer molecules enclose the lipid area. Roughly, each lipid confinement acts as nucleation site. The stress produced through compression is borne by the polymers and later reaches the expanded lipid

islands and force them to condense. Here, the well-known lineactant behavior of polymers is not experienced.
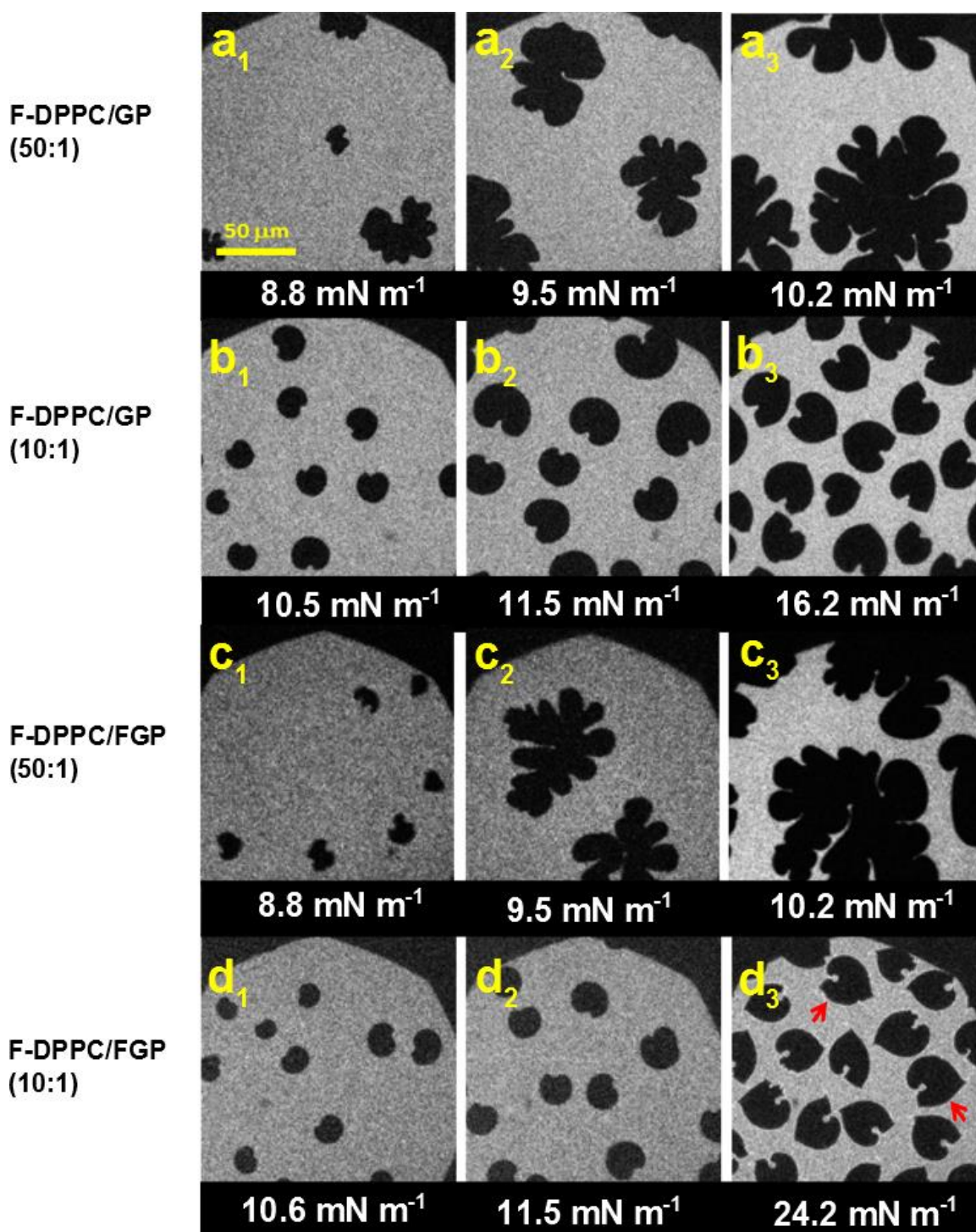
Figure 4.12: FM-images for a) F-DPPC/GP (50:1); b) F-DPPC/GP (10:1); c) F-DPPC/FGP (50:1) and d) F-DPPC/FGP (10:1) co-spread monolayers containing 0.01% RH-DHPE. The corona around the domains in d$_3$ is indicated by red arrows.

_____

A corona appears around the condensed domain with FGP at $\pi \sim 24$ mN m^{-1}, proving the accumulation of dye at the edges of domains despite exclusion from the densely packed lipid molecules (indicated by red arrows in Fig. 4.12d$_3$). This point towards the slow diffusion of FGP from the domain boundaries, which hinders the movement of fluorescent label towards the bulk. Apparently, for a fastly moving interface, the line tension does not come into play and the only operating force is the electrostatic repulsion between lipid molecules, which promotes fractal growth.
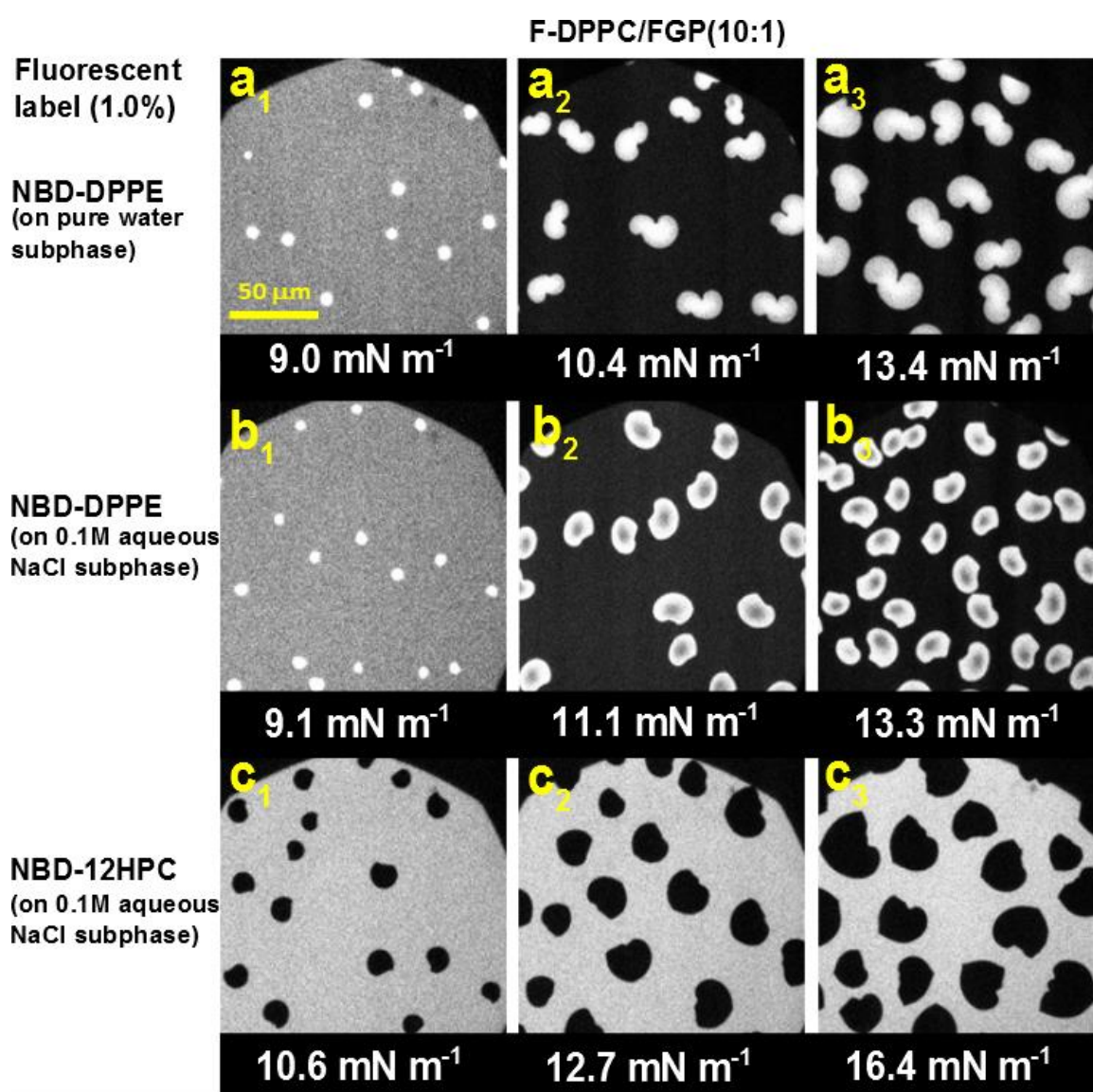
Figure 4.13: FM-images for F-DPPC/FGP (10:1) mixtures in the presence of NBD labelled probes and on different subphase types a) NBD-DPPE on pure water subphase; b) NBD-DPPE on 0.1M aqueous NaCl subphase and b) NBD-12HPC on 0.1M aqueous NaCl subphase (In each case 1.0% of the fluorescent label was added to the mixture)

_____

The epifluorescence microscopy images recorded in the presence of NBD-DPPE probe (Fig. 4.13a) clearly show that the dye does not diffuse away from the domain edges in the monolayer of F-DPPC/FGP (10:1) mixture. The domains are white and peanut shaped on pure water subphase. The background is increasingly darkened upon compression, indicating that the dye is staying in the LC lipid phase and not diffusing into the bulk phase. The domain edges represent a hint of grey, showing relatively lesser dye proportion in this region compared to the core of the LC domain. It has been observed in this work (Fig. 4.4) that the change of subphase from pure water to 0.1M aqueous sodium chloride alters the interactions between the dye label and F-DPPC in the lipid monolayers, and a reversal of contrast is seen, showing the greater presence of dye at the boundaries of LC domains than in the core. The measurements carried out for the monolayers of F-DPPC/FGP (10:1) mixture on 0.1M NaCl subphase (Fig. 4.13b) endorses the same.

On the salt subphase, the bean-shaped LC domains have white edges and greyish core, representing a change in dye distribution compared to that seen earlier on pure water subphase. This behavior is specific to NBD-DPPE, because when the dye label is changed to NBD-12HPC, that is, the head labeled lipid probe, the dye is expelled from the LC domains and black domains are seen. This proves that NBD-DPPE bearing a negatively charged phosphate group responds to the presence of salt in the subphase and as a result, the interactions between the lipid and the dye label are altered.

Effect of PGMA Block Length in Semitelechelic Polymers: GF40 vs GF14

It was seen from the comparison between FGP and GP that there was a second transition in the pressure area isotherms above 25 mN m^{-1} that reflected the mushroom-brush transition of the polymer. This transition was related to the impact of the exclusion of PPO blocks, while the F9 segments retained in the monolayers. In order to further investigate this effect, the semitelechelic polymers devoid of PPO blocks were used. These polymers possessed perfluoroalkyl segments attached with two different lengths of PGMA units. GF14 (*i.e.* PGMA$_{14}$-F$_9$) resembles PGMA$_{20}$-F$_9$ part of FGP. The hydrophilicity of GF40 is similar to that of FGP. However, there is only one F9 chain attached with PGMA block in GF40.

_____

Time dependent Adsorption of Polymer to Preformed Lipid Monolayers
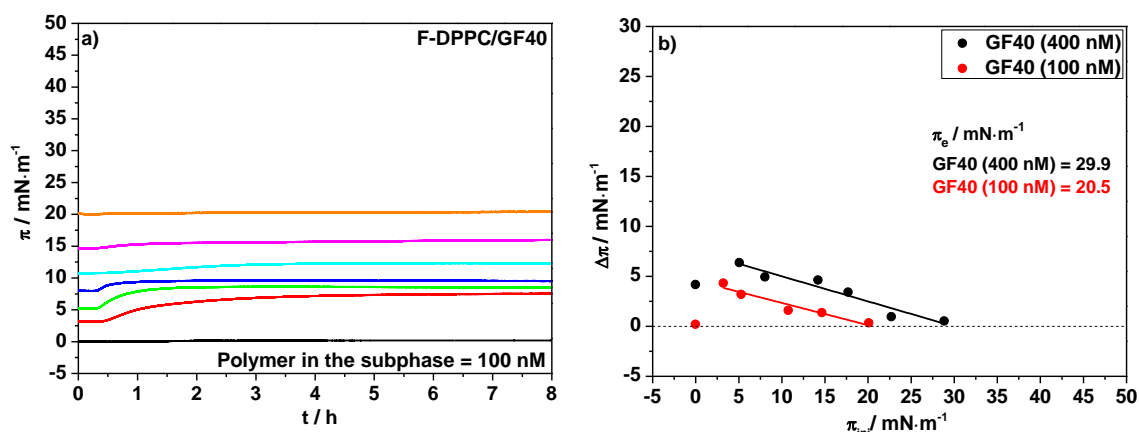
Figure 4.14: a) Effect of subphase concentration of GF40 on its adsorption to F-DPPC monolayer spread at different initial pressures; b) Plot of $\Delta\pi$ vs. π_{ini} for GF40.

It has been reported previously that the PGMA blocks are not very hydrophilic and their enlargement imparts higher surface activity[39]. These polymers are however less surface active in comparison to FGP as well GP.
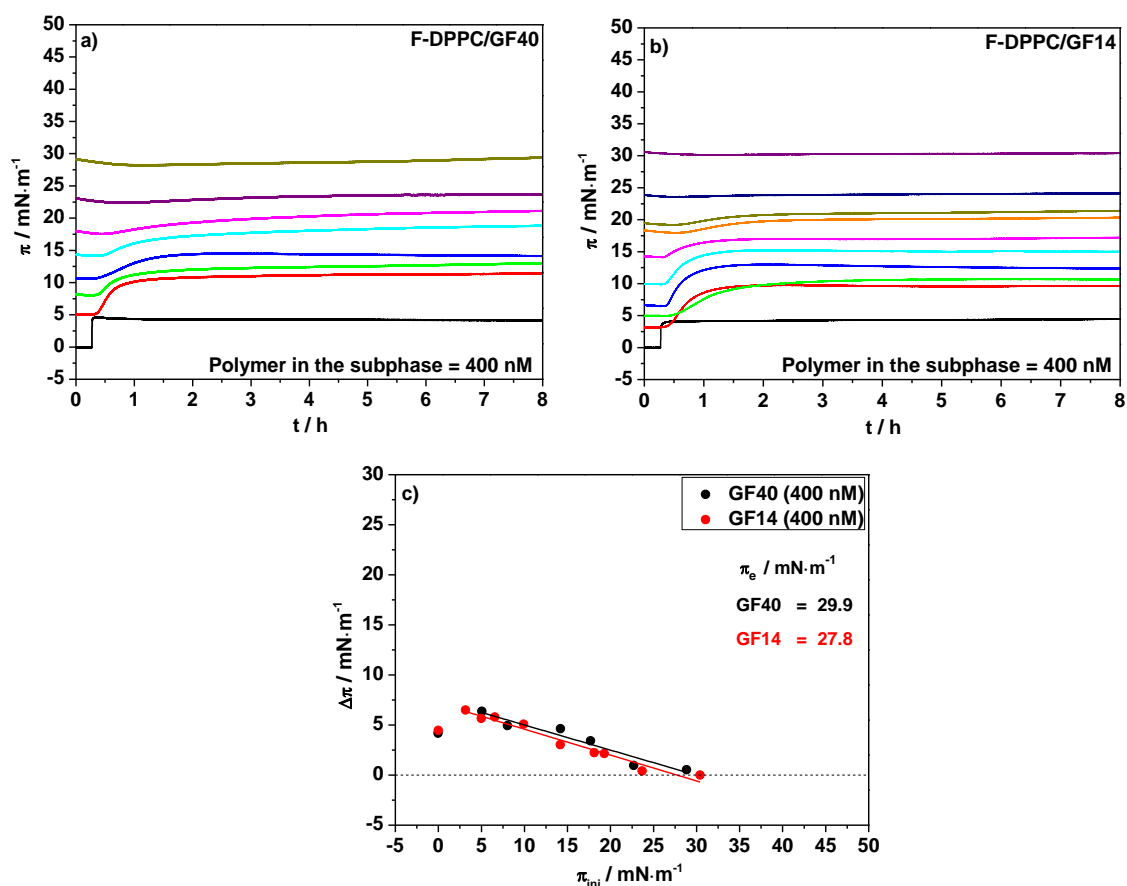
Figure 4.15: Time-dependent adsorption of polymers to F-DPPC monolayers spread at different initial pressures a) 400 nM GF40; b) 400 nM GF14; c) Plot of $\Delta\pi$ vs. π_{ini} for GF40 and GF14.

_____

For 100 nM of GF40 injected into the pure water subphase, the surface pressure remains almost zero (Fig. 4.14). A higher surface activity of GF40 is promoted due to the presence of lipid on the surface. This trait emerges from the possible interaction of -OH groups in PGMA with the head groups of F-DPPC. Here higher polymer concentrations were utilized (400 nM) due to lower surface activity of these polymers in comparison to FGP and GP. The maximal insertion pressures (π_e) obtained for GF14 and GF40 were 28 mN m^{-1} and 30mN m^{-1}, respectively. However, there is very little insertion of polymers above a surface pressure of 20 mN m^{-1} (Fig. 4.15 a & b). Only negligible changes in $\Delta\pi$ values are observed at later stages, when the measurements are continued to run for about 20 hours.

Compression Isotherms and Epifluorescence Microscopy

The pressure-area isotherms for co-spread F-DPPC/GF40 and F-DPPC/GF14 mixtures shown in Fig. 4.16 (a & b) are similar to those reported for the mixtures of these polymers with L-DPPC.[39]
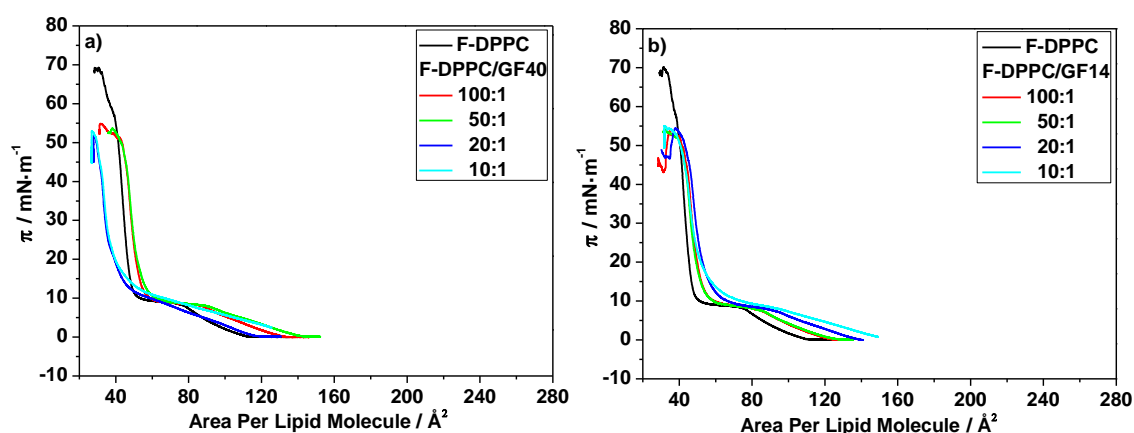
Figure 4.16: Compression isotherms for a) F-DPPC/GF40; and b) F-DPPC/GF14 mixtures.

The magnitudes of shifts in areas are less than those observed for FGP and GP. The changes are more systematic for GF14. The negative ΔA values are exhibited by the co-spread 20:1 and 10:1 mixtures between F-DPPC and GF40. A plausible explanation for this observation is the enlargement of hydrophilic blocks, which makes this polymer more water-soluble and enhances its capacity to self-assemble into aggregates. Upon polymer exclusion from the monolayer, the bound lipid is likely to submerge along with it, reducing the lipid content on the surface. For 10% GF40, the plateau representing the

_____

co-existing LE/LC phases of lipid also starts to disappear, indicating a reduced ability to form condensed domains. Probably the insertion of perfluorinated chains, which are stiffer, promotes the formation of liquid ordered domains or less condensed domains.

Table 4.3: Shift in areas available per lipid molecule (ΔA) in a monolayer after GF40 and GF14 addition recorded at different surface pressures

Lipid/ polymer ratio (moles)	ΔA / $Å^2$ $molec^{-1}$ (F-DPPC) at various surface pressures (π)							
	4 mN m^{-1}		9 mN m^{-1}		15 mN m^{-1}		25 mN m^{-1}	
	F-DPPC/ GF40	F-DPPC/ GF14	F-DPPC/ GF40	F-DPPC/ GF14	F-DPPC/ GF40	F-DPPC/ GF14	F-DPPC/ GF40	F-DPPC/ GF14
100:1	16.1	10.8	0.8	7.4	5.1	5.4	4.2	3.9
50:1	24.4	11.7	4.0	6.3	6.6	5.0	4.6	3.2
20:1	3.2	23.3	-2.8	13.3	-4.4	9.8	-9.6	6.3
10:1	22.2	35.4	6.7	23.4	-1.4	10.8	-8.8	4.5

In epifluorescence microscopy, again the flower-like domains are observed with 100:1 and 50:1 F-DPPC/polymer mixtures (Fig. 4.17a), showing a resemblance to the effects produced by FGP and GP in the lipid monolayers.
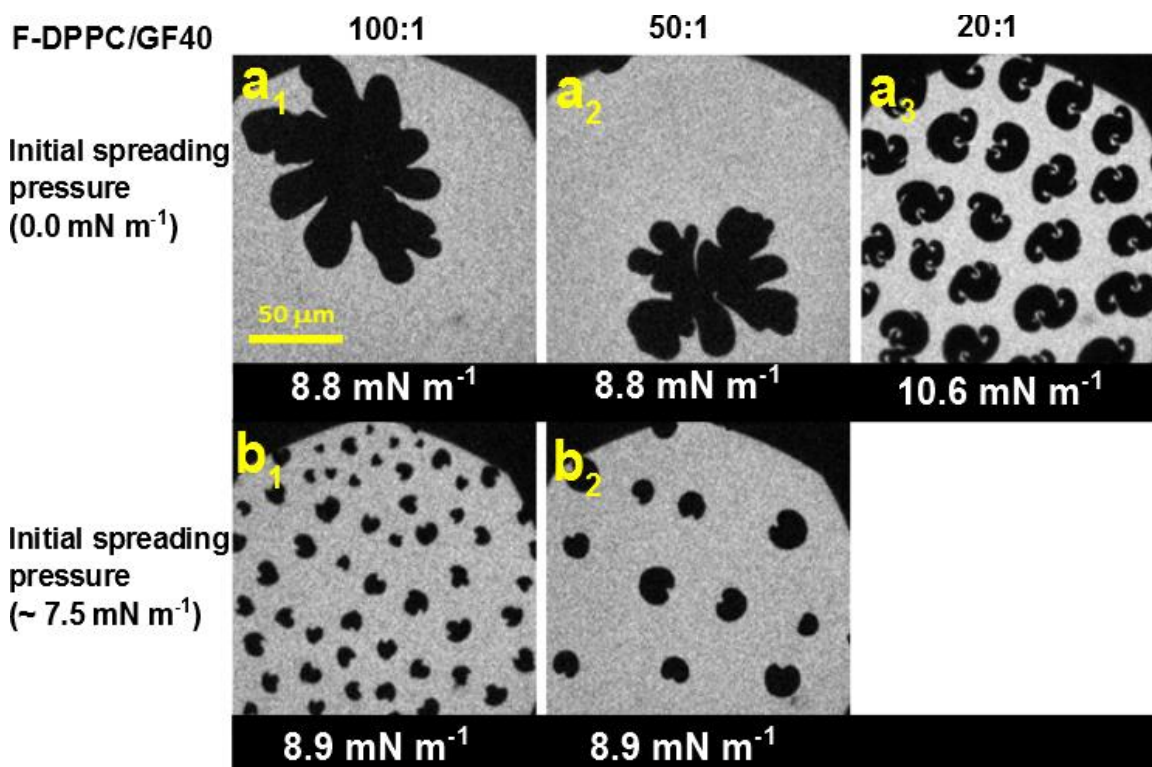
Figure 4.17: FM-images for a) F-DPPC/GF40 mixtures starting from gas phase in a monolayer; and b) F-DPPC/GF40 mixtures starting from LE/LC coexistence phase in a monolayer. In each case 0.01% RH-DHPE was present.

_____

The reduction in line tension above 5% GF40 in the lipid/polymer mixture, causes the thinning of domain boundaries, but no special patterns appear like those observed with DPPC earlier[39]. The start of compression at $\pi > 8.0$ mN m^{-1} through spreading of more lipid produces bean shaped domains (Fig. 4.17b). Increase in number of nucleation sites and limited area available for growth are responsible for such behavior.

An agitation in a three dimensional system favors the secondary nucleation.[206] The surface of already existing crystal acts a breeding ground for aggregation. These weakly bound crystallites are detached from the surface upon agitation. It is, however, difficult to apply the same to a compressed two-dimensional monomolecular layer. The polymer molecules in the case of Gf40 are not able to limit the access of lipid to already nucleated 2D crystals. Similar behavior is observed for GF14 (not shown).

Effect of the Nature of Hydrophilic Block: GF40 vs EF44

As indicated earlier, the PGMA units are not very hydrophilic and tend to enhance surface activity in the case of semitelechelic polymers. In addition, attachment of the perfluorinated chain makes them more capable of staying at the surface and insert into the lipid monolayer. In order to investigate if the hydrophilic block has a significant influence on the insertion of perfluorinated part, a comparative analysis is provided for GF40 and EF44. In the latter, the hydrophilic block consists of ethylene oxide units. The homopolymers of ethylene oxide (PEO) show some surface activity but with the increase in surface concentration, the extension of polymers into the subphase as loops and tails becomes prominent[207]. The study also indicates that at low apparent surface concentration of the polymer, the polymer is stretched fully on the surface and looping occurs only after a critical value is exceeded.

Time-dependent Adsorption of Polymers to Preformed Lipid Monolayers

The exclusion pressure π_e obtained for EF44 is notably lower than π_e for GF40 (Fig. 4.18). The change in surface pressure ($\Delta\pi$) is highest at $\pi_{ini} \sim 2.0$ mN m^{-1}, and gradually decreases with increasing presence of lipid, until the polymer is unable to insert into the lipid monolayers. At smaller initial spreading pressures of the lipid monolayer, the $\Delta\pi$ values recorded for EF44 are higher than those obtained for GF40. The smaller cross-

_____

sectional area of PEO segments and an ease with which they fit in water structure are responsible for this behavior.[208] After π_{ini} = 15.0 mN m^{-1}, EF44 is rapidly excluded from F-DPPC monolayers, whereas GF40 prevails. The π_e values obtained for GF40 and EF44 differ by a magnitude of 8 mN m^{-1}, which highlights the impact of the nature of the hydrophilic units in membrane insertion capability.
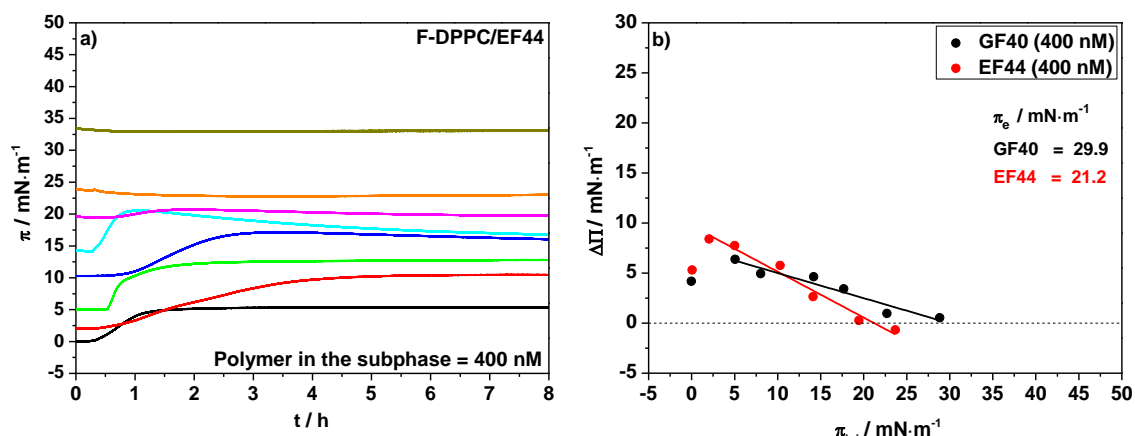
Figure 4.18: Time-dependent adsorption of 400 nM EF44 to F-DPPC monolayers spread at different initial pressures and b) Plot of $\Delta\pi$ vs. π_{ini} for GF40 and EF44.

Compression Isotherms and Epifluorescence Microscopy
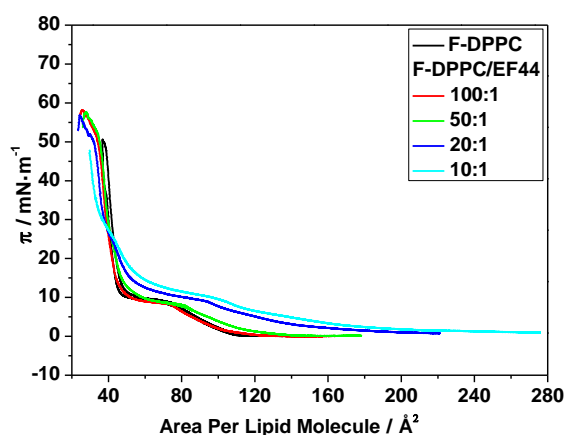
Figure 4.19: Compression isotherms for F-DPPC/EF44 mixtures.

The pressure-area isotherms collected for mixtures containing different ratios of F-DPPC and EF44, co-spread on the water surface are given in Fig. 4.19. With increased polymer content, the lipid LE-LC transition is shifted to higher areas and a significant impact is only observed for 20:1 and 10:1 lipid/polymer mixtures. For smaller amounts of polymer in the lipid/polymer mixtures, the ΔA values for EF44 are lower than those obtained for GF40. The balance is shifted in favor of EF44 for higher polymer content. The overall

effect is due to differences is the size, aqueous solubility and hydrophobicity of GMA and EO units.[209] The binding of PGMA units to lipid head groups allow some lipid to sub-merge along with the polymer. The exclusion of EF44 occurs at 23 mN m^{-1}, which is close to the value reached during the adsorption study.

Table 4.4: Shift in areas available per lipid molecule (ΔA) in a monolayer after GF40 and EF44 addition recorded at different surface pressures.

Lipid/ polymer ratio (moles)	ΔA / Å^2 molec^{-1} (F-DPPC) at various surface pressures (π)							
	4 mN m^{-1}		9 mN m^{-1}		15 mN m^{-1}		25 mN m^{-1}	
	F-DPPC/ GF40	F-DPPC/ EF44	F-DPPC/ GF40	F-DPPC/ EF44	F-DPPC/ GF40	F-DPPC/ EF44	F-DPPC/ GF40	F-DPPC/ EF44
100:1	16.1	-2.0	0.8	-11	5.1	-2.0	4.2	-2.5
50:1	24.4	7.5	4.0	-4.7	6.6	1.1	4.6	-1.2
20:1	3.2	37.9	-2.8	21.8	-4.4	5.9	-9.6	-1.0
10:1	22.2	59.3	6.7	32.6	-1.4	11.8	-8.8	0.4
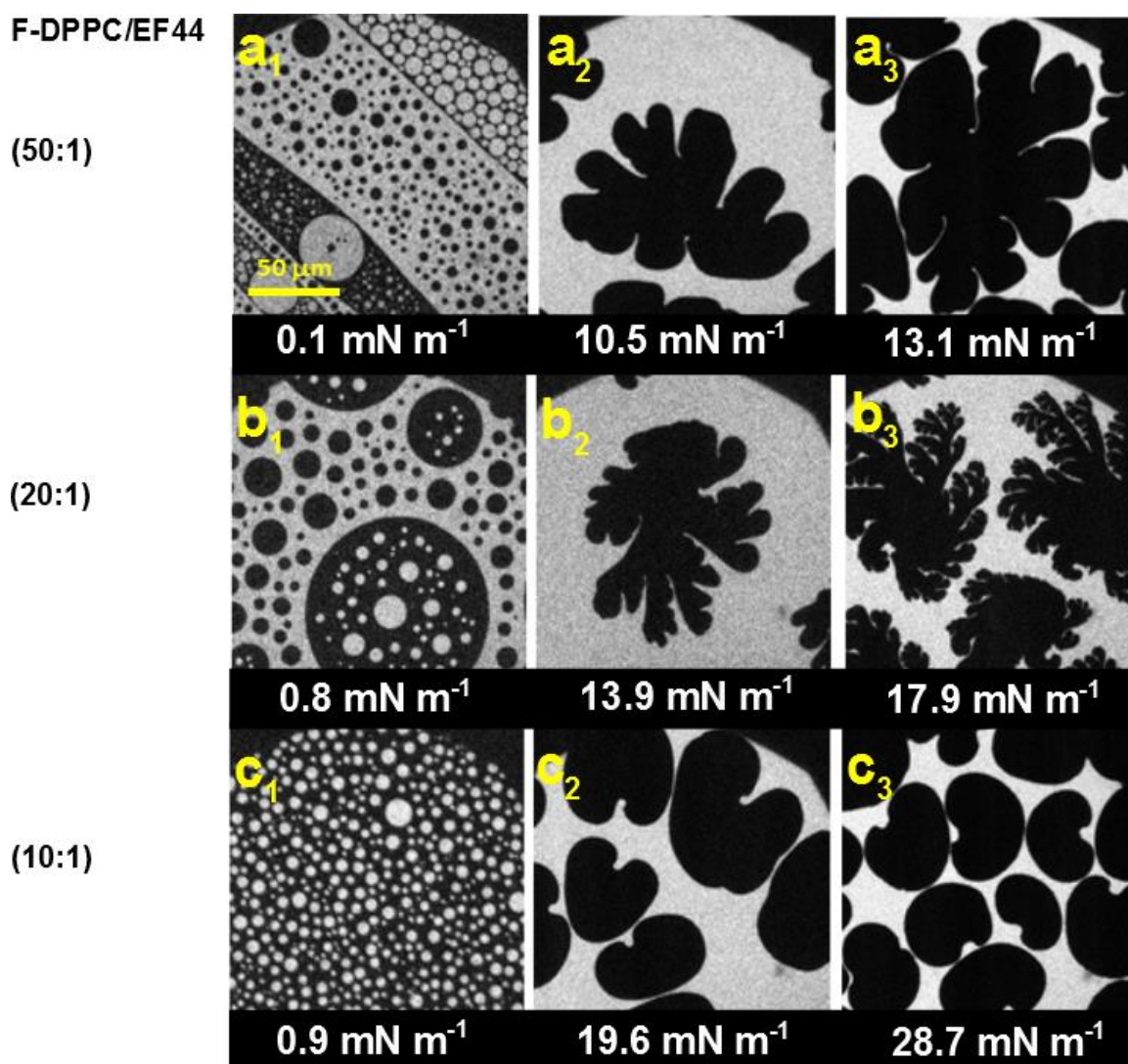
Figure 4.20: LC-domains for co-spread F-DPPC/EF44 mixtures containing 0.01% RH-DHPE.

_____

Effect of Block Sequence / Reversal of Blocks (PFG78)

To understand further the role of perfluorinated moieties on the interactions of polyphilic or triphilic polymers, a polymer with a different block order was investigated. This polymer contains a perfluoroalkyl moiety to which is attached on both sides a diblock of PGMA and PPO. The PPO units on both sides are terminated by n-butyl units. Unlike in FGP, the perfluorinated chain has no free ends in this case, is rigid and attached to PGMA blocks. The possibility of its insertion into lipid monolayers is limited. However, the perfluorinated segment is hydrophobic and prefers to reside in the lipid phase, albeit its lipophobic nature.

Time-dependent Adsorption of Polymers to Preformed Lipid Monolayers

The polymer exhibits low surface activity on a bare water surface. When the surface is covered by a lipid monolayer, an increase in π is observed, indicating insertion into the monolayer (Fig. 4.21). In the coexistence region of LE and LC phases, the penetration is highest and decreases with an increase in lipid density. The polymer's presence forces the lipid to enter into condensed phase by occupying certain surface area.

After injection, the polymer continued to reach the surface with a gradual increase in surface pressure even after 8 hours, so that equilibrium was never reached during the experiment. The insertion of PFG78 is slower than observed for FGP, which is inevitably due to polymer size and the different organization of blocks. On the other hand, the insertion of PPO blocks is facilitated owing to their presence at the polymer's termini. The fluorinated block is flanked by PGMA blocks and it can insert into the monolayers if part of this PGMA block is also pulled into the monolayers, one of the less favorable possibilities. The self-aggregation of PFG78 is possible due to its large size, which can keep all the segments in energetically favorable locations, especially perfluoroalkyl group, which is lipophobic as well as hydrophobic. For instance, if a perfluorinated segment is attached on one side with a hydrophobic block and on the other joined with a hydrophilic block, an intermediate fluorophilic phase may exist.[30] (Fig. 4.22)
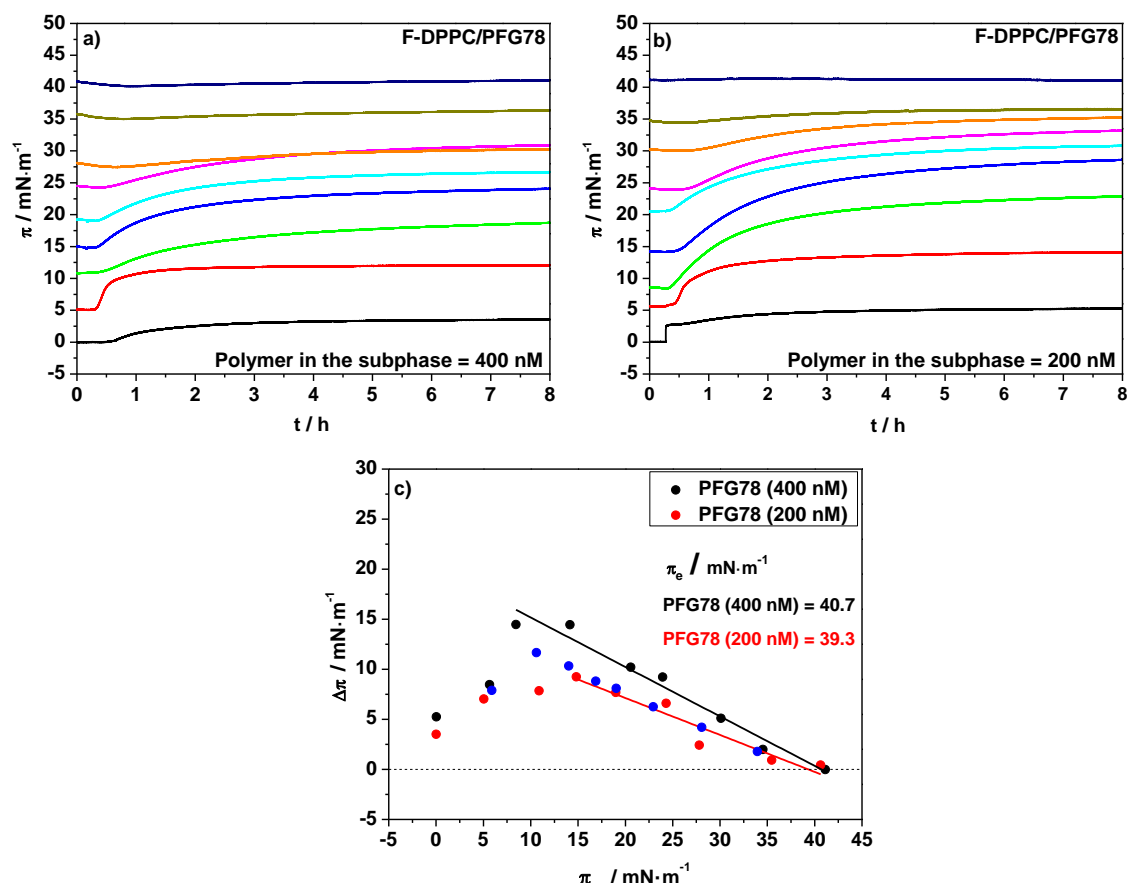
Figure 4.21: Time dependent adsorption of polymers to F-DPPC monolayers spread at different initial pressures a) 400 nM PFG78; b) 200 nM PFG78 ; c) Plot of $\Delta\pi$ vs. π_{ini} for PFG78 (400 nM and 200 nM). The blue circles are for adsorption of 200 nM of PFG78 to pre-existing DPPC monolayers.
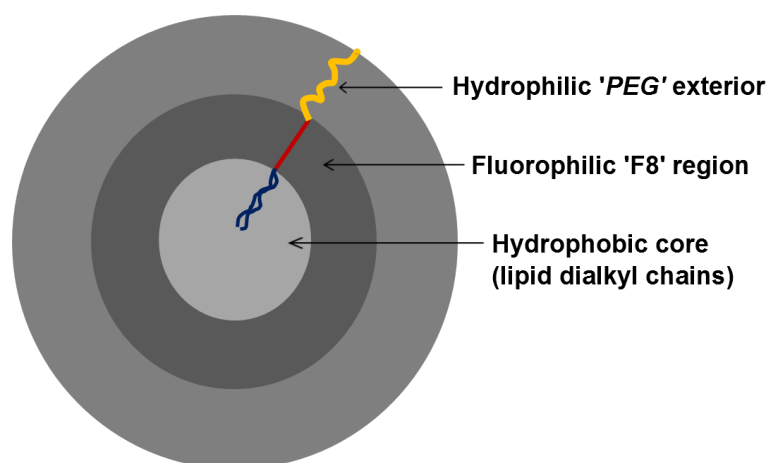
Figure 4.22: Micelles of an ABC type *PEG* derivative comprising of hydrophilic block PEG attached with lipid head group through a perfluorinated alkyl `F8' linker[30].

_____

Compression Isotherms and Epifluorescence Microscopy

The compression isotherms of co-spread PFG78 mixtures with F-DPPC are relatively less shifted compared to those with FGP (Fig. 4.23), despite the fact that PFG78 has both hydrophobic, as well as hydrophilic blocks larger than FGP.
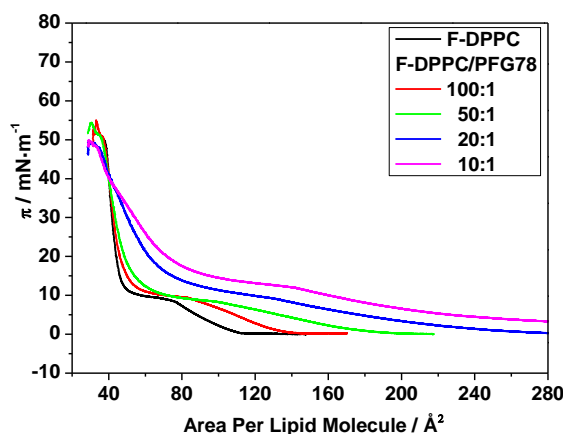
Figure 4.23: Compression isotherms for F-DPPC/PFG78 mixtures.

A closer look at π-A isotherms reveals that the second phase transition takes place at much higher surface pressure that is 35 mN m^{-1} for PFG78. In fact, this transition is hardly visible even for F-DPPC/PFG78 (10:1) mixture.

A comparison between ΔA values obtained for F-DPPC/FGP and F-DPPC/PFG78 co-spread monolayers is given in Table 4.5. When F-DPPC is in LE phase and PFG78 concentration is low in the mixture, the polymer is fully stretched on the surface and its extension into the subphase is minimal. Since the size of PFG78 is greater than FGP, the difference in ΔA values exhibited by mixtures of FGP and PFG78 with F-DPPC is reflective of the difference in the overall lengths of the two polymers.

Above LE-LC phase transition, less surface area is available to the polymers and looping of PGMA blocks into the subphase occurs. When the lipid is already in the LC phase, the differences in areas are due to presence or absence of PPO and perfluorinated segments of the polymers in F-DPPC monolayers. At this stage, the perfluoroalkyl entity is also removed from the surface along with PGMA blocks, simple because PFG78 exhibits much smaller ΔA values in monolayers with $\pi > 25$ mN m^{-1}.

_____

Table 4.5: Shift in areas available per lipid molecule (ΔA) in a monolayer after FGP and PFG78 addition to F-DPPC monolayers

Lipid/ polymer ratio (moles)	ΔA / Å^2 molec^{-1} (F-DPPC) at various surface pressures (π)							
	4 mN m^{-1}		9 mN m^{-1}		15 mN m^{-1}		25 mN m^{-1}	
	F-DPPC/ PFG78	F-DPPC/ FGP	F-DPPC/ PFG78	F-DPPC/ FGP	F-DPPC/ PFG78	F-DPPC/ FGP	F-DPPC/ PFG78	F-DPPC/ FGP
100:1	21.9	7.9	14.2	0.9	4.1	3.9	0.9	1.1
50:1	50.9	29.5	13.9	28.5	7.8	13.5	2.6	7.4
20:1	99.5	73.0	60.4	60.0	28.6	33.0	12.7	17.4
10:1	162.4	152.4	98.9	122.3	49.1	80.2	18.5	47.4

The LC-domains for F-DPPC/PFG78 have fractal patterns of growth with a splitting of the tips as an additional feature (Fig.4.24).
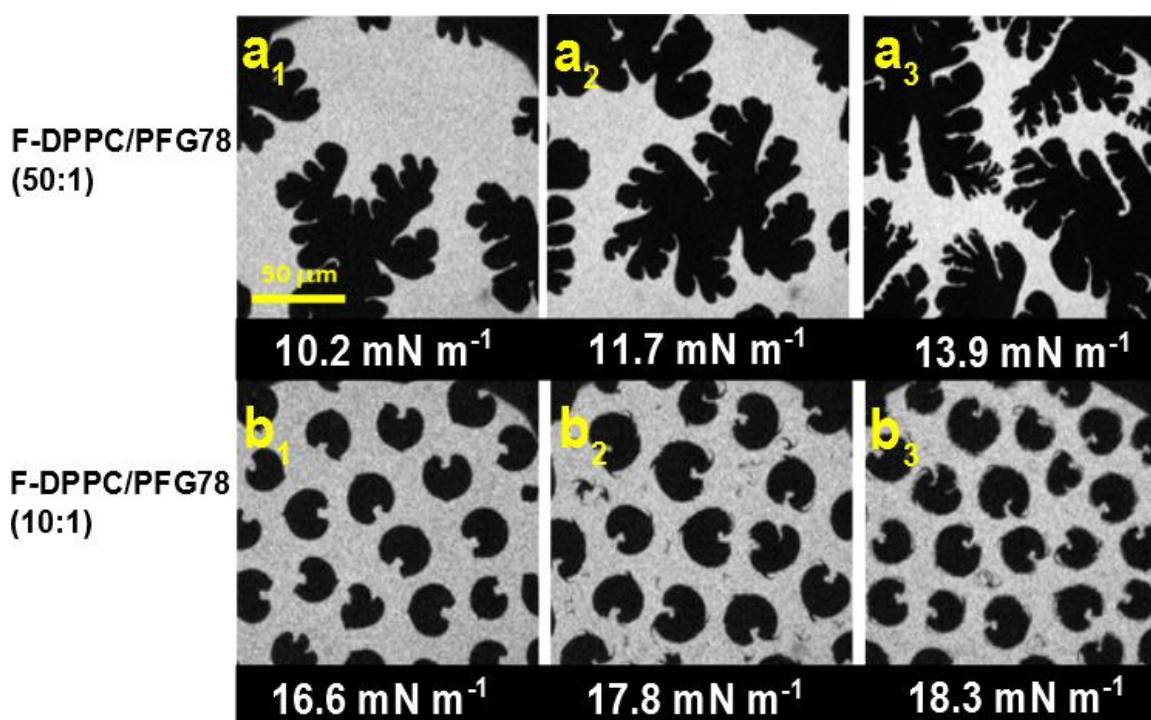
Figure 4.24: LC-domains for co-spread F-DPPC/PFG78 mixtures containing 0.01% RH-DHPE.

The domains get organized with an increase in polymer content in the mixture. Initially existing heart shapes develop fuzzy boundaries at higher surface pressures, indicating a reduction in line tension. In contrast to semi-telechelic polymers, which are lineactant due to perfluorinated chains, the line-active propertyof PFG78 is due to the presence of PPO chains at the LE/LC interface of the lipid.

_____

Adsorption of FGP to F-DPPC/Cholesterol (1:1) Mixed Monolayer

Cholesterol is undeniably amongst the most important lipids existing in cell membranes. Cholesterol addition increases the order in the expanded phase whereas its presence inhibits the condensation of lipid and produces an additional thermodynamic phase that is between fluid and gel states of lipid, so-called liquid ordered phase.[211,212]

Time-dependent Adsorption of FGP to F-DPPC/Cholesterol (1:1) Monolayers

The time dependent adsorption of FGP to a monolayer of 1:1 mixture of FDPPC and cholesterol is shown in Fig. 4.25.
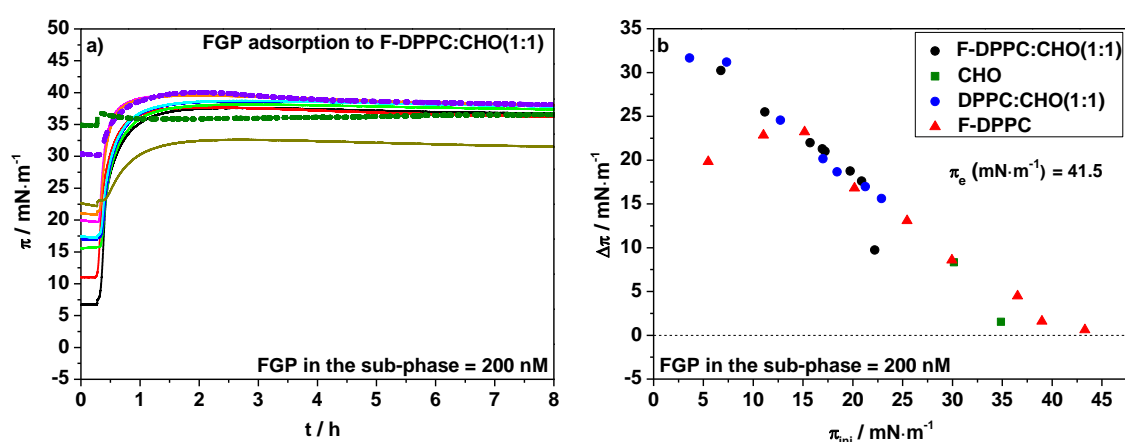
Figure 4.25: (a) Time-dependent adsorption of FGP to F-DPPC/Cholesterol (1:1) mixed monolayers (bold lines) and pure cholesterol monolayers (bold dotted lines) spread at different initial pressures; and b) Plot of $\Delta\pi$ *vs.* π_{ini} for FGP adsorption to F-DPPC/Cholesterol (1:1) monolayers. (For comparison the plots of $\Delta\pi$ *vs.* π_{ini} for F-DPPC, DPPC and DPPC/Cholesterol (1:1) monolayers is also given).

In the presence of cholesterol, a mixed film with the surface pressure above 23 mN m^{-1} could not be obtained through spreading. This is due to fluidization of the monolayers and existence of liquid ordered domains.[213,214] It is however possible to reach the pressure of 35 mN m^{-1} in the case of pure cholesterol monolayer.

At low surface pressure, the polymer inserts more easily into the mixed monolayers compared to a monolayer composed for pure F-DPPC. Similar behavior is observed when FGP is injected underneath a monolayer consisting of an equimolar mixture of L-DPPC and cholesterol (Fig. 4.25b).

The exclusion pressures obtained from the plot of $\Delta\pi$ vs. π_{ini} after extrapolation to $\Delta\pi = 0$ are comparable for pure F-DPPC and F-DPPC/Cho monolayers, but as mentioned above it is not possible for co-spread mixed monolayers to achieve a surface pressure of above

_____

25 mN m$^{-1.}$ This is in accordance with the results of a previously reported study where the initial spreading pressures of above 25 mN m^{-1} are not noticed for DPPC/Cho mixed monolayers[215], It is apparent from Fig. 4.25b that the existence of cholesterol in the expanded lipid phase enhances FGP incorporation into F-DPPC as well DPPC. The surface pressure recorded after FGP incorporation into F-DPPC with and without cholesterol differ by the magnitude of about 10 mN m^{-1} for π_{ini} = 5 mN m^{-1}. The magnitude is markedly reduced for π_{ini} = 10 mN m^{-1}. This is explainable because the monolayer is now more ordered.

Behavior of F-DPPC/Cholesterol Mixed Monolayers

Compression Isotherms and Epifluorescence microscopy

The co-spread films of F-DPPC containing different amounts of cholesterol show a shift in area per lipid molecule, clearly indicating that F-DPPC/Cho monolayers behave differently (Fig. 4.26).
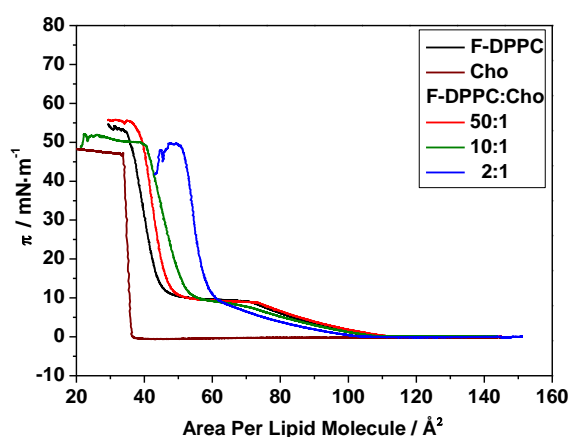
Figure 4.26: Compression isotherms for F-DPPC, Cho and F-DPPC/Cho mixtures.

The plateau representing the co-existing region for LE and LC phases of the lipid smeared-out with the addition of cholesterol and vanished completely in an F-DPPC/Cho (2:1) mixture, reflecting a reduction in packing density. The presence of cholesterol rigidifies the lipid monolayers[215], the isotherms continue to shift to higher areas per F-DPPC molecule with increase in the proportion of cholesterol. The cross-sectional area of cholesterol allows it to fit among the hydrocarbon tails of lipid, while its smaller headgroup, that is a –*OH*, induces hydrogen bonding with the head group.

_____

The interaction of cholesterol with lipid membranes has been reviewed by McMullen *et al.*[211] The cholesterol has condensing effects on the LE phase,. Therefore, it enhances an order in the former giving rise to the L_o-phase. On the other hand, the presence of cholesterol fluidizes the LC phase of the lipid. Consequently, the lipid monolayer exhibits less order.

Table 4.6: Shift in areas available per lipid molecule (ΔA) in a monolayer after Cholesterol addition recorded at different surface pressures

F-DPPC/ Cho ratio (moles)	ΔA / $\mathring{A}^2$ molec^{-1} (F-DPPC) at various surface pressures (π)			
	4 mN m^{-1}	9 mN m^{-1}	15 mN m^{-1}	25 mN m^{-1}
50:1	2.2	-2.2	2.7	2.6
10:1	-2.0	-9.4	6.7	6.2
2:1	-8.1	-8.3	14.0	14.3

The FM-images of the monolayers formed by FDPPC/Cho mixtures are shown in Fig. 4.27. The domain shapes captured at different surface pressures for 50:1 mixture unravel the lineactant role of cholesterol. Thinning, curling and merging of condensed domain takes place during LE/LC coexistence. Similar effects on DPPC domains has been reported by Weiss and McConnell under rapid isothermal compression of the mixed DPPC/Cho monolayers.[216] In their view, cholesterol stabilizes the crystal-liquid interface and the DPPC/Cho system attains the thermodynamic equilibrium. Moreover, a negative effective interfacial free energy is necessary order to separate fluid and condensed domains.

F-DPPC monolayers containing 10 and 33 percent cholesterol, respectively, exhibit circular domains in the gas-LE-coexistence regime. These domains persist up to 6 mN m^{-1}, during which an Ostwald Ripening occurs. Later, the domains start to dissolve above 7.5 mN m^{-1} and disappear at π > 12 mN m^{-1}. This is due to inhibition of condensed phase by cholesterol, as indicated also by the change in shape of the π-A isotherms.
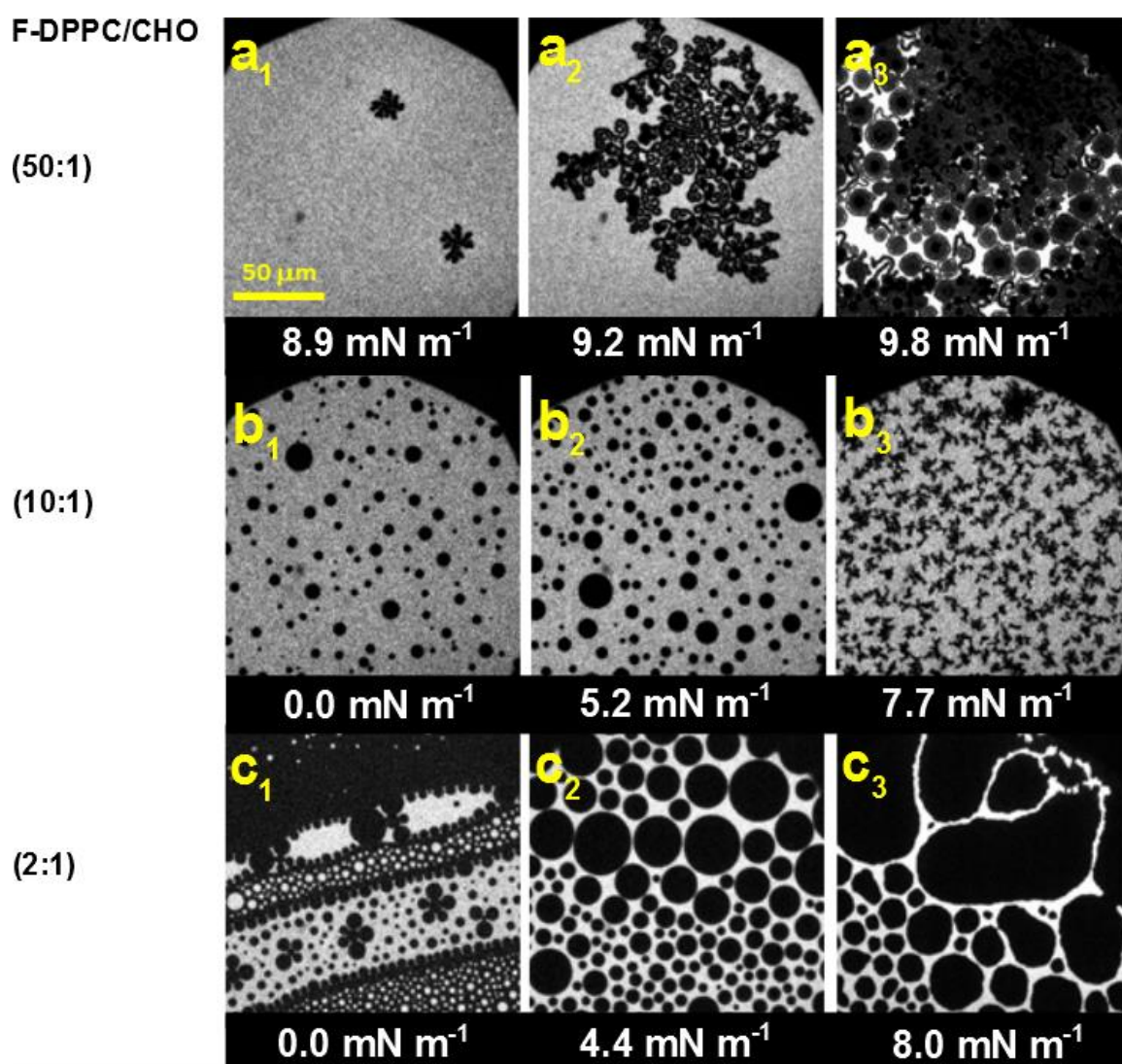
Figure 4.27: FM-images of the monolayers of co-spread F-DPPC/Cholesterol mixtures containing 0.01% RH-DHPE.

Behavior of F-DPPC/FGP (10:1) Monolayers in the Presence of Cholesterol

It has been established in section 4.1.2 that 10% of FGP inhibits fractal domain growth in F-DPPC monolayers. To investigate if FGP could inhibit the domain thinning caused by small percentages of cholesterol in F-DPPC monolayers, the compression isotherms were recorded for co-spread monolayers of the F-DPPC/FGP (10:1) mixtures in the presence of different percentages of cholesterol and phase transitions in the monolayers were observed using epifluorescence microscopy. The FM-images of ternary monolayers are shown in Fig. 4.28. The π-A isotherms (not shown) retain their shape for all mixtures, showing an insignificant effect on the order in these monolayers. Only a slight shift of the lipid phase transition takes place for mixture with 2% cholesterol. These monolayers

exhibit spiral shaped domain, indicative of the line active property of cholesterol, which accumulates at the boundary between LE and LC phases. It is therefore, concluded that FGP could not inhibit the condensing and fluidizing effects produced by the cholesterol in the F-DPPC monolayer.

The perfluorinated moieties in FGP share a common trait of rigidity with cholesterol. They could however, supplement the effects produced by cholesterol provided they are attached with much smaller hydrophilic head.[217]
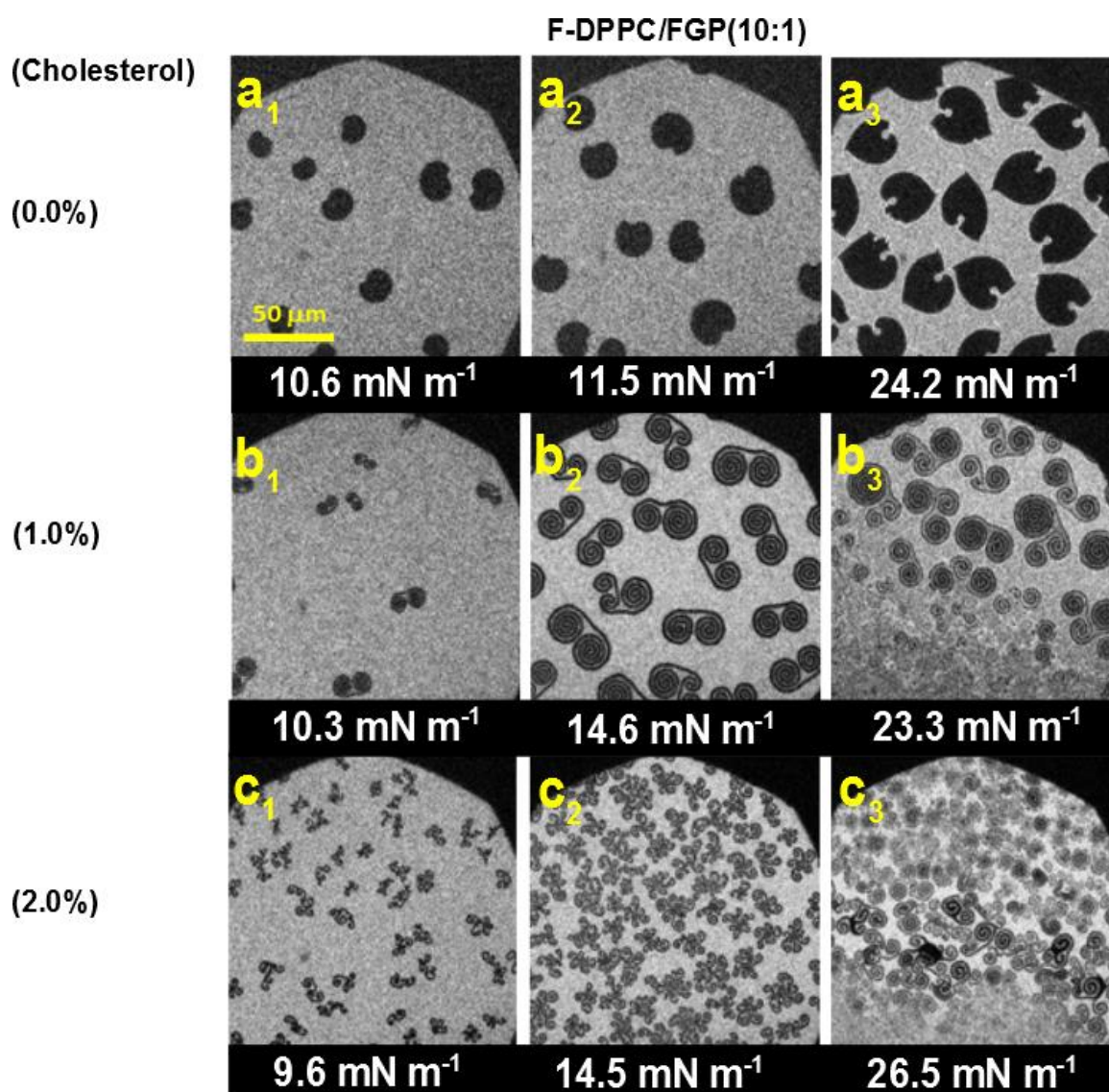
Figure 4.28: FM-images for co-spread monolayers of F-DPPC/FGP (10:1) mixtures containing a) 0 %; b) 1 % and c) 2 % Cholesterol. Each solution possessed 0.01% RH-DHPE.

Impact of Cholesterol on the Anchoring of a Diblock Copolymer

A resemblance between inflexible perfluorinated moieties and rigid cholesterol has been suggested in the previous section. Though the monolayer properties of cholesterol are dominated by its hydrophobic nature, the presence of 3-OH is highly responsible for its residence between lipid molecules in a monomolecular layer.

Time-dependent Adsorption of Polymer to Preformed Lipid Monolayers
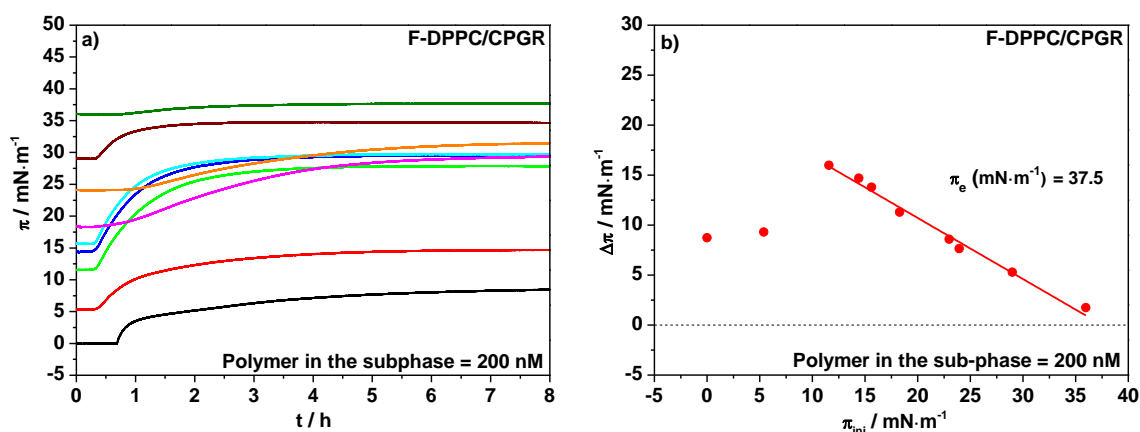
Figure 4.29: a) Time-dependent adsorption of CPGR (200nM) to F-DPPC monolayers spread at different initial pressures; and b) Plot of $\Delta\pi$ vs π_{ini} for CPGR.

To investigate the change in monolayer properties of cholesterol upon derivatization, a block copolymer comprising of a linear polyethylene-glycol block and a hyperbranched polyglycerol block and bearing a cholesterol anchor (*i.e.,* CPGR) was studied for its interactions with F-DPPC. In this polymer, the block lengths of PEG and PG blocks are 30 and 17, respectively. The PG block also carries a rhodamine label attached through a hydrocarbon spacer with it. It has already been reported that this polymer caused extraordinary thinning of triskelion LC-domains in DPPC monolayers.[117]

The time-dependent adsorption of the polymer CPGR to F-DPPC monolayer is depicted in Fig. 4.29. After injection into the subphase, *CPGR* adsorbed to pre-formed F-DPPC monolayers in a similar fashion to that of the polyphilic FGP. The insertion of polymer in LE phase of the lipid is negligible and it is preferably inserted to the monolayers in the coexistence region, where both expanded and condensed lipid phases are present. However, an increase in the amount of condensed lipid and so-called solidification of

_____

domains lead to a gradual elimination of polymer from F-DPPC monolayers. The maximal

insertion pressure is ~ 38 mN m^{-1} for 200 nM polymer in the subphase. This value is

comparable to the *MIP* recorded for F-DPPC/FGP system in the present study. A slightly

higher value of 40 mN m^{-1} has been reported for exclusion of CPGR from DPPC

monolayers, where the subphase concentration of this polymer was 500 nM.[117]

Compression Isotherms and Epifluorescence Microscopy

The compression isotherms of F-DPPC mixed with CPGR are given in Fig. 4.30. There is a

continuous shift of isotherms to higher lateral pressures and isotherm stretches over

larger area with increase in polymer content. The shifts in areas are less pronounced

than those observed for DPPC/CPGR in a previous study.[117] The plateau representing

LE/LC phase coexistence of lipid gradually disappears with increase in moles of polymer

in the co-spread mixture, indicating the tendency of cholesterol to anchor the polymer

in the monolayers.
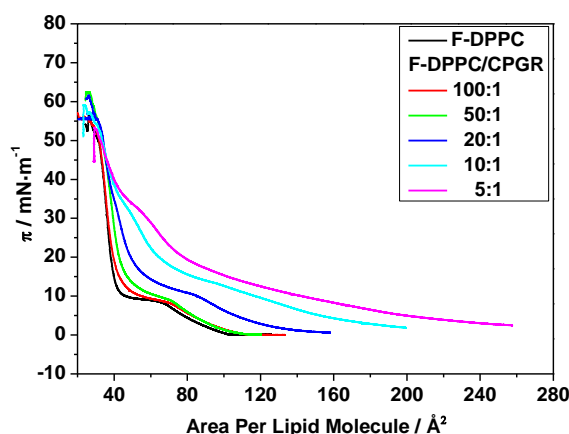
Figure 4.30: Compression isotherms for F-DPPC/CPGR mixtures.

Two transitions are visible in 5:1 mixture, first at π ~ 10 mN m^{-1} and the second above 30

mN m^{-1}. The entrance of polymer from mushroom to brush regime occurs during the

second transition. At at the end of this transition, the π-A isotherms of mixtures start to

overlap with that of pure lipid indicating an exclusion of polymer from the lipid

monolayers. It has been reported[117] that the cholesterol anchor stays in the DPPC

monolayers up to 40 mN m^{-1} and similar inference can be drawn for F-DPPC/CPGR

system. It is not possible to conclude about the removal of cholesterol moiety from F-

_____

DPPC monolayers because the end of the second transition coincides with the collapse of the monolayer.

Table 4.7: Shift in areas available per lipid molecule (ΔA) in a monolayer after CPGR addition recorded at different surface pressures.

F-DPPC/CPGR ratio (moles)	ΔA / Å^2 molec^{-1} (F-DPPC) at various surface pressures (π)			
	4 mN m^{-1}	9 mN m^{-1}	15 mN m^{-1}	25 mN m^{-1}
100:1	5.1	4.0	3.0	0.1
50:1	5.2	10.4	7.4	2.9
20:1	30.4	29.7	18.1	7.2
10:1	81.8	64.0	43.5	18.4
5:1	136.2	92.8	62.0	28.5

The fractal domain shapes are visible in a monolayer comprising a 50:1 mix between F-DPPC and CPGR (Fig. 4.31).
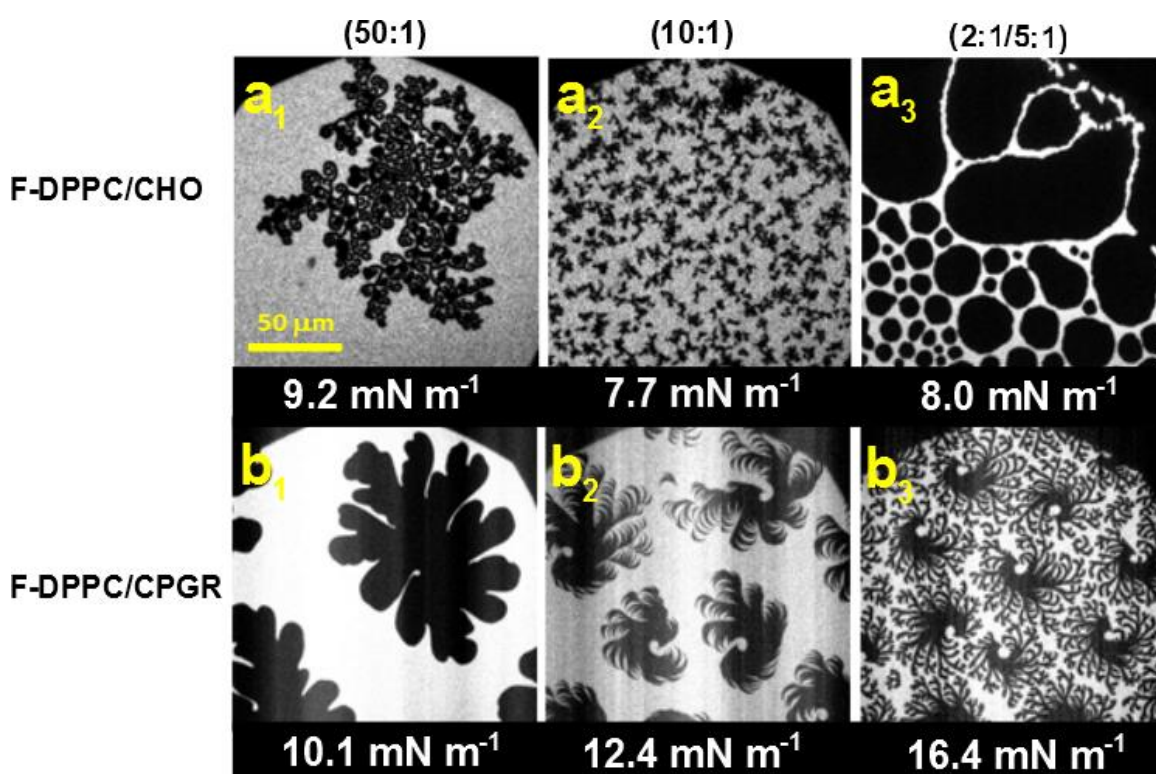
Figure 4.31: FM-images for monolayers of the co-spread mixtures of: a) F-DPPC/Cho; and b) F-DPPC/CPGR containing 0.01% RH-DHPE.

Though the unsubstituted cholesterol is line active in very small percentages, the effect is much reduced upon derivatization of 3-OH in ring A. In fact, the influence of CPGR on LC domains of F-DPPC is not distinguishable from other polymers studied in this work. A splitting of fractal fingers or tips occurs in F-DPPC/CPGR (10:1) mixture, showing the

_____

accumulation of lineactant at domain boundaries. The impact is enhanced for higher percentages of polymer. As mentioned earlier, the hydroxyl group of unsubstituted cholesterol allows hydrogen bonding between lipid head group and cholesterol. When cholesterol is linked to the PEG spacer in the polymer using this 3-OH, the possibility of hydrogen bonding is eliminated.

The hyperbranched PG block contains large number of free hydroxyl groups, which can interact with lipid. However, analysis of domain shapes reveals that the interactions between F-DPPC and CPGR are different from those occurring between unsubstituted cholesterol and the lipid in a mixed monolayer. Another difference arises due to attachment of rhodamine dye with a hydrocarbon linker. This part of the polymer exists in the interfacial region. The hydrocarbon linker pushes itself towards the lipid chains and pulls the dye between lipid head groups, which are possibly spaced at a greater distance due to insertion of cholesterol part. Since, the dye label is attached to the polymer in the case of CPGR, an alteration in polymer concentration leads to change in dye concentration in the mixture as well. An increased dye localization at the 1D interfacial region between fluid and condensed lipid may also produce domain thinning. It is worthwhile to remark that kinetic effects are more prominent during compression in the case of F-DPPC, while they are insignificant for unfluorinated DPPC. The domain shapes acquired for 5:1 mixture of F-DPPC with CPGR in the present study are similar to those reported for DPPC/Cho mixed monolayers after they have been subjected to pressure jumps, a state where monolayer remained in a far from equilibrium state.[216]

4.1.3 Conclusions

- The onset of gas-LE transition occurs at larger area per lipid molecule for F-DPPC compared to DPPC. The phase transition from LE to LC takes place at higher surface pressure than that for DPPC. These differences are due to the affinity of the fluorine atom to the aqueous surface and its bigger size compared to that of a hydrogen atom.

- The LC domains in the monolayers of F-DPPC adopt irregular seaweed like geometries. The splitting of fractal fingers occurs when monolayer compression rates are increased. This reflects that the presence of single fluorine atom at *sn*-2

chain terminus makes the monolayers more prone to kinetic effects and the electrostatic forces between lipid molecules dominate over line-tension in F-DPPC monolayers. This behavior of F-DPPC is in contrast to that exhibited by the unfluorinated analogue, DPPC.

- In the monolayers of an equimolar mixture between D-DPPC and L-FDPPC, complex multi-lobed condensed domain shapes are observed, which are different from those reported for the monolayers of racemic mixture of D-DPPC with L-DPPC.

- Similar to DPPC, the presence of perfluorinated segments increases the polymer retention in the lipid phase for F-DPPC. The exclusion of FGP and GP from F-DPPC and DPPC monolayers takes place at comparable surface pressures. An increased amount of polymer in the subphase does not significantly alter the maximal insertion pressure in the case of FGP.

- In lipid/polymer mixtures, an increase in polymer content counters the kinetic effects resulting from compression of cospread monolayers through confining the lipids molecules into islands separated by the polymer fences. Consequently, the condensed domains adopt bean or propeller shaped morphologies, similar to those seen in DPPC monolayers.

- The semitelechelic polymers (GF40 and GF14) which accumulate at LC domain boundaries cause a reduction in line-tension and induce special pattern formation in LC domains of DPPC. These polymers did not produce similar effects in F-DPPC monolayers. The enlargement of LE-LC interfacial region in F-DPPC monolayers and the diffusion limited domain growth are responsible for this behavior. The polymer retention into lipid monolayers is enhanced when the hydrophilic block is switched from `PEO' to `PGMA'.

- The change in block sequence and size has no notable effect on polymer exclusion from F-DPPC monolayers. However, the polymer insertion into the lipid monolayers is slowed down.

- The attachment of a cholesterol moiety to a diblock copolymer allows the polymer anchoring into lipid monolayers. The condensing and fluidizing effects of cholesterol on lipid monolayers are not present in F-DPPC/CPGR co-spread

monolayers due to alteration in hydrogen bonding interactions. The unusual thinning of LC domains caused by CPGR in DPPC monolayers, could not been observed in F-DPPC monolayers. The thinning of the domain edges resulting from the lineactant behavior of CPGR confirms the accumulation of the polymer at LE-LC interface in F-DPPC monolayers.

4.2   Bilayer Studies

4.2.1 Thermotropic Phase Behavior of F-DPPC

The thermotropic phase behavior of F-DPPC is different from that of DPPC (Fig. 4.32). DPPC exists in a liquid crystalline lamellar phase (L_α) above 40°C, the main phase transition temperature. A lamellar gel phase (L_β') is formed below 35°C and an intermediate rippled gel phase (P_β') exists between 35°C and 41°C.[81]
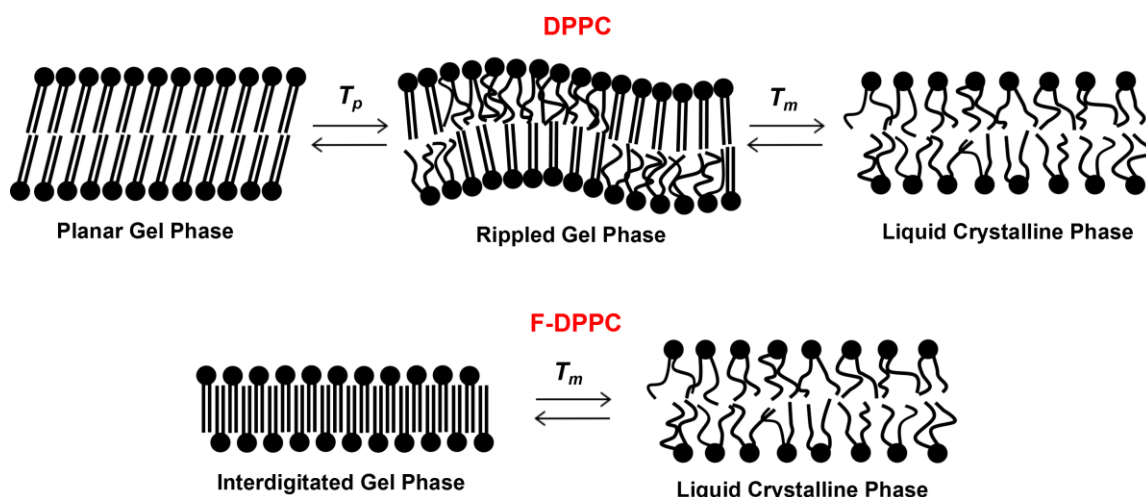
Figure 4.32: Thermotropic phase behavior of DPPC and F-DPPC[91].

In contrast, F-DPPC shows only two phases, a liquid crystalline phase (L_α) above the transition temperature of ~ 50 °C and an a gel phase that is interdigitated ($L_\beta'I$).[95,91] The interdigitated gel phase is more stable than the bilayer gel phase in DPPC. The transition enthalpy is higher with 10 kcal mol^{-1} compared to that of the main phase transition for DPPC (8.7 kcal mol^{-1}). The LE-LC transition in lipid monolayers can be correlated to the gel-fluid phase transition occurring in the bilayers. An increase in the surface pressure for onset of LE-LC transition in the monolayers generally corresponds to a decrease in T_m for gel-fluid transition in the bilayers.[73] Based on this, F-DPPC should exhibit lower T_m

_____

than DPPC. Unexpectedly, the main phase transition temperature for gel-fluid transition

of F-DPPC is 10°C higher than DPPC.[95] The reason for this discrepancy is the existence of

interdigitation in the gel phase of F-DPPC. F-DPPC is among those lipids which undergo

spontaneous interdigitation without any additives or application of pressure.[91]
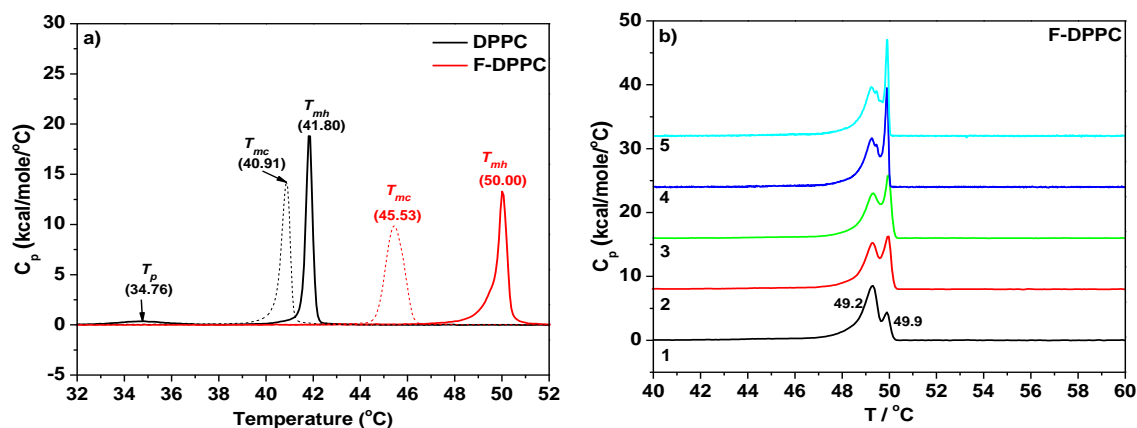
Figure 4.33: a) DSC-thermogram for sonicated aqueous dispersions of DPPC and F-DPPC; and b) Consecutive endotherms for extruded F-DPPC. Bold lines are the endotherms whereas the dotted lines represent the corresponding exotherms.

DSC thermograms shown in Fig. 4.33a gives a comparison between phase transitions in

liposomes prepared by sonication of aqueous DPPC and F-DPPC. The transition from an

interdigitated gel phase to the fluid phase for F-DPPC is broader compared to the one

from ripple gel phase to the fluid phase for DPPC. It has been suggested that this broad

endotherm is in fact a cumulative peak of two closely spaced transitions.[95] In addition,

there is a hysteresis of about 4.5 degrees between the heating and cooling scans, much

larger than the hysteresis seen for the DPPC main transition. For vortexed and sonicated

lipid aqueous dispersions, only one transition is observed, however, for extruded

samples, an additional peak is seen (Fig. 4.33b). The new peak in DSC can be related

either to the heterogeneity in the size of liposomes or due to partially interdigitated

phases, for which the temperature driven fusion of vesicles is responsible.[218] Each

heating-cooling cycle enhances the intensity of main phase transition occurring at 49.9

°C indicating a transformation to a more stable interdigitated state. Concurrently the

intensity of the peak at 49.2°C is reduced and it only appears as a shoulder in all

endotherms beyond the 3rd heating-cooling cycle. It has been observed previously that

F-DPPC undergoes frustrated or incomplete phase transition upon cooling under area

constraints on solid support, leading to partially interdigitated phase[186]. Based on the present work however, it is proposed that the partially interdigitated phases may exist without satisfying the condition of area constraints.
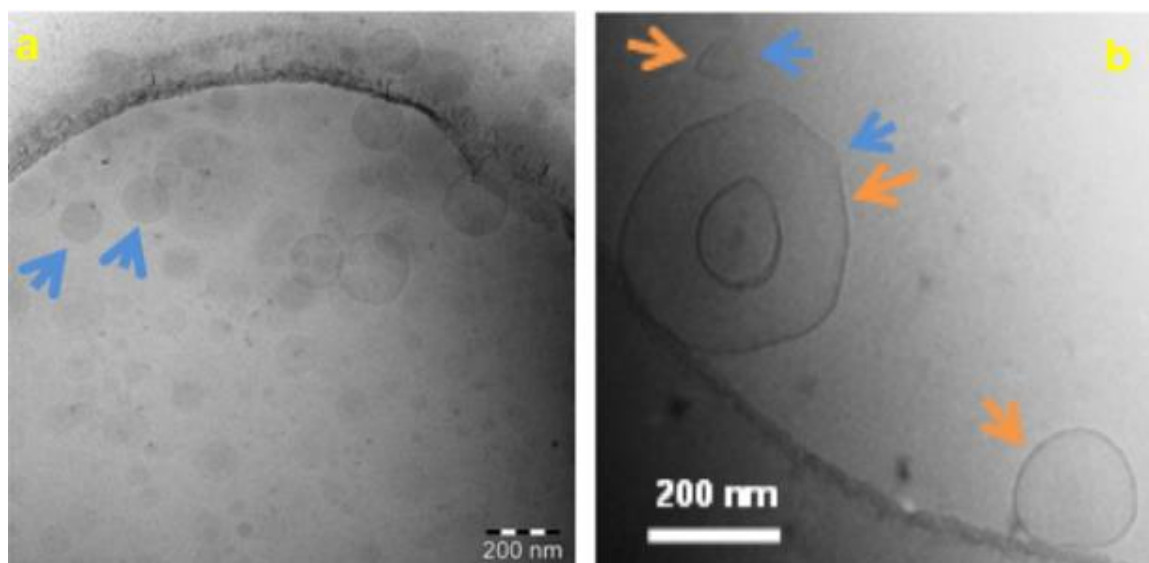
Figure 4.34: Cryo-TEM images for aqueous dispersions of extruded F-DPPC (1.3 mM): a) Quenched from 22°C; and b) Quenched from 55°C.

The extruded samples of the lipid dispersions visualized by cryo-TEM reveal the presence of heterogeneous size distribution among F-DPPC vesicles (Fig. 4.34a). The reduced electron density at the boundary of vesicles represents an interdigitation (see blue arrows). The normal lipid bilayer has higher electron density and appears darker. This is indicated by orange colored arrows. For samples quenched from 55°C, the partially interdigitated phases are also observed.

4.2.2 Effect of Amphiphilic and Polyphilic Block Copolymers on Phase Transition of F-DPPC

Several studies have recently been undertaken on the effect of lanthanum ions, cholesterol and different lipids on the interdigitated gel phase of F-DPPC.[121,122,131,155,185] A single investigation is available on the influence of a peptide antibiotic on F-DPPC and F-DPPG.[130] The investigations on F-DPPC monolayers mentioned in the previous section revealed that the monolayer behavior of F-DPPC in the presence of block copolymers was somewhat different from that of DPPC observed in the presence of these polymers. The proceeding sections explore, whether the polyphilic and amphiphilic block

_____

copolymers insert into F-DPPC bilayers or the presence of $L_\beta I$-phase completely changes the behavior?

Small molecules such as sugars, polyols, urea and amino acids may occupy different positions within membranes, depending upon the polarity of the microenvironment and cause a shift in transition temperature reflective of their position.[219,220] Short chain and polyhydric alcohols favor interdigitation.[92,219] Oligomeric or polymeric additives exert a considerable osmotic stress and are less effective inducers of interdigitation in model membranes.[221,222] Macromolecules could demonstrate different modes of interactions with membranes. They may merely adsorb on the surface, partially penetrate the bilayers and cause their deformation or insert fully into them, and produce a considerable change in the phase transition temperature.[47,223]

Effect of Perfluoroalkylation: GP vs FGP

The binding of hydrophilic blocks of the polymer to charged lipid head groups causes an increase in T_m. On the other hand, hydrophobic and fluorophilic segments can interact with hydrocarbon chains of the lipid and cause a reduction in the main phase transition temperature. The net change in T_m is the summation of both effects.[46] In pre-mixed and sonicated lipid/polymer mixtures, there is a negligible change in phase transition temperatures of DPPC with GP addition. Perfluoroalkylation of polymer increases polymer retention within the bilayer and produces greater decrease in T_m. This information is summarized in Fig. 4.35(b&d).

Mixtures between F-DPPC and GP exhibit continuously broadened endotherms with subsequent increase in polymer concentration, which is accompanied by a decline in T_m (Fig. 4.35(a&c). The cooling scans are also broadened. Initially, there is an increase in hysteresis between melting and crystallization peaks, representing a more hindered transition into the interdigitated phase. Obviously, the PPO block in GP can penetrate the fluid bilayers of F-DPPC and make it more arduous for the lipid to transform to more rigid $L_\beta I$-phase. Very similar results are obtained for F-DPPC/FGP systems. However, for FGP, there is a slight decrease in T_m initially, followed by an emergence of a new peak at comparatively lower temperatures. The peak at 50 °C is related to the phase transition

_____

from an interdigitated gel phase to the fluid phase, while the lower temperature shoulder represents a transition from lipid phase that is partially interdigitated (Fig. 4.36). With increase in polymer content in the mixture, more and more lipid exists as a normal bilayer gel phase. Similar inference can be drawn from the reduction in the hysteresis between endotherms and exotherms in 20:1 and 10:1 mixtures between F-DPPC and FGP.

Figure 4.35: DSC-thermograms for lipid/polymer mixtures: a) F-DPPC/GP; b) DPPC/GP; c) F-DPPC/FGP; and d) DPPC/FGP. Lipids and polymers were pre-mixed and sonicated. Bold lines are endotherms whereas the dotted lines are corresponding exotherms.

A complete adoption of a normal bilayer gel phase motif by the lipid does not occur, because that would have caused the shifting of transition temperatures of F-DPPC/FGP systems in the vicinity of those observed for DPPC/FGP mixtures. The net result is a decline in T_m, which indicates that the hydrophobic interactions between hydrocarbon chains of F-DPPC and hydrophobic/fluorophilic components of FGP dominate in the system. The presence of two peaks in the endotherms also points towards phase separation in the mixtures.

The reformation of the interdigitated phase occurs over a broad temperature range, showing that the conversion to interdigitated phase is hindered upon polymer incorporation and retention. The binding of PGMA block of GP or FGP to lipid heads should favor interdigitation to some extent, similar to polyhydric alchohols.[204] When hydrophobic/fluorophilic components are inserted into the lipid bilayers, the hydrophilic blocks of the polymers are also pulled in the vicinity of head groups. Thus the interactions between lipid head groups and PGMA blocks are augmented. On the other hand, the perfluoroalkyl segments prevent interdigitation upon incorporation into the lipid bilayers and lead to phase separation or partially interdigitated phases.
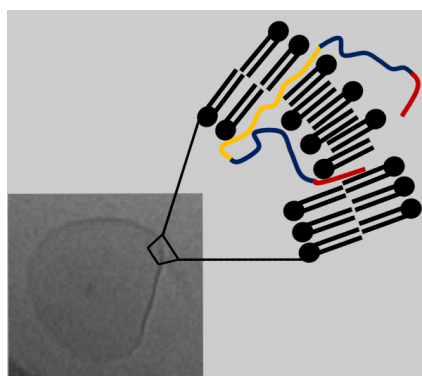
Figure 4.36: Possible existence of partially interdigitated phase in F-DPPC/FGP hybrid vesicle

Effect of the Type of Hydrophilic Block: G40 vs EF44

An essential feature of the thermograms obtained for F-DPPC/GF40 mixtures is the significant broadening of the melting transitions, which now spread over a wide temperature range (Fig. 4.37). In addition, the whole band shifts to lower T_m values. A part of some endotherms overlaps with the relevant crystallization peaks, which makes it difficult to identify the change in hysteresis between them. Similar effects have been reported on melting transitions of DPPC/GF40 mixtures.[39] It is apparent that the presence of the large hydrophilic unit that leads to greater interaction with lipid head groups favors interdigitation similar to polyhydric alcohols.[219] Mixture of F-DPPC with EF44 show somewhat different behavior, especially for lower polymer content. Phase segregation occurs in 20:1 mixture and non-interdigitated phases prevail afterwards, because the endotherms start to overlap with the exotherms and hysteresis is markedly reduced. The broadening of heating scans does not allow drawing an inference about

the complete adoption of a normal bilayer motif by F-DPPC in the presence of EF44. This is however, proposed that the lipid exists in bilayer gel phase only partly. The proposition is supported by the fact that phase transition temperatures observed of F-DPPC/EF44 mixtures in the present study differ by the magnitude of about 5°C from those recorded for DPPC/GF40 system.[39] The crystallization in F-DPPC/EF44 system occurs over a narrow temperature range, and the peak position is negligibly altered.

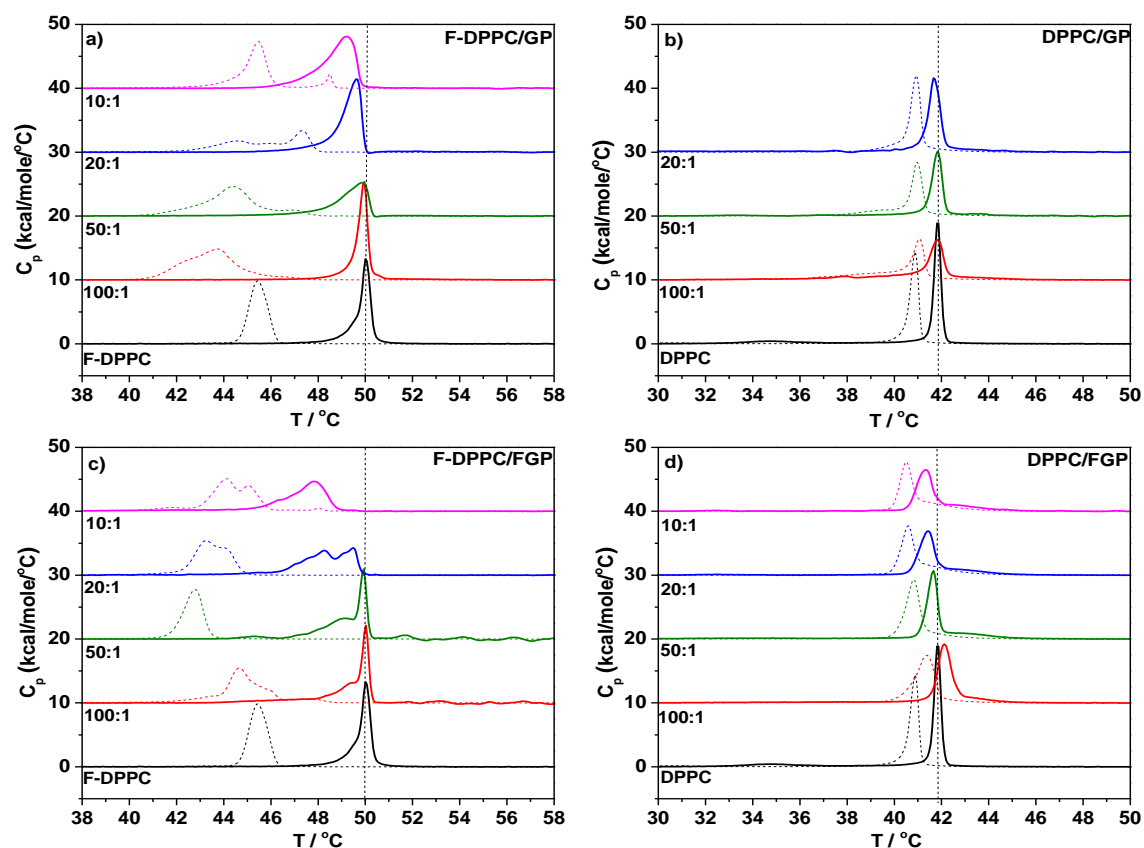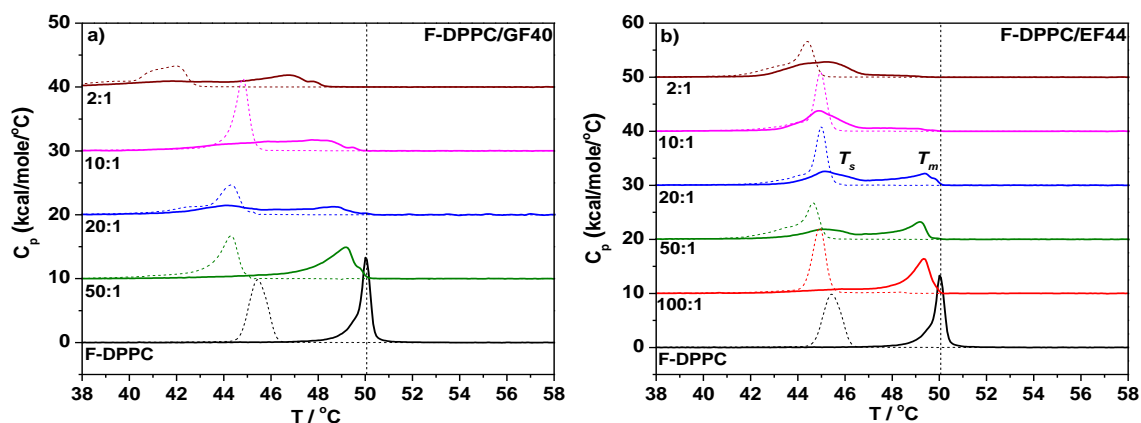**Figure 4.37: DSC-thermograms for lipid/polymer mixtures: a) F-DPPC/GF40; and b) F-DPPC/EF44. Lipids and polymers were pre-mixed and sonicated. The endotherms are represented as bold lines while the exotherms are the corresponding dotted lines.**

Ethylene glycol due to its smaller size partitions to a greater extent into an interdigitated phase and favours a transformation to $L_{\beta}I$.[92,219] The hydrophilic block in EF44 lacks free hydroxyl groups and hence behaves similar to PEG, which prevents interdigitation.[222] This effect is augmented by the F9 chains, causing a phase separation.

Effect of Block Sequence (PFG78)

PFG78 has reversed block sequence compared to FGP and contains only one perfluorinated chain to which is attached on both sides a diblock of PGMA and PPO. The effects produced by this polymer on the phase transition of F-DPPC are shown in Fig. 4.38. The endotherms are broadened and the lipid phase transition occurs over a wide temperature range. Both GF40 and PFG78 have large hydrophilic blocks and since they show similar effects on the thermotropic phase transitions of F-DPPC, it can be inferred that the insertion as well as retention of the polymer in the lipid bilayer is governed by the hydrophilic PGMA blocks.

_____

The height of the melting transition peak at 50°C is much reduced for 10:1 mixture, and it is only slightly regained for 50:1 and 20:1 mixtures of F-DPPC with PFG78. The other transition centered at lower temperatures is stretched over almost 8°C for 100:1 mixture and this width decreases with increasing polymer content in the mixture. For the 10:1 mixture, only one transition occurs with a maximum at about 47°C. This is similar to observation made for F-DPPC/GF40 mixtures. The cooling exotherms are comparatively narrow and demonstrate the ease of crystallization. The hysteresis between endotherms and exotherms shrinks with increased polymer content, implying the presence of partially interdigitated phase.

Figure 4.38: DSC-thermograms for F-DPPC/PFG78 mixtures. Lipid and polymer were pre-mixed and sonicated. The endotherms are represented as bold lines while the exotherms are the corresponding dotted lines.

The binding of free hydroxyl groups in PGMA blocks to the lipid head groups can make it difficult for interdigitated phase (P$_\beta$I) to transform to fluid phase (L$_\alpha$)[92], but the overall decrease in T_m points towards more dominating hydrophobic interactions between lipid alkyl chains and PPO blocks or perfluoroalkyl moieties of the polymer.

Addition of Polymers to Preformed Vesicles of F-DPPC

When polymer and lipid are premixed and later sonicated above the phase transition temperature of F-DPPC, there is greater possibility of polymer penetration and retention within vesicles. The disruptions are obvious if PGMA units are inserted. The polymer incorporates into the bilayer in the fluid phase lipid, and is squeezed out upon cooling to the gel phase bilayer[46], but if the gel phase is an interdigitated, alternating

_____

monolayer, the scenario is different and partially interdigitated phases are formed.[121,155,130] On the other hand, if the interdigitated monolayers are stabilized by the polymer, the recovery to the normal fluid bilayer becomes difficult and hence the melting peaks are significantly broadened. In order to explore whether the polymers can into preformed vesicles, an aqueous polymer solution was added to the extruded aqueous lipid dispersions
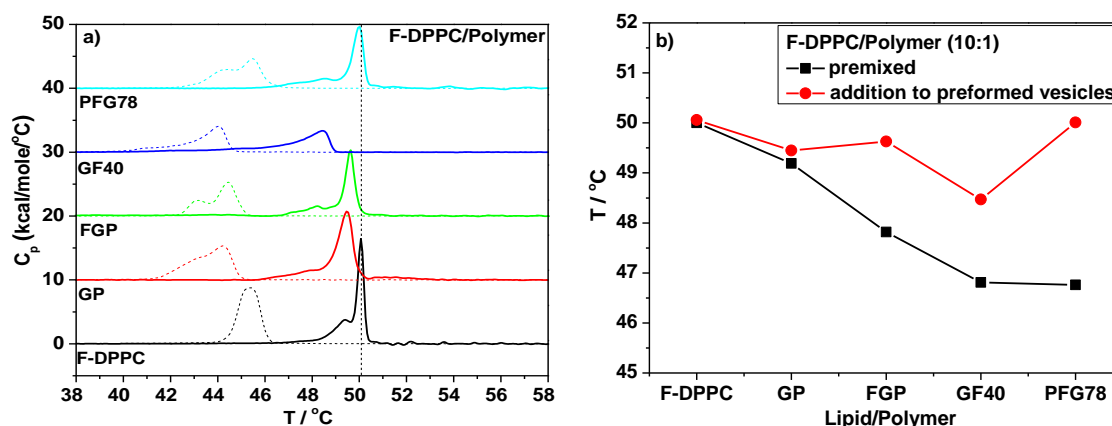
Figure.4.39: a) DSC-thermograms for F-DPPC/polymer (10:1) mixtures. In each case the polymer was added to preformed extruded lipid vesicles.(The endotherms are represented as bold lines, while the exotherms are the corresponding dotted lines; b)Effect on transition temperature of polymer addition to preformed vesicles VS the premixed samples.

Illustrations 4.39 highlight the change in the lipid phase transition temperature upon polymer addition. The depression in T_m is greater for all samples with polymers premixed solutions than for samples where the polymer was added to the preformed vesicles. Here the impact of perfluorinated moieties is highly visible, because GP shows only little dependence of T_m on method of preparation. This indicates that the perfluoroalkyl segments are not excluded from the lipid phase. The PPO block in FGP, GP and PGF78 has a length sufficient to span a normal lipid bilayer. Hence, the insertion of this block does not produce hindrance to the lipid transition involving the transformation from an interdigitated gel phase to a bilayer fluid phase. The additional incorporation of F9 blocks forces the PGMA units to reside near the lipid head groups in the interdigitated phase.

_____

Impact of Cholesterol on the Anchoring of a Diblock Copolymer (CPGR)

The interaction between hydroxyl groups in PGMA units and lipid heads can increase T_m whereas the penetration of perfluoroalkyl chains can reduce the lipid phase transition temperature. In the premixed samples, the insertion of hydrophobic and fluorophilic blocks is facilitated and that is why a significant drop in T_m is seen. On the other hand, such decrease is the phase transition temperature is not observed when polyphilic polymers are added to the performed vesicles, showing that the insertion of F9 and PPO chains is marginalized. In addition, the interaction between lipid head groups and hydrophilic PGMA blocks is enhanced. It is worthwhile to mention that the polymer's tendency to self-assemble in the aqueous solution is also responsible for lowering in the penetration capability into vesicles. The concentration of polymers in lipid/polymer (10:1) mixtures is 0.1M, which is sufficiently high to cause an aggregation of these macromolecules
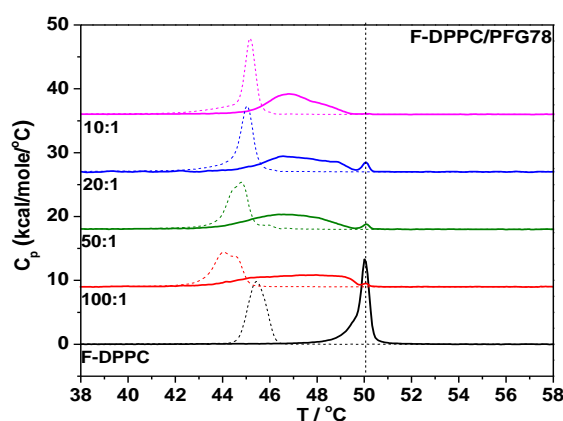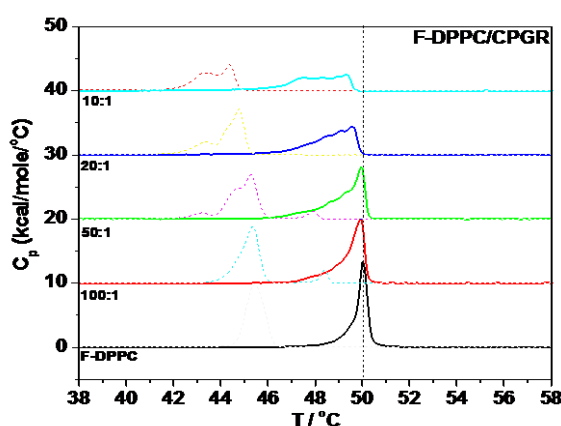

Figure 4.40.: DSC-thermograms for F-DPPC/CPGR mixtures. Lipid and polymer were pre-mixed and sonicated. The endotherms are represented as bold lines while the exotherms are the corresponding dotted lines.

Small molecules such as glycerol favors interdigitation in DPPC[92,219], while its oligomers and polyethylene glycol act in opposition to this.[221,222] Cholesterol eliminates interdigitation in F-DPPC.[155] In CPGR, cholesterol is linked to a copolymer comprising a linear poly(ethylene glycol) block and a hyperbranched polyglycerol. At least one oxygen atom in polyglycerol is attached to the rhodamine dye through a hydrocarbon linker.

The overall effect of CPGR on F-DPPC phase transition is the broadening of melting peaks and lowering of T_m (Fig. 4.40). The crystallization occurs over a wide temperature

_____

range. This is not unexpected due to presence of the cholesterol moiety in the polymer that changes the chain order in membranes. A complete transformation to non-interdigitated phase is not possible, because this requires higher percentage of cholesterol than present in F-DPPC/CPGR (10:1) mix.[155]

4.2.3 Conclusions

- The onset of the LE-LC transition takes places at higher surface pressure in F-DPPC monolayers compared to that in DPPC, but in bilayers, the expected decline in T_m is not observed because of interdigitation in the gel phase.

- The interdigitated unilamellar vesicles are unstable and undergo temperature driven hemifusion, leading to partially interdigitated gel phases. An additional peak in DSC thermograms that exists just below the main transition peak, could be related to the vesicles where lipid molecules partly adopt the normal bilayer motif. This has been confirmed by *cryo-TEM* imaging of the extruded lipid dispersions.

- Amphiphilic and polyphilic polymers have a pronounced effect on the phase transition of F-DPPC, especially when they are premixed. They generate only partially interdigitated phases and the phase transition is considerably broadened.

- A phase separation occurs in lipid dispersions containing FGP, confirming the existence of defects in the gel phase of F-DPPC, induced by the intercalation of perfluorinated moieties among lipid alkyl chains. GP does not produce these effects in mixed dispersions with F-DPPC.

- The semitelechelic polymer GF40 and PFG78 that contain a different block sequence produce comparable effects in aqueous F-DPPC, indicative of multiple closely spaced melting transitions that spread over a wide temperature range. For certain GF40 content a phase separation also occurs, most probably due to the retention of perfluoroalkyl groups in the lipid gel phase. EF44, which contains a PEO block instead-of PGMA produces similar defects in the lipid, and supports the existence of non-interdigitated phases.

_____

- With the exception of GF40, the T_m of the lipid is not altered significantly when polymer is added to the performed F-DPPC vesicles. GP produced similar changes in T_m, whether it was premixed with the lipid or added to the preformed lipid vesicles. On the other hand, all the polyphilic polymers caused greater lowering in T_m in the premixed samples compared to the samples when they were added to the preformed lipid vesicles. In short, the monofluorination of DPPC imparts a capability to recognize the presence of perfluorinated segments in the polymers.

- The penetration of the cholesterol anchor of CPGR inhibits interdigitation in F-DPPC gel phase. In fact, CPGR acts similar to GF40 upon incorporation into the lipid phase. A depression in T_m of F-DPPC occurs and the melting peak is broadened and the occurrence of minor closely spaced phase transitions is visible.

_____

5   INVESTIGATIONS OF THE ETHER LIPID DHPC

The properties of cell membranes are dependent on their composition. Ether lipids are present in the cell membranes of archaea.[143] In ether lipids, the glycerol backbone is linked to alkyl chains through ether bonds in contrast to ester as in DPPC. The absence of carbonyl group in these lipids produces a significant alteration in membrane dipole potential[224]. The decrease in lipid hydrophilicity upon switching the linkage from ester to ether in phosphatidylcholines results in a tighter chain packing near the membrane surface.[225] The conformation of glycerol backbone and the tilt of alkyl chains in monolayers of ether PCs is also different from those of the corresponding ester analogs.[225] Similar to F-DPPC, DHPC also exhibits an interdigitated gel phase, $L_\beta I$. This chapter explains how the ether linkage and interdigitated gel in this DPPC derivative modulates the polymer-lipid interactions?

5.1   Monolayer Studies

5.1.1 Pure Lipid

The compression isotherm of DHPC, along with those of F-DPPC and DPPC are gathered in Fig. 5.1.
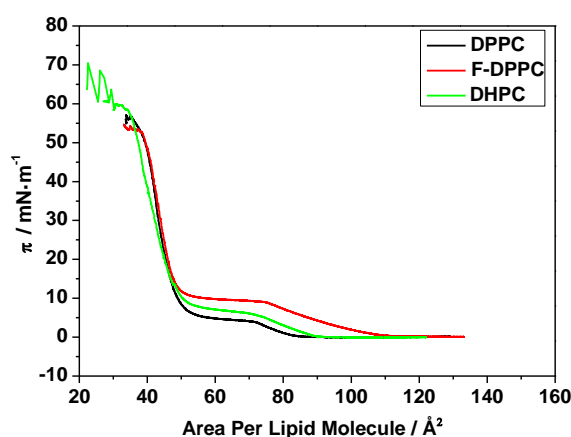
Figure 5.1: Compression isotherms for L-DPPC and F-DPPC monolayers on aqueous subphase at 20°C. The compression speed was 2.0 Å^2 min^{-1} molec^{-1}.

The transition from LE to LC is less clearly defined for DHPC.[148] Despite of the absence of carbonyl groups, the chains are packed in an oblique lattice similar to DPPC with less tilted alkyl chains in the condensed phase.[225] In DHPC monolayers on aqueous subphase,

the condensed domains are observed before the onset of LE/LC coexistence region represented by the a pseudo-plateau in the pressure-area isotherms.[127] The LE-LC transition occurs at slightly higher surface pressure compared to DPPC, but at lower surface pressure compared to F-DPPC.

Epifluorescence micrographs of DHPC monolayers reveal that for this ether lipid, the LC-domains do not possess a defined shape, are smaller in size compared to those observed for DPPC, and grow fuzzy upon further compression (Fig. 5.2). At higher surface pressures they get blurred, produce grey merging boundaries and vanish. Nearly, similar behavior has been reported for DHPC in the presence of NBD-cholesterol fluorescent probe.[127] The greyish corona visible in LC domains of DHPC monolayer is due to the enormous thinning of these domains that does not allow their detection below the resolution limit of the microscope. This thinning of domain boundaries and domain destabilization is due to alterations in attractive van der Waals forces between lipid molecules in the LC phase.[127] The domain deformation in the LC phase of DHPC also shows that the electrostatic repulsive forces between the charged lipid heads dominate the line-tension.
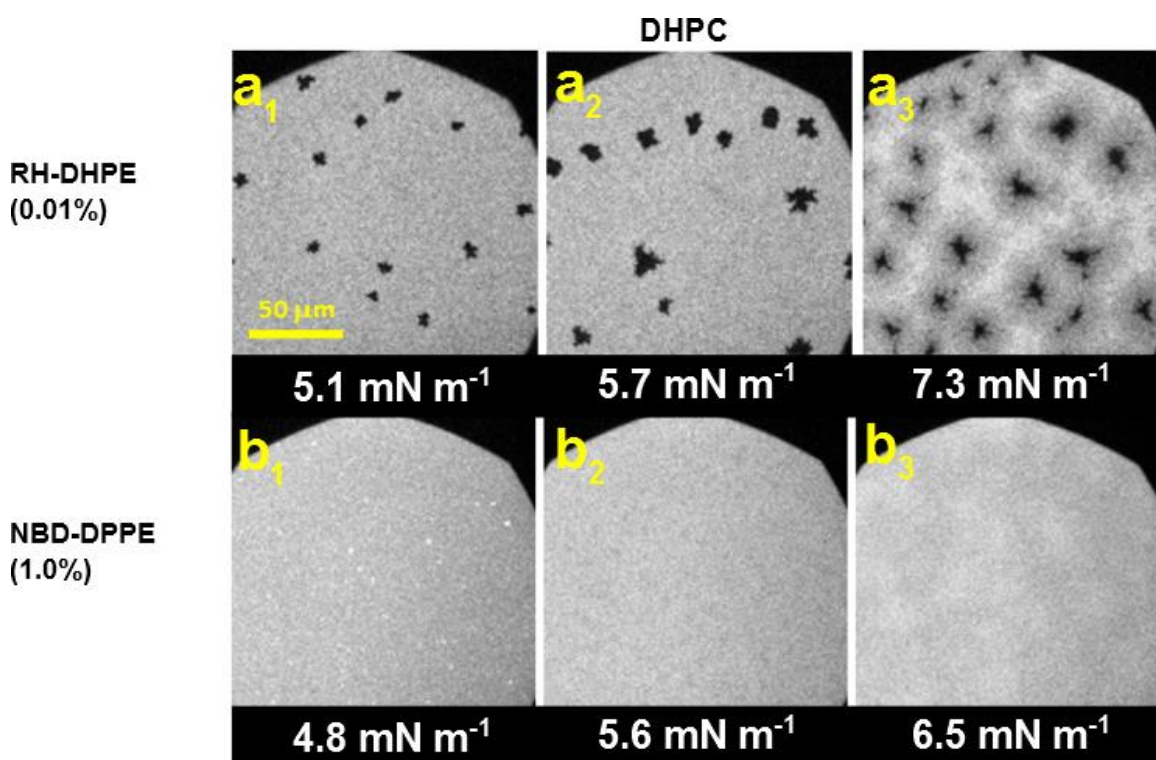
Figure 5.2: LC-domains of DHPC monolayers in the presence of different dyes a) 0.01% RH-DHPE; and b) 1.0% NBD-DPPE.

When the DHPC monolayers are visualized by using NBD-DPPE as fluorescent probe, an anomalous behavior is observed. At the beginning of the LE-LC coexistence region, white and thin condensed domains are seen. Later, when the lateral pressure is raised to 5.6 mN m^{-1}, very small light grey domains appear, indicating the exclusion of probe from the LC phase of the lipid. For $\pi \sim 6.5$ mN m^{-1} only grey and white dim patches exist. It is therefore, deduced that NBD-DPPE is not appropriate for probing the LE-LC transition in monolayers of DHPC. Based on the above mentioned observations, it can be concluded that NBD-DPPE fits well into the LC phase of the ester lipids such as F-DPPC. Again, the monolayer of DHPC is only representative of fluid phase of the bilayer, because the gel phase of DHPC is interdigitated.[144]

5.1.2 Interactions of Amphiphilic and Polyphilic Polymers with DHPC Monolayers

Effect of Perfluoroalkylation: GP vs. FGP

The lateral density of DHPC monolayers is different from DPPC due to absence of carbonyl group[128]. The presence of ether or ester linkage in the lipid affects the interactions with cholesterol in the lipid monolayers[127] and consequently alters interactions with polymeric additives. Therefore, the incorporation into the lipid monolayers of FGP containing rigid perfluorinated chains should also be different from that of GP possessing only PPO and PGMA blocks.

Time-dependent Adsorption of Polymers to Preformed Lipid Monolayers

It is clear from π vs. t plots (Figs. 5.3a & 4.10a) that the no GPinsertion takes place above 30 mN m^{-1}, neither for F-DPPC nor for DHPC. Since DHPC is an ether lipid whereas in F-DPPC the alkyl chains are linked to glycerol by an ester linkage, it can be inferred that the GP insertion into phospholipid monolayers is not linkage (or packing density) dependent. Based on these results the involvement of carbonyl group in the interactions with GP can also be ruled-out. The pressure increase observed for GP below the LE-LC phase transition is less than that obtained immediately above it.

In DHPC monolayers, the penetration capacity of FGP is higher than that of GP. After the polymer injection under bare water surface, the surface pressures exceed 15 and 20 mN

_____

m^{-1} for GP and FGP, respectively. A lowering in $\Delta\pi$ occurs for $\pi_{ini} \sim 5$ mN m^{-1}. This is simply due to decline in surface area available for adsorption of polymer from the subphase when part of the surface is occupied by a lipid monolayer. An increase in $\Delta\pi$ is seen initial spreading pressure of 10 mN m^{-1}, which reflects an interaction between lipid head groups and hydrophilic blocks of the injected polymers. Beyond this point, the $\Delta\pi$-values decrease with an increase in π_{ini}. The exclusion pressures computed for GP and FGP are 30 mN m^{-1} and 40 mN m^{-1}, respectively. This difference of $\sim$10 mN m^{-1} magnitude was also observed in the case of F-DPPC and DPPC and is chiefly due to preference of perfluorinated chains for the lipid chains or air.

Figure 5.3: Time-dependent adsorption of polymers to DHPC monolayers spread at different initial pressures a) 200 nM GP; b) 200 nM FGP; c) Plot of $\Delta\pi$ vs. π_{ini} for FGP and GP.

Compression Isotherms and Epifluorescence Microscopy

The compression isotherms recorded for DHPC/polymer mixtures are shifted to higher areas per lipid with increase in polymer content (Fig. 5.4). This shift is nearly comparable

_____

to that in the F-DPPC/GP mixtures. The ΔA values recorded for DHPC/FGP mixtures are either comparable or higher than the corresponding lipid/polymer mixtures containing GP. DHPC occupies lesser area per molecule than F-DPPC. In addition, it enters into condensed phase much earlier than F-DPPC and possesses tighter packing as well. Therefore, it recognizes the presence or absence of F9 chains easily.
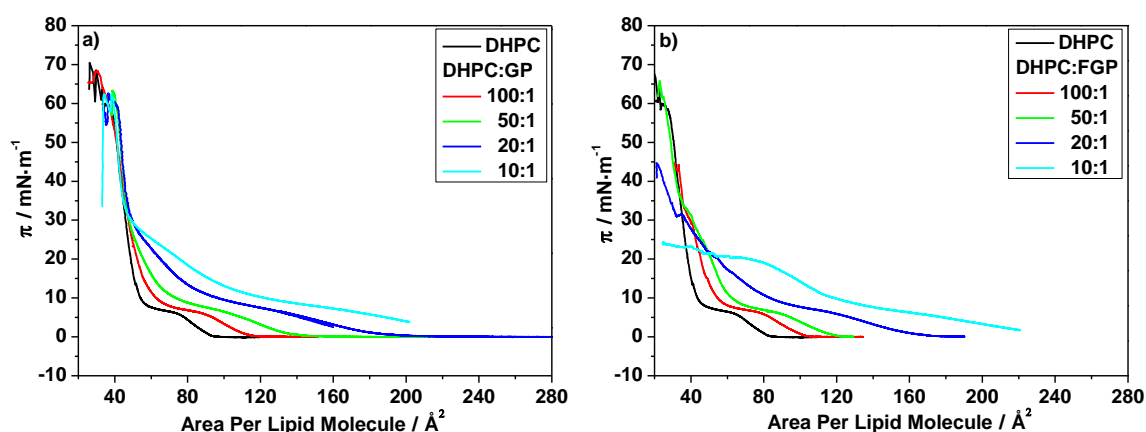
Figure 5.4: Compression isotherms for a) DHPC/GP; and b) DHPC/FGP mixtures.

With increase in FGP content, the mixed monolayer is destabilized and exhibits lower collapse pressures. The condensation of lipid is not inhibited though, and LC-domains for DHPC/FGP mixtures are quite similar to those recorded for DHPC/GP monolayers (Fig. 5.5).

Table 5.1: Shift in areas available per lipid molecule (ΔA) in a monolayer after FGP and GP addition recorded at different surface pressures.

Lipid/ polymer ratio (moles)	ΔA / Å^2 molec^{-1} (DHPC) at various surface pressures (π)							
	4 mN m^{-1}		7 mN m^{-1}		15 mN m^{-1}		25 mN m^{-1}	
	DHPC/ GP	DHPC / FGP	DHPC / GP	DHPC / FGP	DHPC / GP	DHPC / FGP	DHPC / GP	DHPC / FGP
100:1	16.5	16.4	13.2	15.1	5.4	9.1	2.3	5.8
50:1	34.5	28.9	30.6	24.8	11.0	15.3	3.6	9.0
20:1	72.4	64.1	60.7	54.0	24.8	26.5	8.6	7.6
10:1	118.7	120.6	99.2	93.9	41.3	57.3	13.5	--

For lower polymer content, the fractal domain growth is visible in the mixed monolayers. The LC domains attain star like geometries with increased amount of the polymer in the mixture, with five or six thin branches emerging from the compact core. Later, the domains grow fuzzy and disappear. Wang *et al*[226] have related fractal domain growth to both diffusion limited aggregation and positional relaxation of molecules.

_____

Figure 5.5: LC-domains in a) DHPC/GP (100:1); b) DHPC/GP (20:1) c) DHPC/FGP(100:1) and d) DHPC/FGP (20:1) co-spread monolayers containing 0.01% RH-DHPE.

Effect of PGMA Block Length in Semitelechelic Polymers: GF40 vs GF14

The next investigation involves the impact of PGMA block length of semitelechelic polymers on their insertion into DHPC monolayers. These polymers represent the

_____

PGMA-F9 segment of FGP. These polymers lack PPO block, which is why they are less surface-active than GP and FGP. Though the PGMA block is hydrophilic, the lengthening of this block imparts higher surface activity.[39]

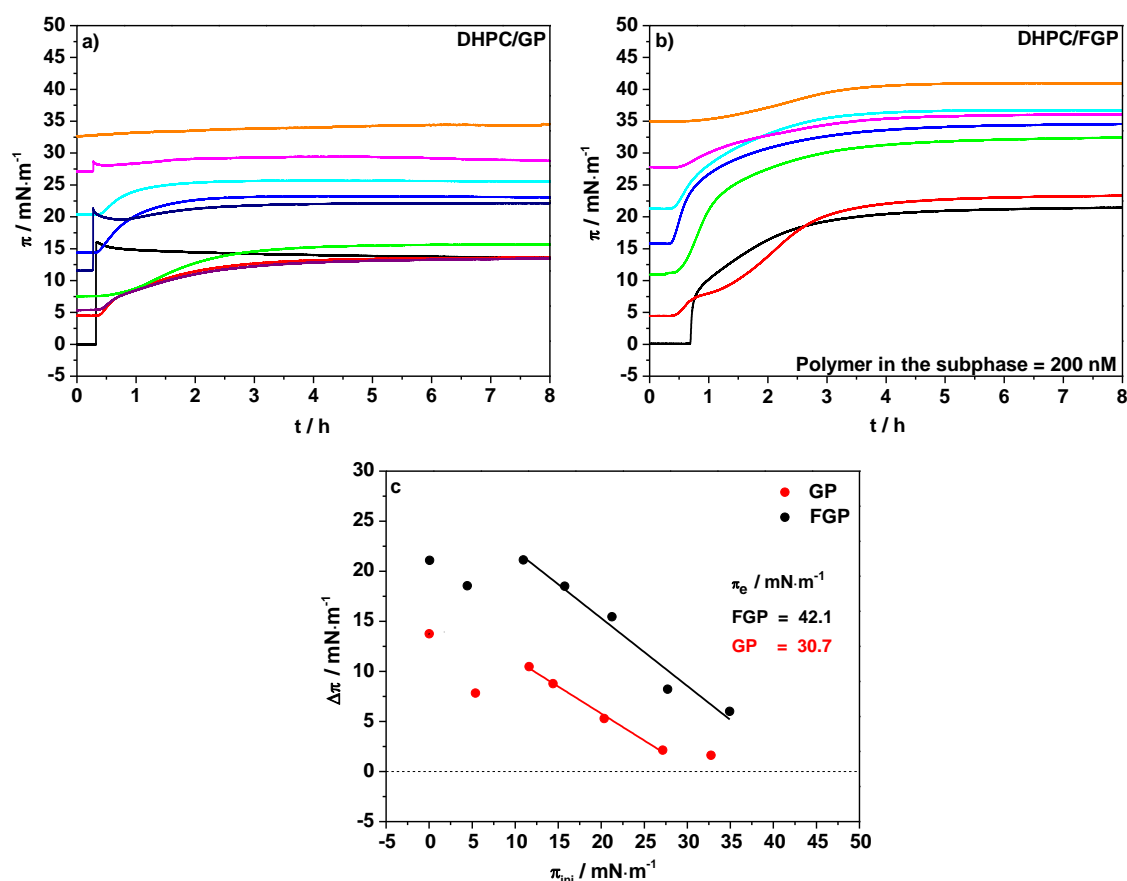## Time-dependent Adsorption of Polymers to Preformed Lipid Monolayers
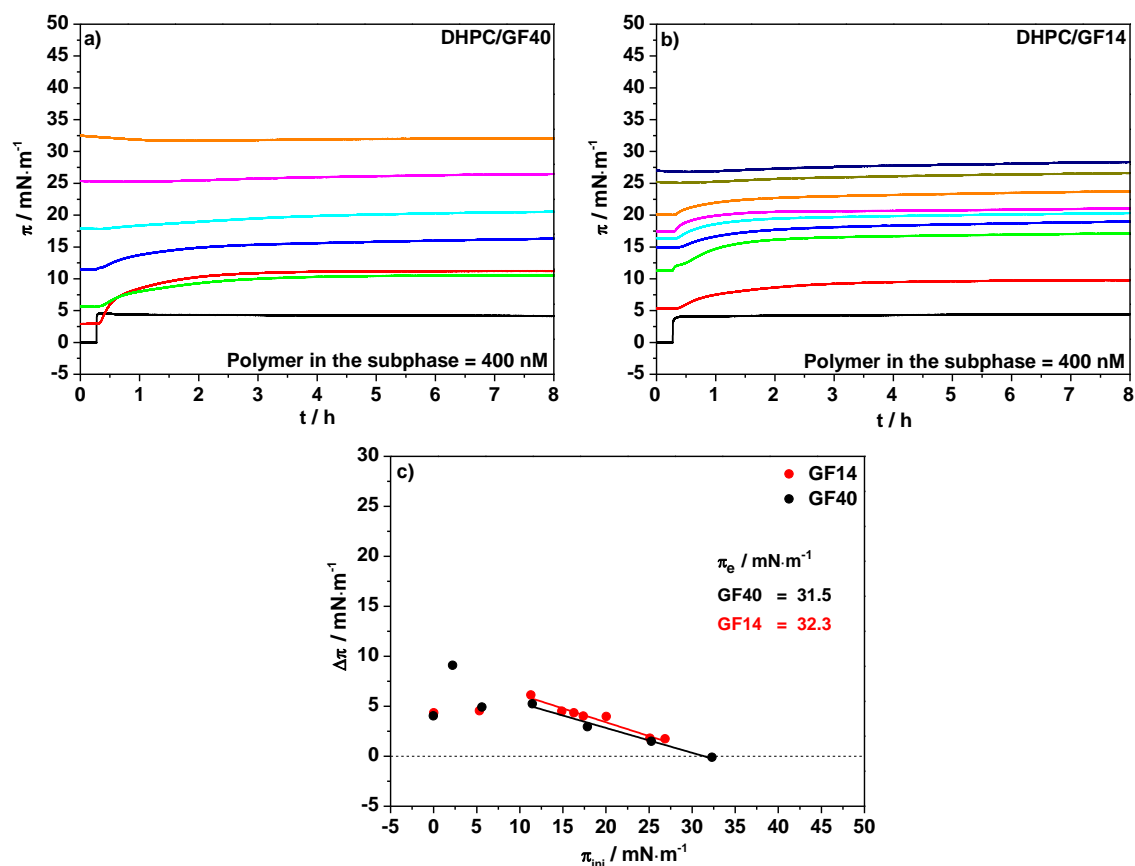
Figure 5.6: Time dependent adsorption of polymers to DHPC monolayers spread at different initial pressures a) 400 nM GF40; b) 400 nM GF14; c) Plot of $\Delta\pi$ vs π_{ini} for GF40 and GF14.

The semitelechelic polymers when adsorb onto bare air-water interface, produce a comparable increase in surface pressure averaging at 4.1 mN m^{-1}. When the polymer is injected underneath a monolayer of DHPC, so that its sub-phase concentration is 400 nM, the surface pressure reaches ~ 9 mN m^{-1} for DHPC monolayer spread initially at 2 mN m^{-1}. This means that DHPC has been pushed into condensed phase by the polymer insertion-a similar effect described before for F-DPPC in this study and DPPC[39] after polymer injection underneath lipid monolayers. Pure DHPC undergoes condensation at much lower surface pressure and LE-LC transition the pressure-area isotherms is smeared out[127]. At lower lipid density on the surface, there is always some area of

interface available for polymer adsorption. The occupation of certain surface by the polymer brings the lipid molecules closer to each other. This produces phase transition in significant part of the lipid monolayer and change in surface pressure is greatest for the system. When the initially spread monolayer has a higher density, the polymer has less space available for adsorption and hence the elevation in the surface pressures becomes smaller. A limit reaches, where the pressure virtually remains unaltered after polymer injection, showing that polymer could not make it to the surface (Fig. 5.6 (a&b).

The $\Delta\pi$ values are about 1 mN m^{-1} for π_{ini} of 25 mN m^{-1}, showing a significant retardation of polymer's capability to insert into DHPC monolayers. Both semitelechelic polymers are excluded from DHPC monolayers at similar pressures that are just about 32 mN m^{-1} (Fig. 5.6c). These exclusion pressures are slightly higher than observed for F-DPPC/GF40 and F-DPPC/GF14 monolayers. These values are also comparable to those measured for GP when its subphase concentration was 200 nM (after injection) underneath the DHPC monolayers. This indicates that GP's insertion capability is roughly two fold that of semitelechelic polymers. The slight difference between the accessibility of DHPC and F-DPPC to polymers could be due to the difference in the ratio of cross-sectional areas of the lipid head groups to the corresponding tail groups.

Compression Isotherms and Epifluorescence Microscopy
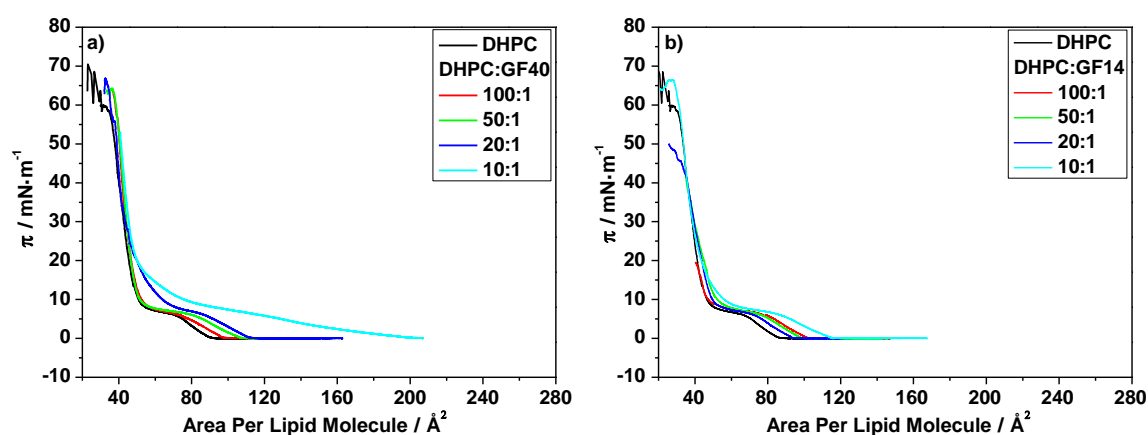
Figure 5.7: Compression isotherms for a) DHPC/GF40 and b) DHPC/GF14 mixtures.

The pressure-area isotherms of the monolayers of DHPC mixtures with GF40 and GF14 are shown in Fig. 5.7. The change in area per lipid is greater for GF40, which is expected due to difference in size of the PGMA block, which in the case of GF40 is nearly twice as

_____

large as that of GF14. The extension of PGMA unit enhances the surface activity of the polymer[39] and allows the polymer to contribute significantly to the change in area occupied by a single lipid molecule.

Table 5.2: Shift in areas available per lipid molecule (ΔA) in a monolayer after GF40 and GF14 addition recorded at different surface pressures.

Lipid/ polymer ratio (moles)	ΔA / Å² molec⁻¹ (DHPC) at various surface pressures (π)							
	4 mN m⁻¹		7 mN m⁻¹		15 mN m⁻¹		25 mN m⁻¹	
	DHPC/ GF40	DHPC / GF14	DHPC / GF40	DHPC / GF14	DHPC / GF40	DHPC / GF14	DHPC / GF40	DHPC / GF14
100:1	4.9	6.1	2.9	10.1	1.1	0.8	1.3	--
50:1	12.1	10.7	7.4	10.8	1.7	4.6	1.5	2.3
20:1	18.2	13.4	17.8	6.7	7.8	2.9	2.1	1.7
10:1	61.1	22.9	43.5	20.4	11.4	4.9	3.1	1.0

The ΔA values for DHPC/GF14 and DHPC/GF40 co-spread monolayers are collected in Table 5.2. When GF14 concentration is low in the mixture, it fully stays on the surface due to its smaller size. The hydrophilic PGMA block in GF40 remains at the bare air/water interface, but in the presence of lipid it dangles into water, due to its greater affinity for the aqueous medium. At higher polymer content, the difference between the ΔA values exhibited by the two systems start to vanish and for lipid/polymer (10:1) mixtures, a greater change in area per lipid molecule is affected by GF40 than GF14. The adsorption of polymer to an existing monolayer on the surface reveals that the exclusion of GF14 occurs at slightly higher surface pressure than GF40. This could be related to size of the hydrophilic block bearing hydroxyl groups that act as hydrogen bond donors as well acceptors. The absence of carbonyl groups in the lipid also reduces the possibility of bonding with the hydroxyl bearing PGMA units in the polymers.

Clejan *et al*[220] have indicated in the study of the permeability properties of sterol-containing liposomes prepared from DPPC and DHPC that the presence of ester linkage in the lipid has a negligible effect on interactions with cholesterol. Since rigidity is a common feature between cholesterol and perfluorinated moieties, they are expected to insert into monolayers in a similar fashion. Therefore, the effect seen in the case of semitelechelic polymers is mostly due to PGMA.
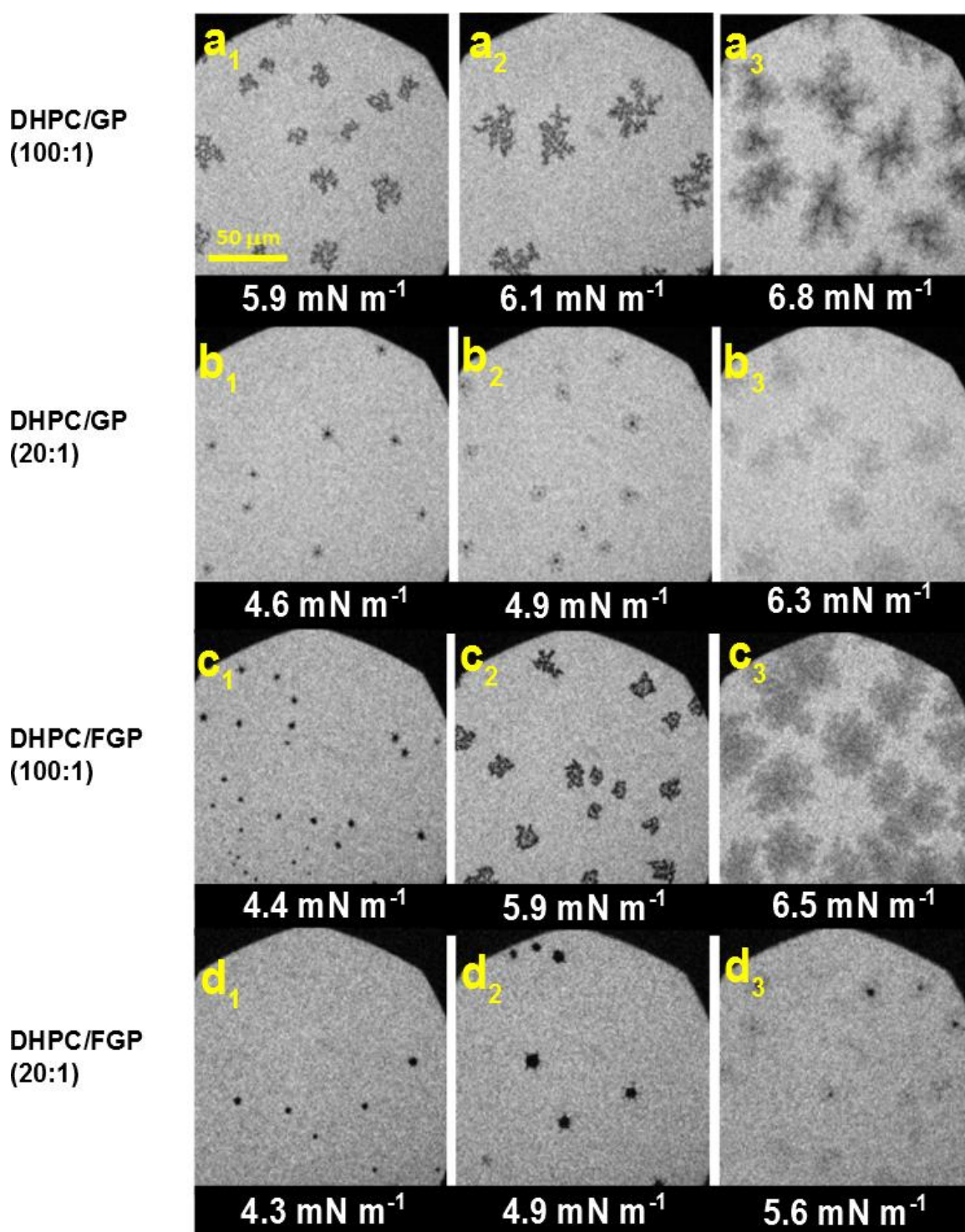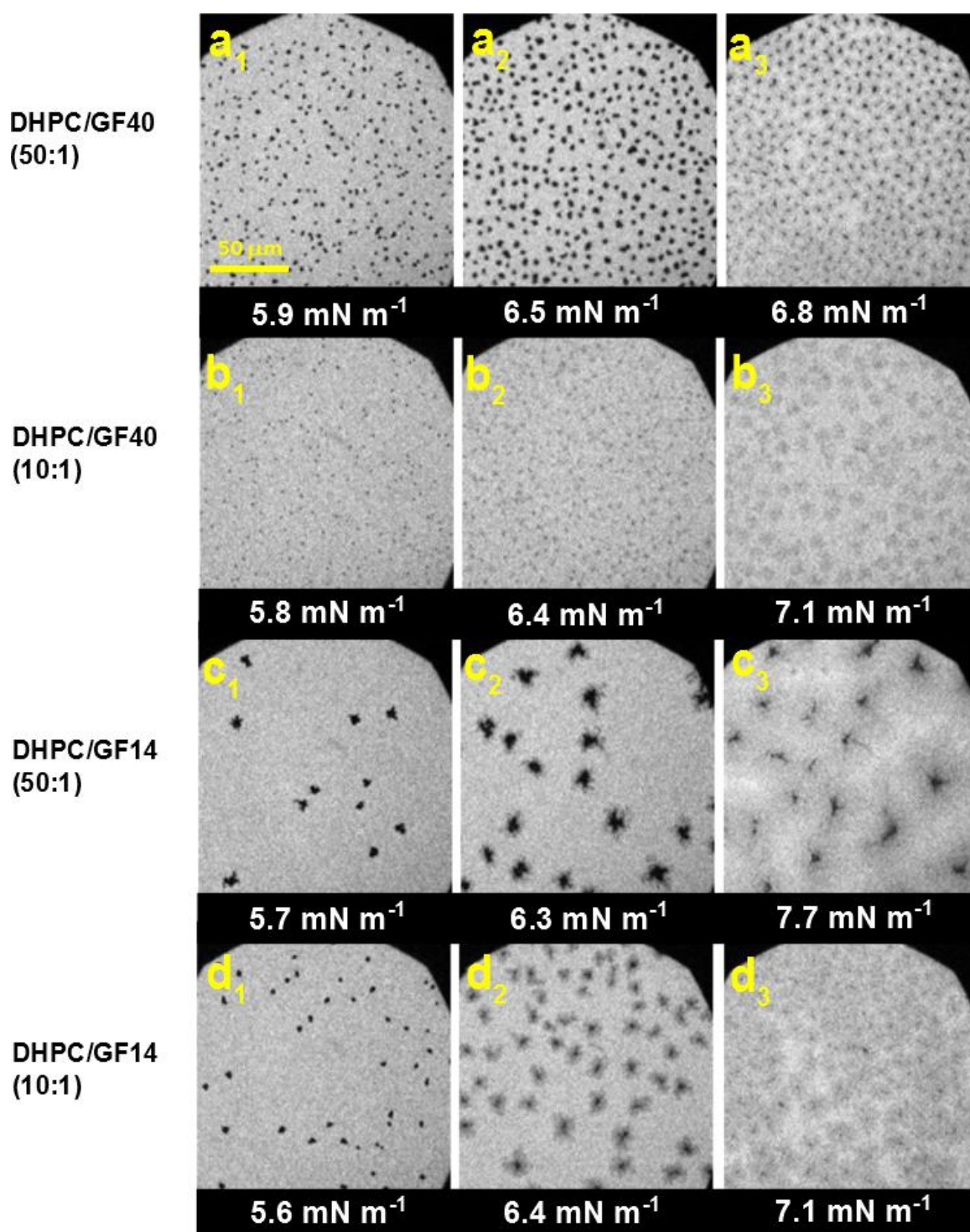
Figure 5.8: LC-domains in a) DHPC/GF40 (50:1); b) DHPC/GF40 (10:1) c) DHPC/GF14 (50:1) and d) DHPC/GF14 (10:1) co-spread monolayers containing 0.01% RH-DHPE.

Fig. 5.8 shows the LC domains observed in the co-spread monolayers of DHPC mixtures with GF40 and GF14. The domain size depends not only on the polymer content in the lipid/polymer mixture, but also on the length of the PGMA unit. GF40, which contains larger PGMA units compared to GF14 causes, marked reduction in the size of LC domains

in mixed lipid/polymer monolayers. The condensed domains get fuzzy with increasing surface pressure. They show fractal growth patterns and branching occurs in all directions, unlike in DHPC monolayers with FGP and GP, where domains are more symmetrical with five or six thin branches emerging from a compact core. The perfluorinated chains of the semitelechelic polymers GF40 and GF14 are probably arranged at interfacial region between LE and LC phase and cause a reduction in the line tension. As a consequence, the branching and thinning of domain edges occurs. This work endorses the lineactant behavior of semitelechelic polymers previously observed through imaging of their co-spread monolayers with DPPC.[39]

5.1.3 Conclusions

- In DHPC monolayers, the onset of LE-LC transition occurs at slightly higher surface pressure than that for the DPPC monolayers. The transition is less clearly defined and is of low cooperativity for DHPC.[127]

- LC domains in DHPC monolayers are irregularly shaped and fuzzy. The lateral density in DHPC monolayers is larger than that in DPPC monolayers and probably responsible for the fractal domain morphologies. The anomalous behavior of NBD-DPPE in DHPC monolayers endorses the limited utility of this probe for the monolayers of the ether-linked lipids.

- The exclusion of GP and FGP from DHPC monolayers occurs at slightly lower lateral pressures in comparison to those obtained for the elimination of these polymers from F-DPPC monolayers. Thus, it is concluded that the lipid-polymer interactions are not largely affected by the type of link present between the glycerol backbone and the lipid alkyl chains.

- The intercalation of perfluoroalkyl segments of FGP among the DHPC alkyl causes the destabilization of the mixed monolayers, which then exhibit lower collapse pressures.

- LC domains attain more compact geometries with increased polymer (GP and FGP) content in the mixed monolayer. However, the thinning of the domain edges continues to happen due to accumulation of hydrophobic/fluorophilic segments of the polymers, indicating an alteration in the van der Waals forces. This lineactant behavior was not observed in F-DPPC/polymer monolayers.

_____

- The semitelechelic polymers, GF40 and GF14 demonstrate higher retention in DHPC monolayers compared to the F-DPPC monolayers. More organized LC domains in the cospread DHPC/GF40 monolayers indicate a reduction in the lipid headgroup repulsions due to the enlargement of the hydrophilic block of the polymer. The fuzziness of condensed domains in the mixed monolayers reflects the presence of perfluorinated moieties at the domain boundaries.

5.2   Bilayer Studies

5.2.1 Thermotropic Phase Behavior of DHPC
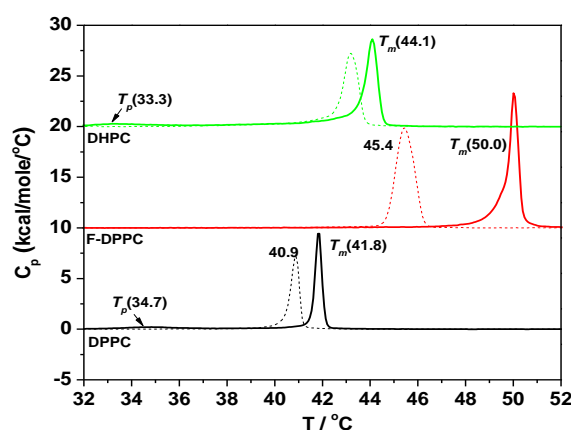
Figure 5.9: DSC-thermograms for aqueous sonicated DPPC, F-DPPC and DHPC. The bold lines are the melting transitions whereas the dotted lines are the corresponding crystallization peaks.

The phase transitions in DHPC appear similar to those observed for the corresponding ester lipid DPPC. The main transition occurs at relatively higher temperature of 44°C, which is from the rippled gel phase to fluid bilayer phase. However, the pre-transition occurs from an interdigitated gel phase to rippled gel phase and takes place at 33.3°C. The observed DSC transitions are in agreement with those available in literature.[144–146,227] Hence, DHPC is different from both DPPC and F-DPPC in a way, that it produces an interdigitated gel phase, but it is transformed to ripple gel phase instead of going directly to fluid phase like F-DPPC (Figs. 5.9 & 5.10). The enthalpies for pre-transition and main phase transition are 1.3 kcal mol^{-1} and 8.1 kcal mol^{-1}, respectively.[144] The molecular arrangements are dependent on degree of hydration and only the fully

hydrated dispersions show interdigitation.[94] The LE-LC transition begins at higher lateral pressure for DHPC monolayers compared to that of DPPC. From this, one would expect the exhibition of lower T_m for gel-fluid phase transition by DHPC than for the similar transition in DPPC.[73] This relationship between the LE-LC onset pressure in monolayers and T_m in the corresponding bilayers state does not hold for DHPC because of interdigitation in the gel phase of this ether lipid.
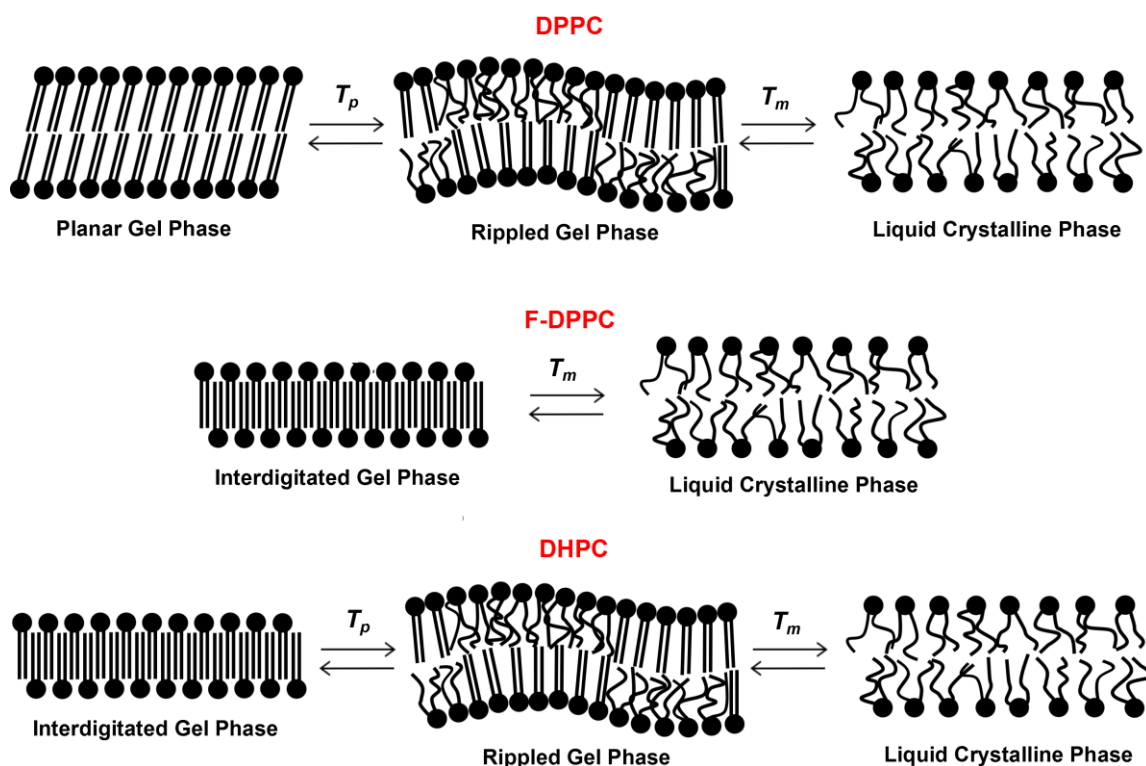
Figure 5.10: Phase transitions in fully hydrated DPPC, F-DPPC and DHPC.[91]

The studies done with mixtures of DPPC and DHPC reveal that the interdigitation persists in the presence of DPPC, and the main transition is affected most upon DPPC incorporation[146]. The interdigitated phase in DHPC has low tolerance for cholesterol and vanishes completely in mixtures containing only 5% cholesterol.[147] A sub-transition in DHPC also occurs, showing a change in packing from orthorhombic to hexagonal.[89]

5.2.2 Effect of Amphiphilic and Polyphilic Block Copolymers on Phase Transition of DHPC

The perfluorinated hydrocarbons are rigid structures and lack flexibility shown by the hydrocarbons. To our perception, they resemble cholesterol's backbone. Since

cholesterol eliminates interdigitation in DHPC, the insertion of inflexible perfluorinated moieties might produce similar effects, especially when osmotic stress produced by hydrophilic block could also prevent interdigitation.[222]

Effect of Perfluoroalkylation: GP vs FGP

The addition of GP or FGP to DHPC bilayers eliminates the pre-transition and reduces the main phase transition temperature (Fig. 5.11). The trade-off between interactions at the lipid heads and hydrophobic van der Waals forces determines the overall change in T_m.[46]
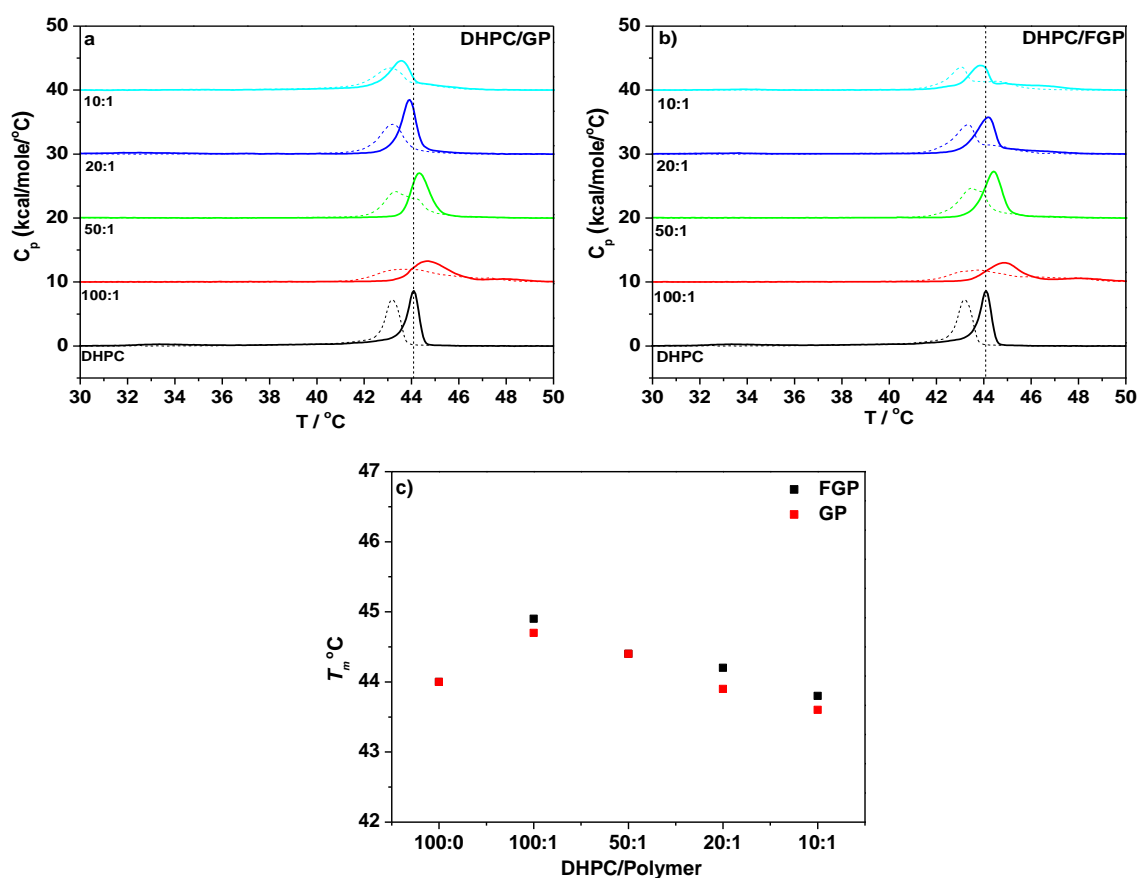
Figure 5.11: DSC-thermograms for lipid/polymer mixtures: a) DHPC/GP; and b) DHPC/FGP. d) Transition temperature for DHPC/GP and DHPC/FGP sonicated mixtures.

For DHPC, the pre-transition disappears in the mixtures showing that interdigitation is abolished upon polymer addition. T_m increases slightly for 1% polymer, but further addition causes a decrease in the transition temperature. The peaks are broadened and a higher temperature shoulder becomes visible with scans rates of 0.5°C min^{-1}. These thermograms resemble DHPC scans observed in the mixtures comprising 10 to 20 percent cholesterol[147]. For 100:1 mixture, the change in T_m is affected by the interactions between the PGMA blocks and lipid head groups. With an increase in the

_____

polymer content in the lipid dispersions, the intercalation of hydrophobic/fluorophilic segments of polymers into the lipid alkyl chains takes place and causes a lowering in the main phase transition temperature.

Effect of PGMA Block Length in Semitelechelic Polymers: GF40 vs GF14

A comparison of DSC thermograms of mixtures of DHPC with GF14 and GF40 are shown in Fig. 5.12. The DSC thermograms are quite similar, which indicates that PGMA block length has a negligible effect on the main transition temperature.
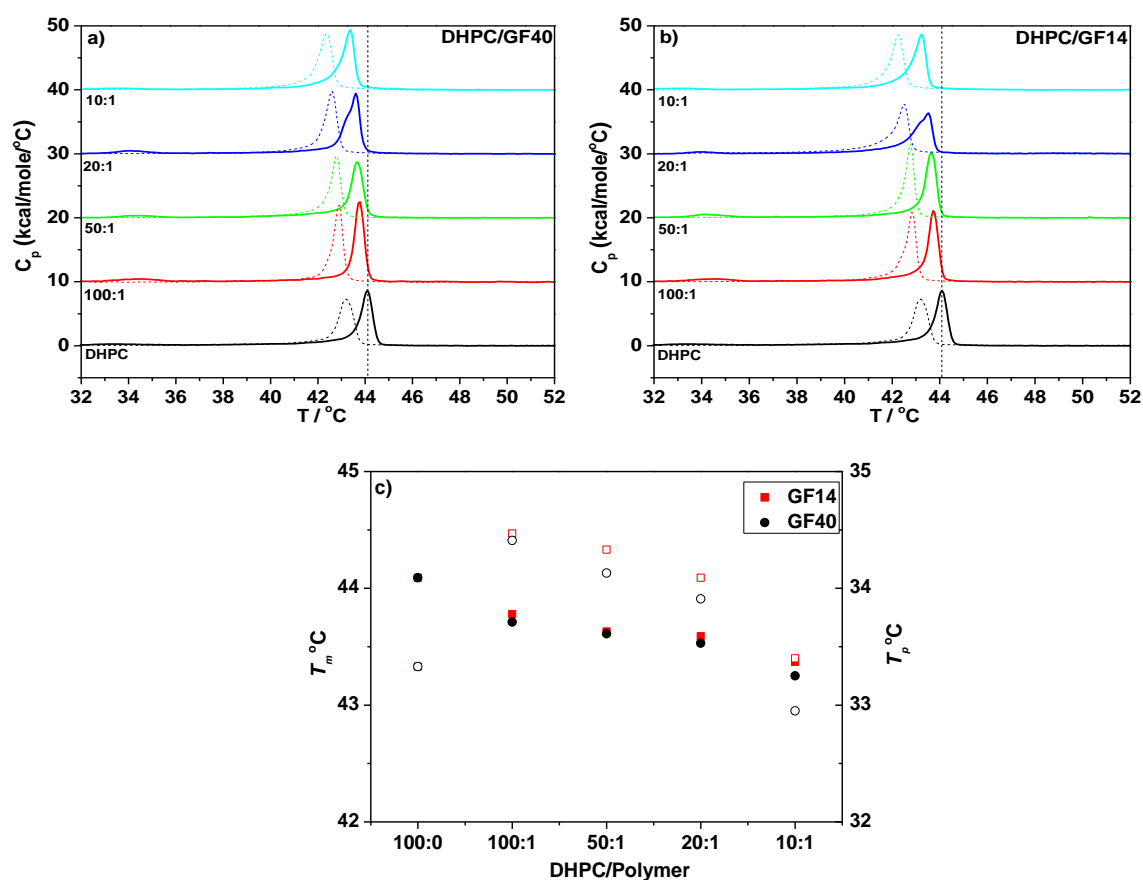
Figure 5.12: DSC-thermograms for lipid/polymer mixtures: a) DHPC/GF40; and b) DHPC/GF14. c) Transition temperature for DHPC/GF14 and DHPC/GF40 sonicated mixtures (Open symbols are for pre-transition).

T_m decreases with increase in polymer content in the lipid/polymer mixtures. However, the effect is only slightly greater for GF40. The value of ΔT_m is 1°C. The transition from rippled gel phase ($P_{\beta'}$) to fluid phase (L_α) in DHPC is similar to that of DPPC, which is not altered much after GF14 addition.[39] A less clear trend in T_m has been reported previously for DPPC mixtures with GF40.[39] The endotherms are slightly broadened, reflecting a

reduction in cooperativity of the transition from $P_\beta{}'$ to L_α phase of the lipid, owing to polymer presence.

The behavior of lipid/polymer mixtures is rather complex and minor transitions appear as shoulder in the heating scans. A micro phase separation may result from incorporation of F9 segments in the lipid bilayers, giving rise to additional transitions overlapping with the main phase transition. Obviously, the parts of membrane still lack order in the ripple gel phase and polymer retention is possible. The packing density in DPPC monolayers is lower than that in DHPC monolayers. This is due to an ether link between alkyl chains and glycerol unit in DHPC compared to an ester as in DPPC. The pre-transition temperatures of DHPC dispersions initially increase and then decrease with subsequent increase in proportion of semitelechelic polymers.

The pre-transition that represents transformation of an interdigitated gel phase ($L_\beta I$) to rippled gel phase ($P_\beta{}'$) in DHPC is affected to a greater extent compared to the main phase transition, and the impact of block length is visible. The ethanol partitioning is facilitated in the $L_\beta I$-phase, where more sites are available for binding of small solutes (such as ethanol) compared to those available in the L_β-phase.[92] Interaction of lipid head groups with hydroxyls in PGMA may favor interdigitation and produce an increase in transition temperatures. On the other hand, interaction of lipid alkyl chains with intercalated fluorophilic F9 segments can produce the opposite effects and cause a decrease in T_m. The overall change in T_m is reflective of both the above mentioned impacts. Another scenario is that the insertion of perfluoroalkyl chains into the lipid bilayers may also pull PGMA blocks in the vicinity of lipid headgroups, thus enhancing the probability of polymer-lipid interaction.

5.2.3 Conclusions

- In DHPC dispersions, first a transition from an interdigitated to rippled gel phase occurs before the main transition into the liquid-crystalline phase is seen. This is different for F-DPPC, where the main phase transition occurs directly from an interdigitated gel phase to the corresponding fluid phase.

_____

- The pre-transition of DHPC vanishes upon polymer (FGP or GP) addition to the lipid dispersions reflecting an adoption of normal bilayer motif by the DHPC molecules. The trends in T_m indicate the binding of PGMA units to the lipid headgroups for low polymer content in mixed dispersions. With an increase in polymer content, the insertion of PPO blocks and perfluoroalkyl segments into the lipid alkyl chains occurs, causing the hydrophobic forces to dominate.

- In the case of semitelechelic polymers, comparable impacts on T_m are produced by GF40 and GF14, with a negligible effect of the PGMA block length. T_m values are lowered with increase in polymer content in the DHPC/polymer mixtures, reflecting the prevalent hydrophobic interactions. On the other hand, the trend in T_p is representative of some stabilization of the interdigitated states and the impact of GF40 is greater than GF14.

_____

6   INVESTIGATIONS OF THE CATIONIC LIPID EDPPC

The additional esterification of the phosphate group of DPPC with an ethyl group produces the cationic derivative 1,2-dipalmitoyl-*sn*-glycero-3-ethylphosphocholine (EDPPC) which is highly biocompatible and degradable by the *phospholipases.*[138] In fact, this lipid represents a class of synthetic lipids that is used for DNA and RNA transfection.[138,137] The phase transition behavior of EDPPC is similar to that of F-DPPC, because it forms an interdigitated gel phase ($L_\beta I$) that transforms directly to liquid crystalline phase (L_α), without passing through an intermediate rippled gel phase (P_β').

6.1   Monolayer Studies

6.1.1 Pure Lipid
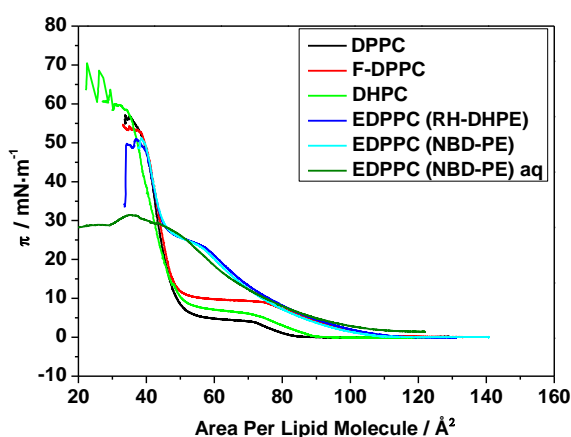
Figure 6.1: Compression isotherms for different lipids (DPPC and F-DPPC on aqueous subphase and EDPPC on 0.1M sodium chloride subphase and aqueous subphase).

The pressure-area isotherms for various lipids including EDPPC are given in Fig. 6.1**.** The area per lipid molecule occupied by EDPPC is greater than that of DPPC, DHPC and F-DPPC. This is due to electrostatic repulsive forces and larger cross-sectional area of the cationic head form other lipids investigated in the present work. When EDPPC is spread on pure water, it does not undergo condensation upon compression and remains in the expanded phase until the monolayer collapses at a low surface pressure of 28 mN m^{-1}. On 0.1M aqueous sodium chloride as subphase, the head group repulsions are reduced and LE-LC transition is observed at π = 23.5 mN m^{-1}.

Fig. 6.2 contains a collection of FM-images of EDPPC monolayers on 0.1M NaCl subphase. The LC-domains are small and disappear with further condensation when visualized using RH-DHPE.
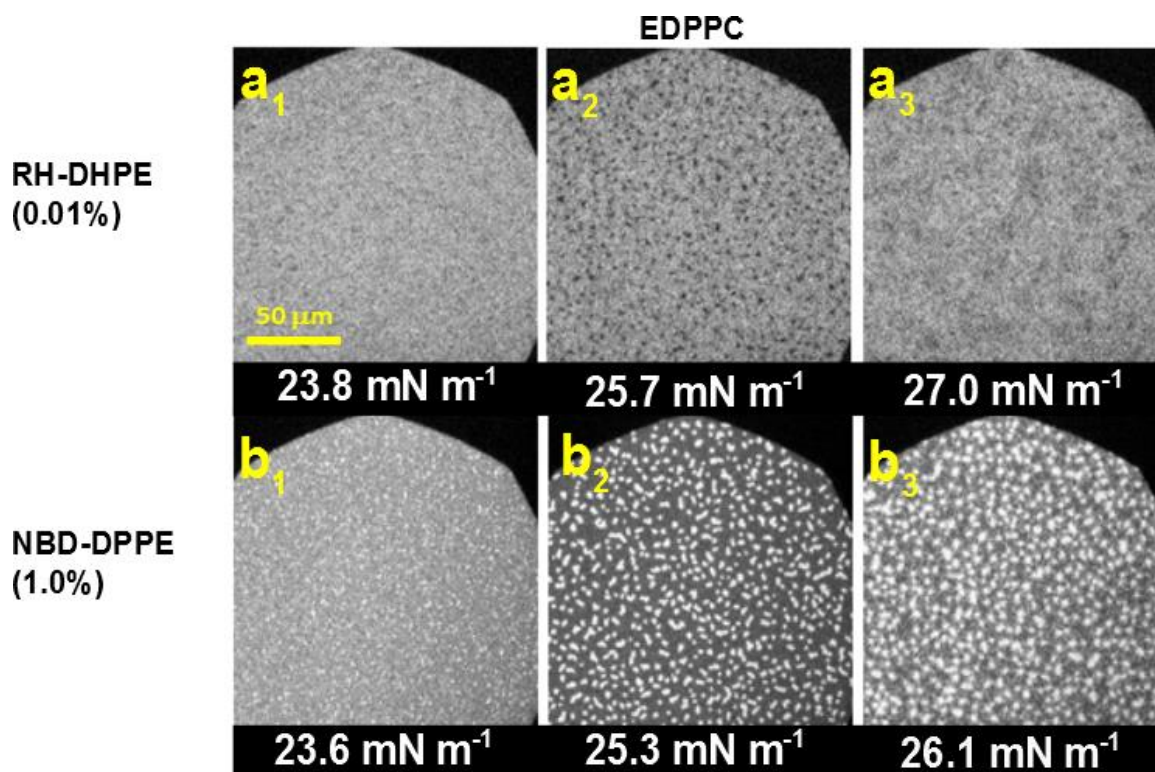
Figure 6.2: LC-domains of EDPPC monolayers in the presence of different dyes a) 0.01% RH-DHPE; and b) 1.0% NBD-DPPE. The recordings were made on 0.1M sodium chloride subphase.

The probing of phase transition utilizing NBD-DPPE produces white condensed domains, which are irregular shaped and slightly bigger in size. This fluorescent probe undergoes condensation it-self[198] and can initiate nucleation of EDPPC. The π-A isotherms of EDPPC recorded in the presence of RH-DHPE and NBD-DPPE overlap showing that the small percentages of probes have no effect on LE-LC phase transition of EDPPC. The difference in the lipid LC domains in the presence of two probes is explainable, keeping in view the presence of the negatively charged phosphate group in NBD-DPPE, which allows a stronger binding with cationic lipid head. The smaller size of NBD moiety allows this probe to fit among the lipid head groups in the LC phase and prevents it exclusion. RH-DHPE, on the other hand is larger in size and is essentially excluded from the LC lipid.

_____

6.1.2 Effect of Amphiphilic and Polyphilic Block Copolymers on Phase Transition of EDPPC

Effect of Perfluoroalkylation: GP vs. FGP

Time-dependent Adsorption of Polymers to Preformed Lipid Monolayers
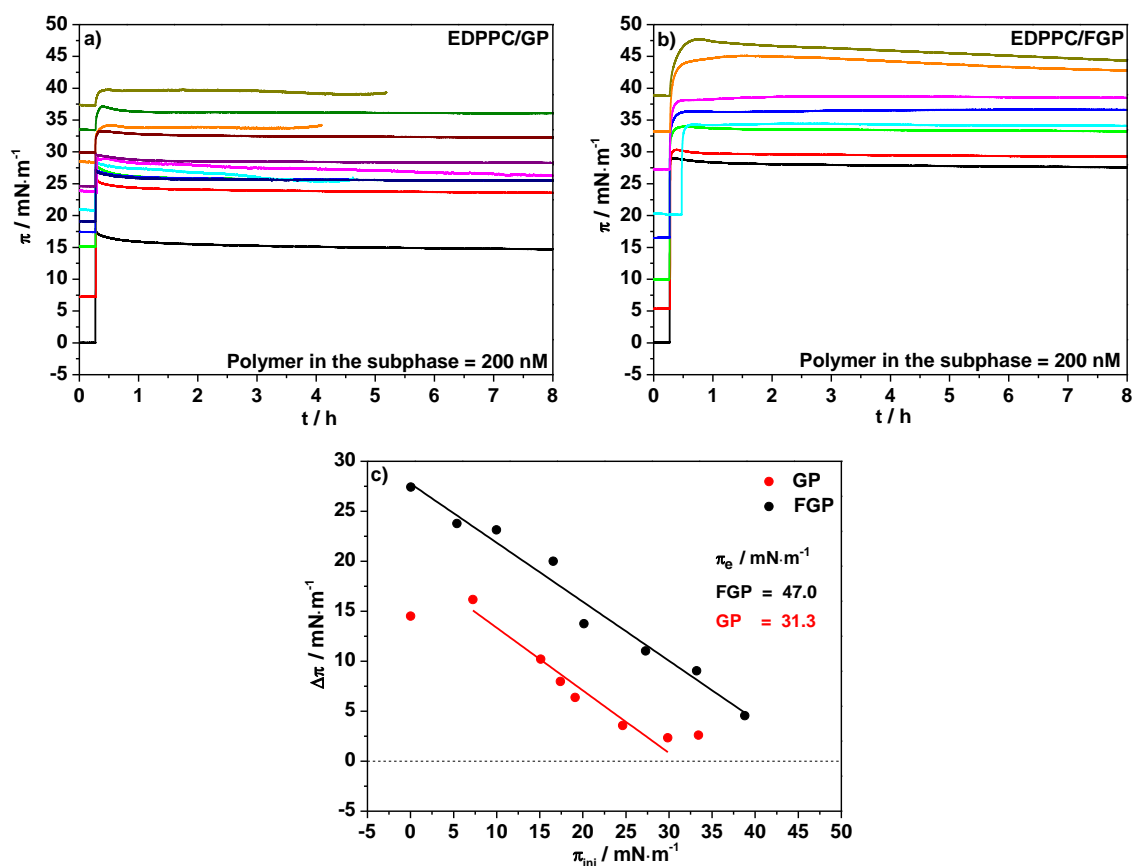
Figure 6.3 : Time dependent adsorption of polymers to EDPPC monolayers spread at different initial pressures a) 200 nM GP; b) 200 nM FGP; c) Plot of $\Delta\pi$ *vs.* π_{ini} for FGP and GP.

Polymer injection under EDPPC monolayers causes an increase in surface pressure (Fig. 6.3). At smaller initial pressures of an EDPPC monolayer, the insertion takes place immediately after injection, because the lipid remains in the liquid expanded phase mostly. A reduction in polymer insertion occurs for $\pi_{ini} > 25$ mN m^{-1}, indicated by a decrease in $\Delta\pi$-values. Nevertheless, some polymer reaches the surface even at high π_{ini}. Again, FGP inserts to a larger extent into EDPPC monolayers than GP. The maximal insertion pressures obtained by extrapolating π_{ini} vs $\Delta\pi$ plot to $\Delta\pi = 0$ reveal much higher value for FGP, that is, 47 mN m^{-1}., whereas GP is excluded from EDPPC at pressures comparable to those obtained with F-DPPC and DHPC. In the case of EDPPC, π_e

_____

~ 31 mN m^{-1} for GP (Fig. 6.3c). For same amount of the polymer injected into the subphase, the surface activity of FGP is higher on 0.1M sodium chloride subphase than on a pure water subphase. On the other hand, the surface activity of GP is hardly dependent on the subphase type. Since FGP and GP differ only in the presence or absence of perfluoroalkyl segments, it can easily be concluded that the presence of perfluorinated moieties are directly responsible for enhanced surface activity in FGP. Also, the π_e exhibited by FGP is significantly large for its adsorption to EDPPC monolayers, which is also reflective of a preference of perfluoroalkyl segments for lipid alkyl chain over salt containing subphase.

Compression Isotherms and Epifluorescence Microscopy
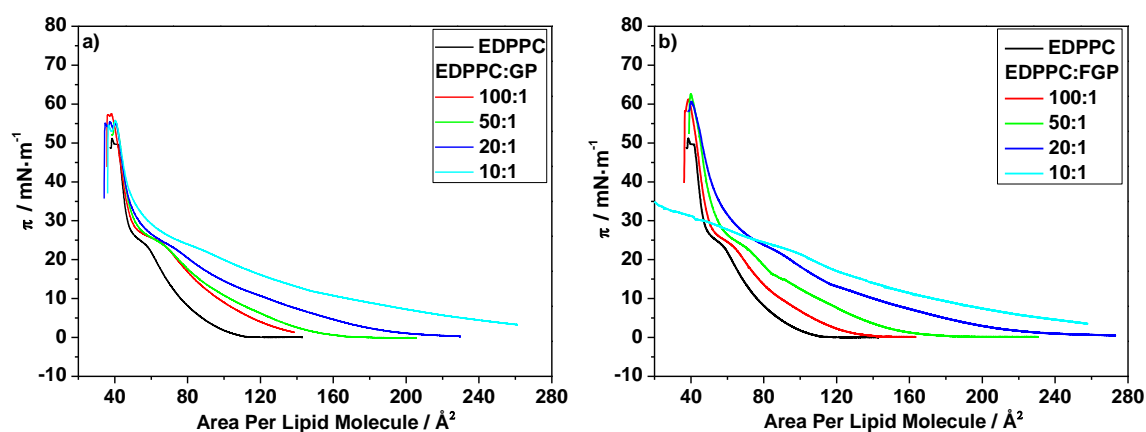
Figure 6.4: Compression isotherms for a) EDPPC/GP; and b) EDPPC/FGP mixtures.

The difference in the behavior of FGP and GP observed in the adsorption study is also visible in the compression isotherms given in Fig. 6.4. The π-A plots show that GP is excluded at π = 35 mN m^{-1}. For FGP, the exclusion occurs near 50 mN m^{-1} depending upon the amount of polymer in EDPPC/FGP mixtures. There is a shift in area per lipid molecule with increased polymer content in the mixtures. With 1% polymer, the $\varDelta A$ (FGP) < $\varDelta A$ (GP), pointing towards the phenomenon of looping of hydrophilic blocks in sub-phase because of hydrophobic nature of F9 chains, which abstain from lying flat on the water surface. For 10% FGP, a destabilization of EDPPC monolayer occurs during condensation, and surface pressure rises less steeply than for the other mixtures. Here the second phase transition of polymer is not observed because the LE-LC phase transition of EDPPC coincides with the mushroom-brush transition of the polymer that

involves the expulsion of PPO-blocks. The plateau is smeared out with an increase in polymer content due to greater overlapping of the two phase transitions mentioned above.

Table 6.1: Shift in areas available per lipid molecule (ΔA) in a monolayer after FGP and GP addition recorded at different surface pressures.

Lipid/ polymer ratio (moles)	ΔA / Å^2 molec^{-1} (EDPPC) at various surface pressures (π)							
	4 mN m^{-1}		15 mN m^{-1}		27 mN m^{-1}		35 mN m^{-1}	
	EDPPC/ GP	EDPPC/ FGP	EDPPC/ GP	EDPPC/ FGP	EDPPC/ GP	EDPPC/ FGP	EDPPC/ GP	EDPPC/ FGP
100:1	28.9	20.0	15.5	8.8	5.0	3.6	1.3	2.2
50:1	39.9	46.4	18.4	21.7	6.5	9.3	2.3	5.6
20:1	73.8	97.9	29.9	43.0	9.5	19.6	3.0	10.3
10:1	156.9	158.9	58.5	65.4	17.0	14.4	5.2	--

The head group of EDPPC is more hydrophobic than DPPC and insertion of hydrophobic/fluorophilic components is facilitated. The π-A isotherms recorded for EDPPC/FGP monolayers do not overlap with that of pure EDPPC monolayer, indicating the retention of FGP in the lipid, even at surface pressures in the vicinity of the collapse pressures. This polymer retention is a most probable cause of the destabilization of the monolayer in EDPPC/FGP (10:1) mixture.

The thin white LC-domains for EDPPC containing 1% FGP vanish over a short range of pressures (Fig. 6.5). The size of domain decreases after FGP/GP addition to F-DPPC and DHPC. EDPPC acts likewise. For mixtures containing GP, the domains are organized and more compact. Thinning occurs for 2% polymer. For 20:1 and 10:1 mixtures, the condensed domains could not be visualized due to the resolution limit of the microscope. The LE-LC coexistence region is reduced in width and smeared out.

An increased presence of the perfluorinated chains among the lipid alkyl chains on the dilute aqueous NaCl subphase causes the destabilization of the cationic monolayer. On contrary, the binding of PGMA block to the cationic heads reduces the headgroup repulsions. Consequently, the LC domains attain more organized patterns and grow bigger in size in EDPPC/GP mixed monolayers, compared to those in pure EDPPC monolayers. With an increase in polymer content in the mixture, the hydrophobic

interactions between PPO chains and the lipid alkyl segments start to dominate, causing a reduction in the domain size.
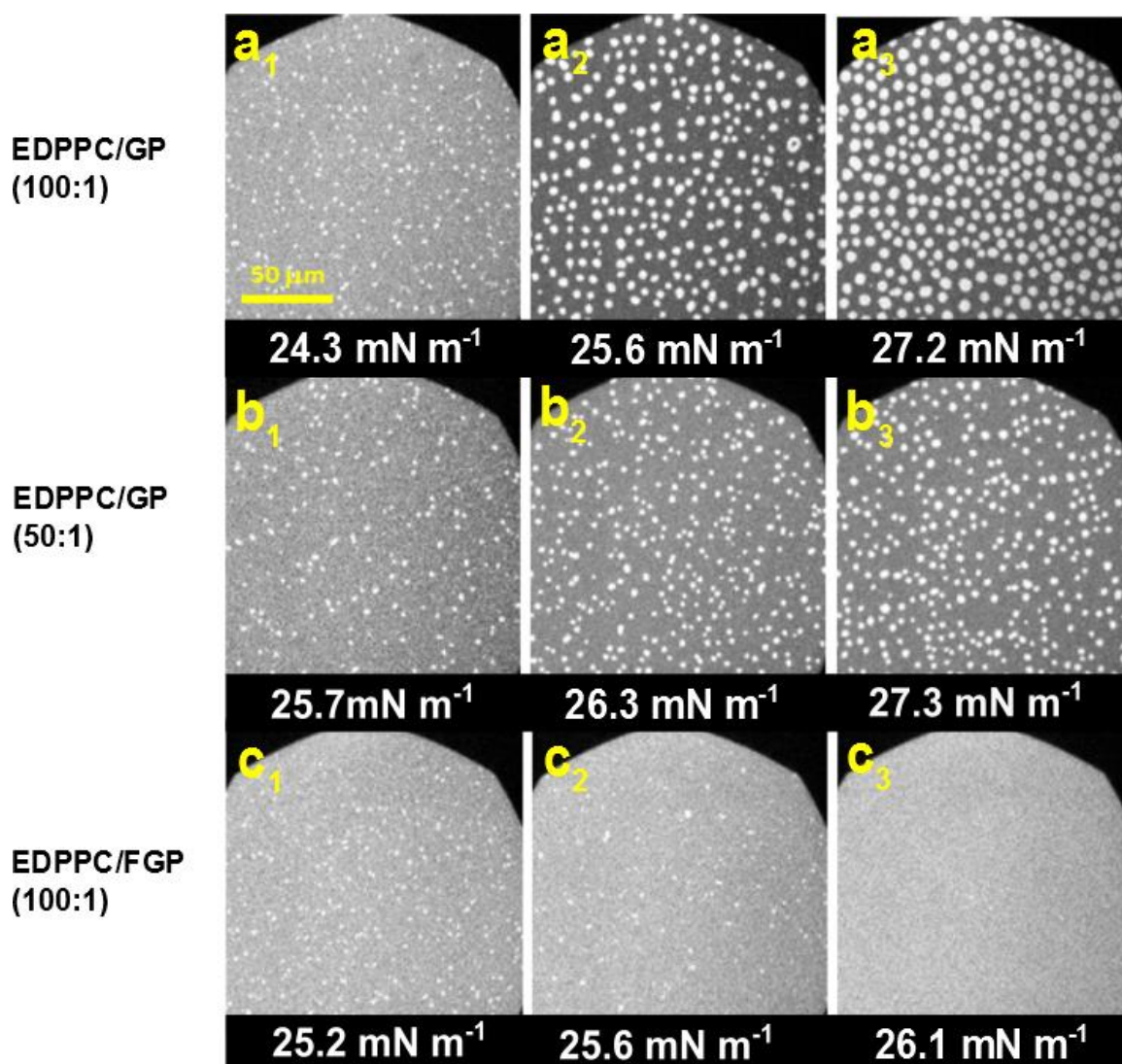
Figure 6.5: LC-domains for a) EDPPC/GP (100:1); b) EDPPC/GP (50:1) and c) EDPPC/FGP (100:1) co-spread monolayers containing 1.0% NBD-DPPE and on 0.1M NaCl subphase.

Effect of PGMA Block Length in Semitelechelic Polymers: GF40 vs GF14

Finally, the semitelechelic polymers GF40 and GF14 were studied again to learn about the impact of PGMA block length on interactions with EDPPC. This provides also an insight into effects produced by the absence of hydrophobic PPO block. Because these polymers demonstrate lower surface activity, their concentration used in the subphase was twice as high as that of GP/FGP. Again, 0.1M aqueous sodium chloride instead of pure water was used as subphase.

Time-dependent Adsorption of Polymers to Preformed Lipid Monolayers

The polymer injection under bare air/water interface produced a change in surface pressure of ~ 4.5 mN m^{-1} for GF14 and about 6.5 mN m^{-1} for GF40 possessing a PGMA block twice as large as GF14 (Figs. 6.6 a & b).
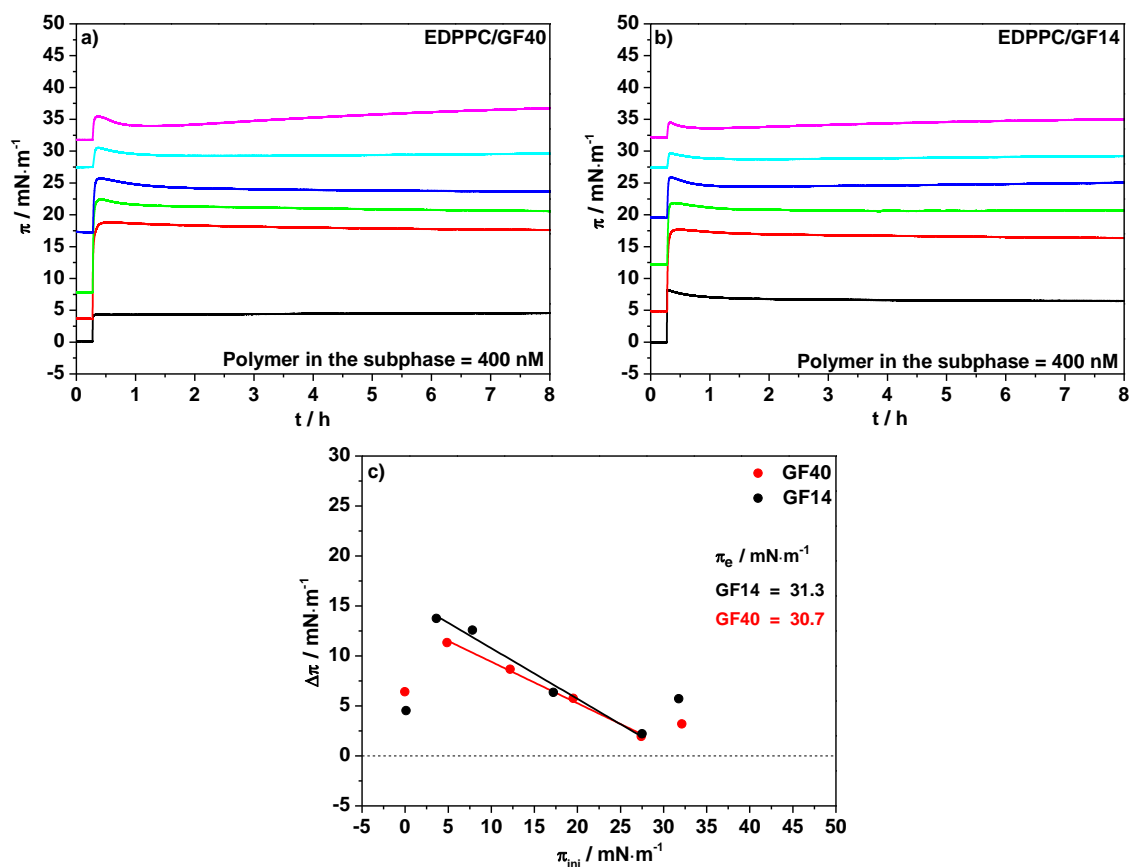
Figure 6.6: Time-dependent adsorption of polymers to EDPPC monolayers spread at different initial pressures a) 400 nM GF40; b) 400 nM GF14; c) Plot of $\Delta\pi$ vs. π_{ini} for GF40 and GF14.

The surface activity of GF14 does not change in the presence of sodium chloride, however the surface activity of GF40 appears to be higher than that on pure water. It has already been established in the preceding section that the attachment of PGMA block with perfluorinated cap is necessary for enhancement of surface activity in salt solution, but negligible change in surface activity of GF14 revealed that the PGMA block was not sufficiently long for such effects. The presence of saturated aqueous salt solution in the subphase significantly alter the surface activity of hydrophilic PEO polymers.[228] However, the low salt concentration used in this work is hardly enough to produce similar effects on PGMA units in the semitelechelic polymers. The plot of $\Delta\pi$ vs. π_{ini} shows a decrease in $\Delta\pi$ values for higher π_{ini} (Fig. 6.6c).

_____

For surface pressures representing the LE-LC co-existing region of the lipid, the $\Delta\pi$ values fall to a minimum, showing that the lipid molecules allow very little access to polymer. The exclusion pressures derived for GF14 and GF40 are comparable, in spite of different slopes. They are indistinguishable from those obtained for the injection of these polymers into the subphase underneath F-DPPC and DHPC monolayers.

Compression Isotherms and Epifluorescence Microscopy
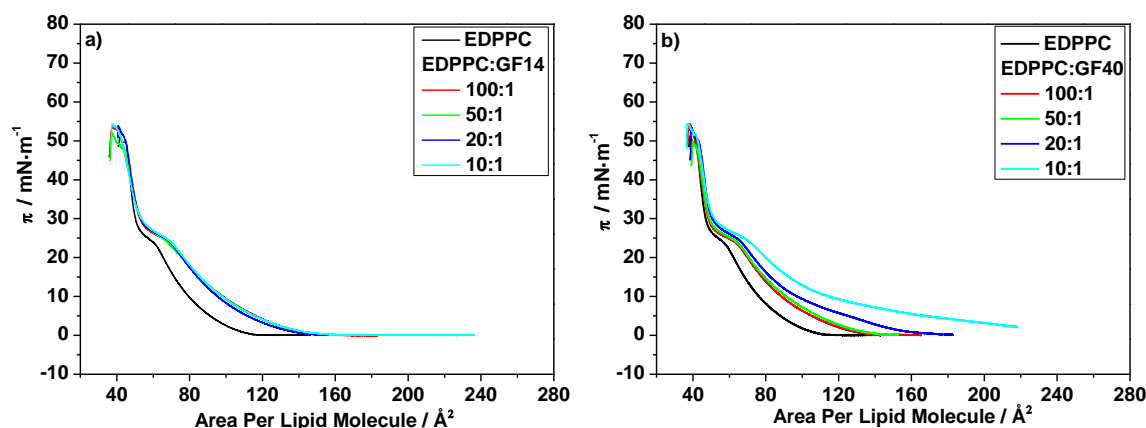
Figure. 6.7: Compression isotherms for a) EDPPC/GF14; and b) EDPPC/GF40 mixtures.

The compression isotherms for EDPPC/GF14 mixtures show very little dependence on the percentage of polymer in the mixtures. Not only, the π-A plots overlap for all mixtures, but also give comparable ΔA values. DPPC monolayers when co-spread with 10% GF14 experience similar shifts.[39] This is expected because of small PGMA block that on average contains only 14 GMA units.

Table 6.2: Shift in areas available per lipid molecule (ΔA) in a monolayer after GF40 and GF14 addition recorded at different surface pressures.

Lipid/ polymer ratio (moles	ΔA / Å^2 molec^{-1} (EDPPC) at various surface pressures (π)							
	4 mN m^{-1}		15 mN m^{-1}		27 mN m^{-1}		35 mN m^{-1}	
	EDPPC/ GF40	EDPPC / GF14	EDPPC / GF40	EDPPC / GF14	EDPPC / GF40	EDPPC / GF14	EDPPC / GF40	EDPPC / GF14
100:1	18.7	26.6	9.6	13.9	2.6	4.9	1.1	1.4
50:1	22.3	25.9	11.0	13.6	4.2	6.0	1.3	1.6
20:1	40.9	21.8	14.2	12.5	7.2	6.0	2.6	1.7
10:1	94.0	25.9	24.3	14.3	10.3	7.0	2.8	1.1
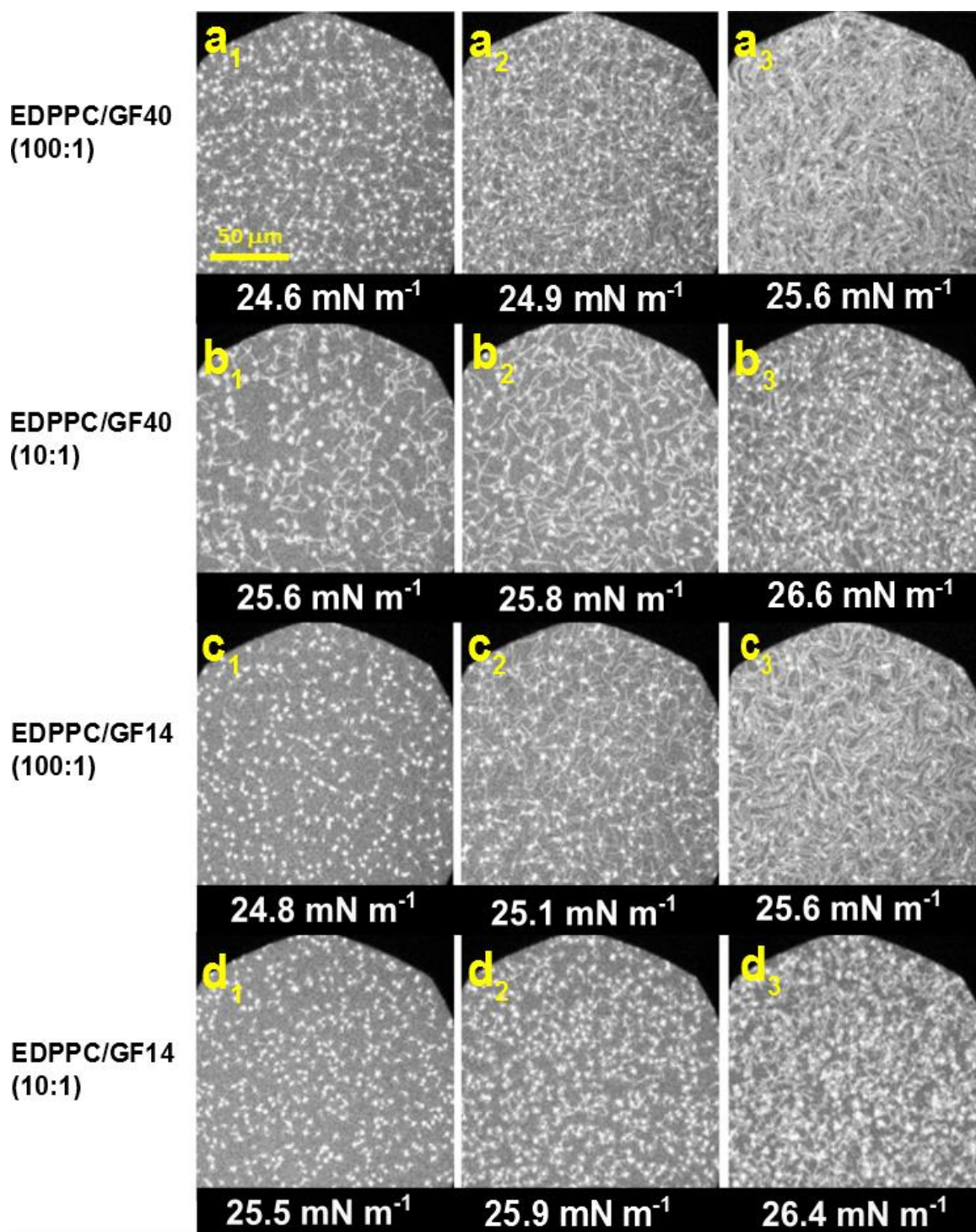
Figure 6.8: LC-domains for a) EDPPC/GF40 (100:1); b) EDPPC/GF40 (10:1); c) EDPPC/GF14 (100:1); and d) EDPPC/GF14 (10:1) co-spread monolayers containing 1.0% NBD-DPPE and on 0.1M NaCl subphase.

Another factor is the larger head group of EDPPC, which contains an ethyl group attached to oxygen of phosphate group and can be considered as a DPPC monolayer

with ethanol molecules existing in the head group region. For GF40, variation in ΔA is clearly dependent on moles of polymer. These results are summarized in Fig. 6.7.

The LC-domains occurring upon compression were imaged with NBD-DPPE. The domain shapes are quite exceptional. The small white domains first grow spikes, which upon compression, evolve into strands and finally lead to a thin thread like network extending over the whole area of monolayer (Fig. 6.8).

The semitelechelic polymers act as lineactant and cause thinning of DPPC domains[39], but the effect noted in this study has a greater resemblance to DPPC mixtures with CGPR, where an unusual triskelion pattern was observed.[117] It is possible to correlate the thinning effect to the length of PGMA block by comparing EDPPC mixtures containing equal percentages of GF14 and GF40, where larger PGMA block has a greater impact. This effect in our view is due to retention of the polymer in the condensed monolayers of lipids, which is in accordance with the observation made during the adsorption studies, where the polymer injection underneath EDPPC monolayers at π_{ini} above 30 mN m^{-1} still produced an increase in surface pressure. Apparently, the polymers can insert into regions adjacent to LC domains leading to a reduction of line tension with concomitant thinning of the domains.

6.1.3 Conclusions

- The cationic lipid EDPPC remains in the LE phase on pure water subphase but exhibits an LE-LC phase transition on aqueous NaCl subphase due to the reduction in the headgroup repulsions. The onset of LE-LC phase transition in cationic monolayers occurs at a surface pressure of about 23 mN m^{-1}, which is markedly different from those recorded for phase transition in F-DPPC (8.1 mN m^{-1}) and DHPC ($\sim$ 3 mN m^{-1}) monolayers.

- The condensed domains in EDPPC monolayers are small and disorganized. They appear either white or black depending upon the type of fluorescent lipid probe and NBD-DPPE appears to be more suitable to monitor the domain formation than RH-DHPE.

_____

- FGP with its fluorinated alkyl chains has a higher surface activity on NaCl subphase than pure water is used. It has a greater affinity than the other polymers to the EDPPC monolayers, and is retained in the lipid monolayers up to surface pressures of above 45 mN m^{-1}. The exclusion of GP from EDPPC monolayers occurs at a surface pressure of about 31 mN m^{-1}, which is similar to that obtained after the injection of this polymer underneath F-DPPC and DHPC monolayers.

- Both, FGP and GP, cause enormous thinning of LC domains in EDPPC/polymer monolayers having low polymer content. The increase in FGP content has a destabilizing effect on mixed monolayers, which exhibit an early collapse.

- The semitelechelic polymers, GF14 and GF40 are easily retained also in the rims of the condensed domains and produced thread like structures, a clear indication for their accumulation at the domain boundaries and their line active properties.

6.2   Bilayer Studies

The cationic P-O-ethyl phosphatidylcholines are degradable by the enzymes such as *phospholipase A*, and therefore are considered biocompatible lipids despite their cationic nature.[138] Their most promising application is the delivery of genetic materials to cells, commonly known as gene transfection.[136] In the past, studies have been contributed to unveil the mechanism of this phenomenon[229] and to highlight the properties of EDPPC and EDOPC bilayers.[134,96] In the proceeding sections, the effect of polymers on the thermotropic phase behavior of EDPPC will be described.

6.2.1 Thermotropic Phase Behavior of EDPPC

The thermotropic phase behavior of DPPC along with its derivatives used in present study, as observed by microcalorimetry (DSC) is given in Fig. 6.9. The main phase transition temperature is 41.8°C, which represents a transition from an interdigitated gel phase ($L_\beta I$) to a liquid crystalline phase (L_α) without passing through a rippled gel phase (P_β'). This value of T_m is is comparable to those available in the literature.[96,134] The LE-LC transition begins at significantly higher surface pressure for EDPPC monolayers compared to those of DPPC. Therefore, the transition temperature for corresponding

gel-fluid phase transition in EDPPC bilayers is expected to be much lower than that of DPPC. In actual, the T_m of EDPPC is greater than gel to fluid transition temperature exhibited by DPPC membranes.[73] This discrepancy originates from the interdigitation in the gel phase of the cationic lipid EDPPC.
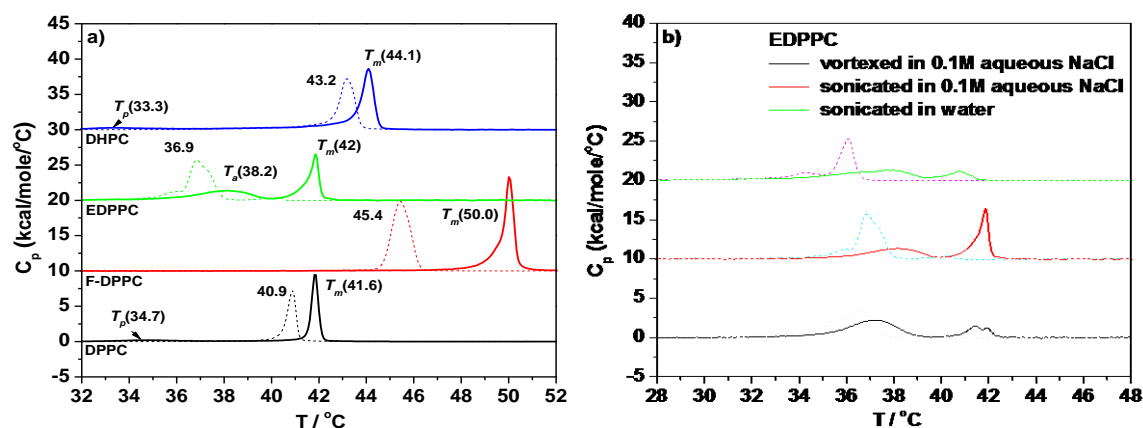
Figure 6.9: a) DSC-thermograms for aqueous sonicated DPPC, F-DPPC and DHPC; b) Thermotropicphase behavior of EDPPC samples prepared in different ways. The bold lines are the melting transitions whereas the dotted lines are the corresponding crystallization peaks.

Another lower temperature transition centered at 38.2°C was observed in our sample in pure water and also in preparations in 0.1M aqueous NaCl and vortexed or sonicated above phase transition temperature. This transition designated as an additional transition (with transition temperature T_a) has never been reported before for the pure lipid, however a presence of the stacks of interdigitated bilayers manifest itself as an additional peak in the exotherm[135]. Koynova and McDonald reported an additional transition in the similar region for DPPC containing 30% EDPPC.[230] This was only possible after significant sample degradation. Before further investigation, the acquired sample of EDPPC was checked for its purity by TLC where it gave only a single spot. It was therefore assumed that the additional transition was due to the existence of the stacks of interdigitated or normal bilayers. This is not far-fetched considering the fact that ethanol addition causes a lowering in transition temperature and leads to the formation of interdigitated sheets[231] and also because sonication (*i.e.,* agitation) partially extinguishes the transition occurring at ~ 38°C (Fig. 6.9b). The vesicle formation is prevented in lipid dispersions in pure water[232], which also supports this proposition. A reduction in electrostatic repulsive forces among cationic lipid head groups is possible in

_____

the presence of sodium chloride. However, it appears that the salt concentration, *i.e.,* 0.1M is not sufficient to completely eliminate these repulsions and therefore, the vesicle formation is partly inhibited. The hysteresis between endotherms and exotherms is comparable to that of F-DPPC, which is reflective of the phase transition from an interdigitated gel phase to the corresponding fluid phase.

The presence of an additional phase transition in DSC has been reported for anionic lipid DPPG in the presence of different amounts of sodium chloride.[233,234] When NaCl concentration is low, the T_m of DPPG dispersions are shifted to lower values compared to that in pure water. Small cations such as Na$^+$ and K$^+$ inhibit interdigitation in the gel phase of DPPG.[235] Since $T_a < T_m$ for EDPPC and the additional transition peak is very broad, it is probable that the lamellar stacks comprise partly of the non-interdigitated bilayer gel phase.

DMPG membranes show an unusual melting behavior and vesicles convert to a three dimensional membrane network in aqueous dispersions, depending upon the ionic strength.[232] Consequently, the melting peak splits into three overlapping transitions. Also, there exists a temperature dependent equilibrium between the flat and curved membrane segments. In conclusion, a coexistence of stacks or sheets (or neworks) and vesicles is highly probable in charged phospholipid membranes.

6.2.2 Effect of Amphiphilic and Polyphilic Block Copolymers on Phase Transition of EDPPC

Effect of Perfluoroalkylation: GP vs. FGP

The DSC thermograms of EDPPC/GP and EDPPC/FGP mixtures are collected in Fig. 6.10. These mixtures were treated in the similar fashion to that of pure EDPPC, that is, they were premixed, hydrated with 0.1M aqueous NaCl and the resulting dispersions were sonicated above the main phase transition temperature of the lipid.

The transition at 38.2°C disappears in all lipid/polymer mixtures, which indicates that the vesicle formation is facilitated by the polymers. Since the intercalation of PPO and F9 segments of the polymers into lipid alkyl chains promotes non-interdigitation, the

_____

disappearance of this additional transition suggests that this peak in DSC is not due to presence of partially interdigitated phases. The DNA molecules due to their anionic nature form lipoplexes with cationic lipids, where the DNA is sandwiched between the adjacent layers in the lamellar stacks comprising of interdigitated bilayers[135]. The polymers utilized in the present study carry no charged moieites, therefore their complexation with EDPPC and resulting stabalization of lipid stacks is not possible.
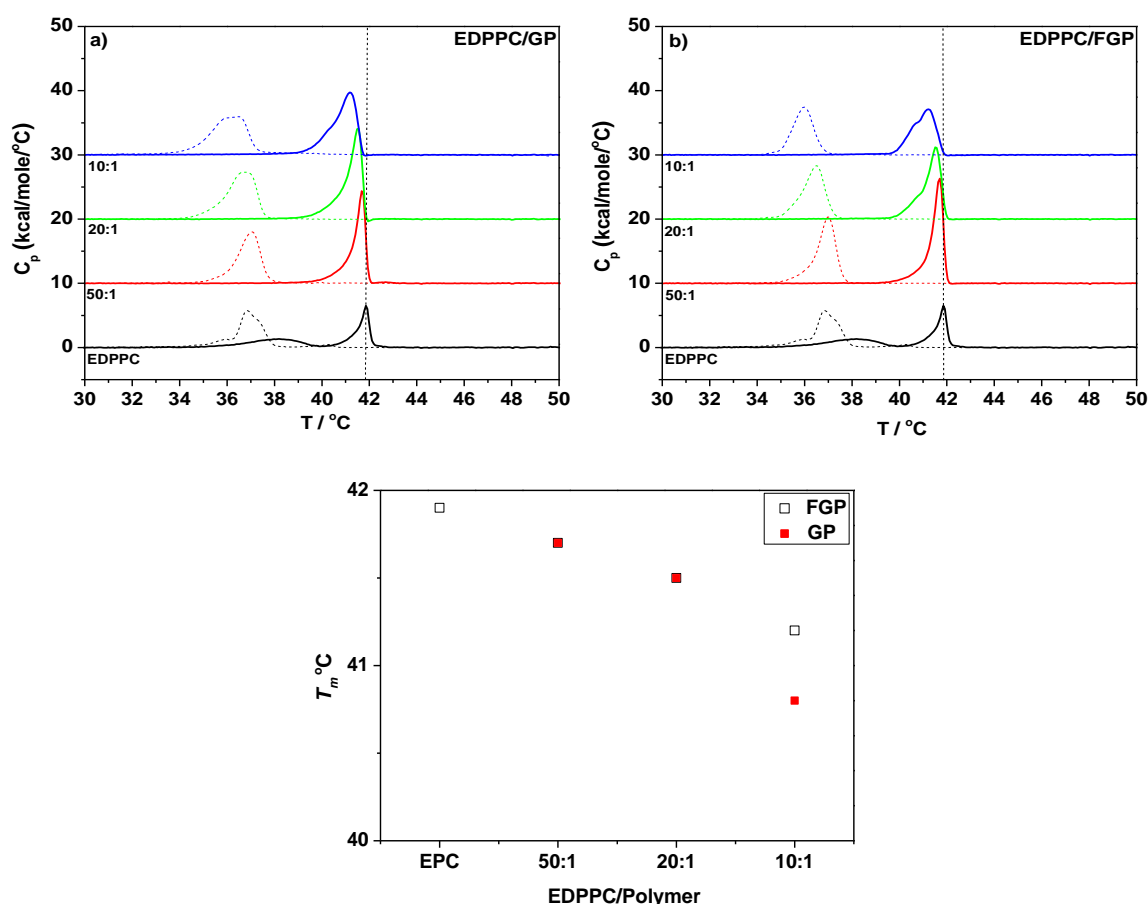
Figure 6.10: DSC-thermograms for lipid/polymer mixtures: a) EDPPC/GP; and b) EDPPC/FGP. (The dotted lines are the corresponding cooling scans); c) Transition temperature for EDPPC/GP and EDPPC/FGP sonicated mixtures.

A lowering in the main transition temperature, T_m occurs with increased polymer content. In fact, hardly any differences of the effect of FGP and GP on T_m could be observed. Smith and Dea[91] have recently reviewed most of the aspects of the interdigitated gel phase. Due to an additional esterification of the phosphate in lipid with an ethyl group makes the lipid head more hydrophobic and causes a decrease in polarity of the interface.[110,134] This enhances the probability of the localization of the

_____

hydrophobic blocks of GP and FGP in the lipid head group region. For EDPPC/FGP (10:1) mixture, a shoulder appears in the endotherm showing the occurrence of a minor transition that overlaps with the main phase transition. Such behavior is likely because of the inhibitory effects of FGP on interdigitation, as observed also in the case of F-DPPC and DHPC.

Effect of PGMA Block Length in Semitelechelic Polymers: GF40 vs GF14
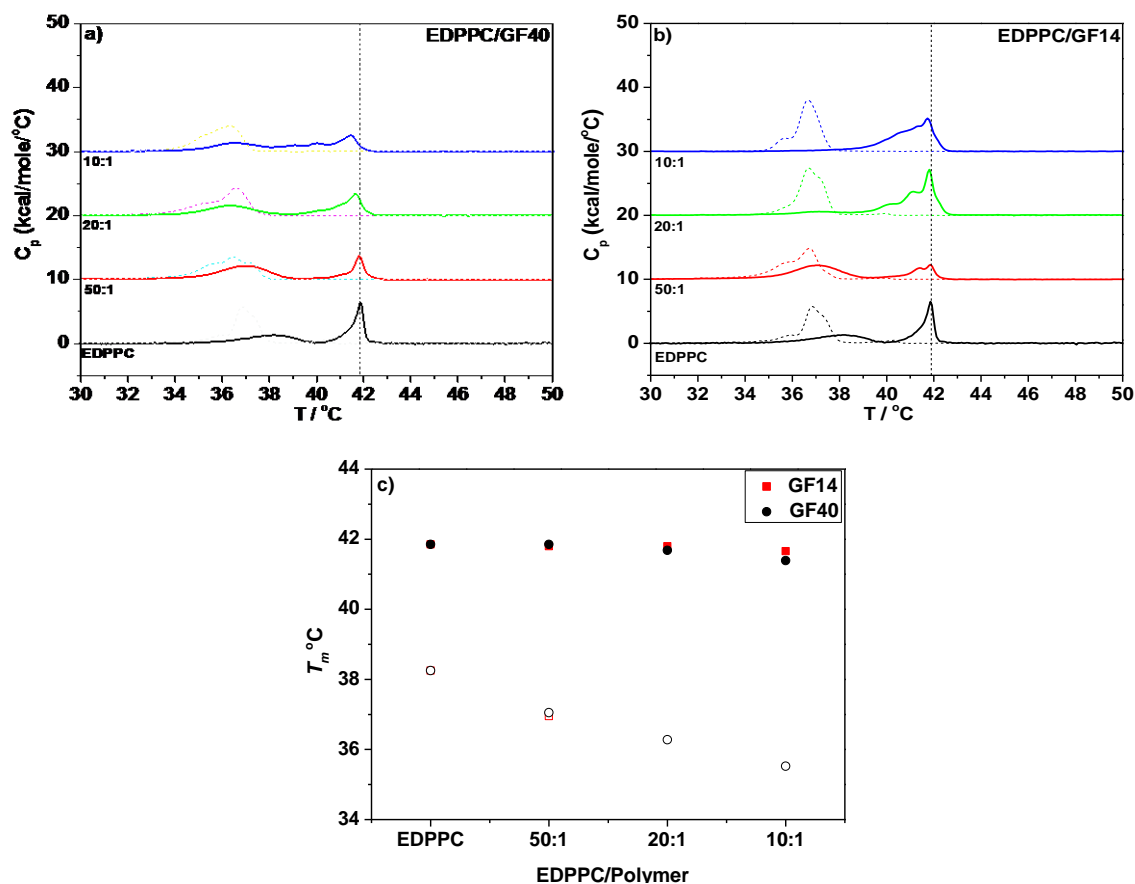
Figure 6.11: DSC-thermograms for lipid/polymer mixtures: a) EDPPC/GF40; and b) EDPPC/GF14. The dotted lines are the corresponding cooling scans. d) Transition temperature for EDPPC/GF40 and EDPPC/GF14 sonicated mixtures. (Open symbols are for pre-transition).

The DSC thermograms for EDPPC/GF40 and EDPPC/GF14 mixtures are gathered in Fig. 6.11. In both the cases, the main phase transition temperature, T_m is hardly altered with increase in polymer content. For EDPPC mixtures with GF40, the transition temperature T_a decreases with increase in moles of polymer in the mixture. The endotherms are significantly broadened in 10:1 mixture and two transitions start to overlap. On contrary, the second transition occurring at 38.2°C for the pure lipid vanishes with increase in polymer content for EDPPC/GF14 mixtures. Based on these observations, it can be

inferred that the lengthening of PGMA block in the semitelechelic polymers favors the existence of interdigitated lipid bilayers into stacks or sheets. Most probably the elongation of the hydrophilic PGMA block allows the polymer to occupy the inter-bilayer space and stabilize these stacks. Similar diversity in populations based on lipid vesicles and lamellar stacks have also been observed in EDPPC complexes with DNA.[135] The hysteresis between heating and cooling scans for lipid/polymer systems, which reflects interdigitation, is prevalent and it is because the interdigitation for EDPPC is not dependent on hydration degree, and EDPPC undergoes interdigitation even in the dry form.

6.2.3 Conclusions

- Two endothermic transitions are observed in EDPPC dispersions prepared in pure water or 100 mM aqueous sodium chloride, indicative of the coexistence of lamellar sheets (comprising of non-interdigitated bilayers) and interdigitated vesicles.

- The hydrophobic interactions dominate in EDPPC/polymer dispersions. For FGP and GP T_m is reduced with increase in polymer content, simply because the head group in EDPPC is more hydrophobic than that of DPPC. The additional transition vanishes after polymer addition to EDPPC dispersions, which suggests that this additional transition does not originate from the presence of the partially interdigitated phases.

- The main phase transition splits into overlapping transitions and the endotherm is broadened in EDPPC dispersions containing G40/GF14, showing a phase separated system.

- The additional transition prevails in all mixtures of EDPPC with GF40, clearly showing a support for existence of lamellar stacks upon elongation of the hydrophilic PGMA block.

- Interdigitation is sustained in all EDPPC/polymer mixtures because the hysteresis between endotherms and exotherms is not changed, at least for the main phase transition.

7   SUMMARY

The water-soluble amphiphilic and polyphilic polymers based on hydrophilic PGMA block/s, hydrophobic PPO block/s and fluorophilic perfluorinated segments have significance for pharmacy and related areas of application. The interactions of some of these polymers have been studied with model membranes composed of phospholipids. It has been reported previously by our group that the binding of the polymers to these model membranes is dependent on the length and type of alkyl chains and the nature of the head group in the lipid. In order to extend these investigations, the present study was designed with three aims:

- To highlight the response of the above mentioned polymers to change in phospholipid structure other than alteration of the alkyl chain length or switching of choline moiety by ethanolamine in the lipid head. For this purpose, a tail modified monofluorinated F-DPPC, a head group modified cationic EDPPC, and an ether linked DHPC were investigated in monolayers as well as bilayers for their interactions with different types of block copolymers.

- To unravel the potential of these synthetic phospholipids to mimic biomembranes through comparison with DPPC, especially in monolayers.

- To observe the impact of these block copolymers on the interdigitated gel phase of the above mentioned lipids.

Interactions in Langmuir and Gibbs monolayers and monitoring of the phase transitions in pure and mixed monolayers utilizing epifluorescence microscopy allowed the portrayal of the candidature of the lipids as membrane models and brought into light some additional aspects of lipid-polymer interactions. The differential scanning calorimetry was employed to observe the impact of the block copolymers on interdigitated gel phases. The vesicle fusion in extruded F-DPPC dispersions was studied by the cryo electron microscopy.

Monolayers of Pure Lipids and Lipid Mixtures

Monolayer compression experiments reveal the following trends in lateral pressure at the onset of LE-LC phase transition in the monolayers of the investigated lipids.

EDPPC > F-DPPC > DHPC > DPPC

EDPPC due to large head group repulsions and increased head group hydrophobicity, F-DPPC due to the affinity of fluorine atom for aqueous surface and its larger size compared to hydrogen atom and DHPC because of the absence of carbonyl groups differ in their packing density in the monolayers than that of DPPC monolayers. The preliminary IRRAS studies indicate that the alkyl chains tilt in the LC phase of F-DPPC is similar to that of DPPC.

The LC domains in lipid monolayers have fractal patterns and the domain size is dependent on the type of lipid. The size decreases in the following order:

$$F\text{-}DPPC > DPPC \geq DHPC > EDPPC$$

The LC-domain size and form of F-DPPC monolayers are highly sensitive to the compression rate. Kinetic effects are responsible for irregular LC domain shapes. The widening of the LE-LC transition region is possible due to localization of the fluorine atom at sn-2 chain terminus close to water surface, which can lead to branching in the condensed aggregates.

The high LE-LC onset pressure, small LE-LC coexistence region, and low screening of charges on a dilute aqueous sodium chloride subphase are responsible for small sized LC-domains in EDPPC monolayers.

Unlike DPPC, the headgroup region of DHPC is less hydrated the subphase due to the absence of carbonyl groups. The cross-sectional area is smaller leading to a reduced chain tilt compared to DPPC. The the LE-LC transition in DHPC is less clearly defined and has a low cooperativity.

The appearance of LC-domains of lipids showed a dependence on the type of fluorescent probe used. Black domains were observed with RH-DHPE and NBD-12HPC because both of these labels were expelled from the LC phase. The retention of NBD-DPPE in the LC phase of the lipids resulted in white LC domains. RH-DHPE was found to be the appropriate probe to monitor the phase coexistence in monolayers of F-DPPC ,

DHPC and DPPC whereas NBD-DPPE appeared better suited for visualizing EDPPC monolayers.

The *quasi-racemate* between D-DPPC and L-FDPPC exhibited multi-lobed complex patterns of condensed lipid different from those reported for monolayers comprise of the equimolar mixture between L- and D-DPPC. Such complex patterns reflected a chiral phase separation.

Adsorption of Polymers to Preformed Lipid Monolayers

All polymers utilized in the present study (except EF44) showed a tendency to insert near or above the monolayer-bilayer equivalence pressure in PC membranes. FGP demonstrated significantly high penetrability into EDPPC monolayers and was retained in cationic monolayers up to a surface pressure of 47 mN m^{-1}. The insertion capacity of FGP and other polyphilic and amphiphilic polymers into the monolayers of other modified lipids was similar to that demonstrated for their adsorption to DPPC monolayers. The reversal of block sequence and enlargement of hydrophilic and hydrophobic blocks (as in PFG78) slowed down polymer insertion into DPPC and F-DPPC monolayers, but did not alter the maximal insertion pressure appreciably. This indicates that the modified lipids did not differ much from DPPC in the order of their alkyl chains and compressibility and hence it is possible to harness their potential as model membranes.

Approximately, three lipid molecules exist on the surface for each polymer molecule, when 400 nM of polymer is present in the subphase, underneath the lipid monolayer in the condensed phase. The lipid/polymer ratio exceeds 6:1, when the subphase concentration is reduced to 200 nM. This also depends on polymer size and its surface activity. Based on the adsorption experiments, it was possible to develop a general trend of the penetration capacity of polymers into the monolayers of the modified lipids:

FGP (200 nM) > PFG78 (200 nM) > CPGR (200 nM) > GP (200 nM) $\geq$ GF40 (400 nM) $\geq$ GF14 (400 nM) > EF44 (400 nM)

The perfluoroalkyl segments have greater impact on membrane insertion capability of the polymer when they are not constrained (as in PFG78). A comparison between FGP

_____

and CPGR indicates that perfluorinated segments can anchor the polymer in a lipid monolayer similarly as a cholesterol anchor. It can be concluded that the presence of PPO block as well the perfluoroalkyl segments in the same polymer were requisite for demonstration of better penetrability in the lipid monolayers and bilayers.

Monolayer Behavior of Lipid/Cholesterol and Lipid/Polymer/Cholesterol Mixtures

Cholesterol produces condensation and fluidization of LE and LC phase of lipid, respectively. The LE-LC coexistence region is smeared out in a 2:1 mixture between F-DPPC and cholesterol. The surface pressure of above 23 mN m^{-1} could not be reached by spreading of an equimolar lipid/cholesterol mixture. Polyphilic FGP could not reduce the effects produced by small amounts of cholesterol (1-2%) in the monolayer comprising of F-DPPC/FGP (10:1) mixture.

LC-domains in Mixed Lipid/Polymer Monolayers

In the presence of about 10% polymer in the mixture, the fractal LC domains in lipid monolayers became more compact but their size was also reduced. The line active properties of the polymers, exhibited in mixed monolayers with DPPC was not observed in the monolayers consisting of their mixtures with F-DPPC. The widening of the LE-LC transition region, due to kinetic effects, probably did allow the line-tension to come into play. An exception was CPGR, which caused the thinning of domain boundaries owing to the presence of the cholesterol anchor in the lipid monolayers. However, this effect was different from the unusual thinning of triskelion patterns induced by this polymer of the LC domains in DPPC monolayers. The reduction in line tension was observed in monolayers of the lipid/polymer mixtures of other modified lipids, where for DHPC the LC domains grew fuzzy upon compression. A thread like network was formed in EDPPC monolayers in the presence of GF40 and GF14 . FGP caused the destabilization of mixed monolayers in the case of DHPC and EDPPC. The domain size was also markedly reduced and no LC domains were seen for all mixtures containing more than 1% polymer in the co-spread monolayers.

Interdigitated Phases in Pure Lipids and Lipid/Polymer Mixtures

In extruded aqueous dispersions of F-DPPC, fusion of interdigitated unilamellar vesicles occurred and caused the endotherm to split into two closely spaced transitions. This temperature driven hemifusion that generated partially interdigitated phase was confirmed by cryo-TEM images of the lipid dispersions. The main phase transition temperature was reduced in the presence of all the polymers, indicating the dominance of hydrophobic interactions resulting from the intercalation of PPO blocks and perfluoroalkyl segments into the lipid alkyl chain region. The lipid molecules increasingly adopted the normal bilayer motif with increase in polymer content in the mixture, giving rise to a phase segregated system, as indicated by the broadening of endotherms and the appearance of new peaks at temperatures lower than T_m. However, a complete change to the normal bilayer gel phase was not achieved. The polyphilic polymers produced greater impacts when premixed with F-DPPC, compared to when they were added to preformed lipid vesicles. The amphiphilic polymer GP showed insensitivity to method of preparation of the mixed dispersion.

The interdigitation was completely eliminated in sonicated premixed dispersions of FGP and GP with DHPC, because the pre-transition that represented the change from interdigitated gel phase to the rippled gel phase was abolished. Only the transition from the rippled gel to the liquid-crystalline phase prevailed. The penetration of hydrophobic PPO and fluorophilic F9 segments of these polymers produced voids or defects in the interdigitated phase of DHPC. The initially produced partially interdigitated phase transformed to normal bilayer in order to prevent exposure of lipid alkyl chains to water. On the other hand, the semitelechelic polymers stabilized the interdigitated states in DHPC, showing the favorable binding of PGMA blocks with lipid head groups. Therefore, both pre- as well as the main transition were observed with GF40 and GF14.

Two transitions were observed in EDPPC dispersions due to presence of lamellar sheets comprised of lipid bilayers and vesicles with interdigitated lipids. The thermotropic phase behavior of EDPPC was somewhat similar to that reported for DMPG dispersions[232]. This esterified DPPC derivative has a larger cross-sectional area of

headgroup, which is also more hydrophobic than that of DPPC. Hence, the incorporation of hydrophobic and fluorophilic polymer chains into the bilayers was facilitated, causing a lowering in T_m. The splitting and broadening of endotherms reflected the phase separated system, most probably comprised of a partially interdigitated phase coexisting with a normal bilayer phase. The additional transition was abolished in EDPPC mixtures with FGP and GP, but it prevailed in more hydrophilic GF40, indicating the stabalization of lamellar sheets by PGMA blocks.

8 APPENDIX

8.1 Materials

8.1.1 Lipids and Lipid Probes

1,2-dipalmitoyl-*sn*-glycero-3-phosphocholine (L-DPPC) and 2,3-Dihexadecanoyl-*sn*-glycero-1-phosphocholine (D-DPPC) were purchased from Sigma-Aldrich (Schnelldorf, Germany), whereas 1-palmitoyl-2-(16-fluoropalmitoyl)-*sn*-glycero-3-phosphocholine (F-DPPC); 1,2-di-O-hexadecyl-*sn*-glycero-3-phosphocholine (DHPC) and 1,2-dipalmitoyl-*sn*-glycero-3-ethylphosphocholine (EDPPC) as chloride salt were acquired from Avanti Polar Lipids (Alabaster, Alabama, USA). Cholesterol was also the product of Avanti Polar Lipids. Fluorescently labelled lipids 1,2-dipalmitoyl-*sn*-glycero-3-phosphoethanolamine- N-(lissamine rhodamine B sulfonyl)(triethylammonium salt) (RH-DHPE); 2-(12-(7-nitrobenz-2-oxa-1,3-diazol-4-yl)amino)dodecanoyl-1-hexadecanoyl-*sn*-glycero-3-phosphocholine (NBD-12HPC) and 1,2-dipalmitoyl-*sn*-glycero-3-phosphoethanolamine-N-(7-nitro-2,1,3-benzosadiazol-4-yl))(triethylammonium salt) (NBD-DPPE) were from Invitrogen (Karlsruhe, Germany). The purity of all these products was above 99% and they were used as received.

8.1.2 Block Copolymers

PGMA based amphiphilic and polyphilic block copolymers were supplied by working group of Prof. Jorg Kressler, Physical Chemistry of Polymers, Institute of Chemistry, Martin-Luther University, Halle-Wittenberg. Their synthesis has been reported elsewhere.[28,39,150,152,153] Rhodamine labelled block copolymer possessing the cholesterol anchor was synthesized at Institute of Organic Chemistry, Johannes-Gutenberg University, Mainz in the group of Prof. Dr. Holger Frey, which recently appeared in the literature.[117]

8.1.3 Other Chemicals

Chloroform and methanol of HPLC-grade were obtained from Carl Roth GmbH & Co KG (Karlsruhe, Germany). Sodium chloride was supplied by the same company. Ultrapure water from a Milli-Q Advantage A10 System of Millipore S.A.S., Molsheim Cédex, France

_____

was utilized. The conductivity of water was below 0.055 μS cm^{-1} and *TOC* less than 5 ppb

at 25°C. Hellmanex$^{\circledR}$ was from Hellma GmbH, Müllheim, Germany.

References

1.	Singer, S. J. & Nicolson, G. L. The fluid mosaic model of the structure of cell membranes. *Science* **175,** 720–731 (1972).

2.	Nicolson, G. L. The Fluid—Mosaic Model of Membrane Structure: Still relevant to understanding the structure, function and dynamics of biological membranes after more than 40years. *Biochim. Biophys. Acta - Biomembr.* **1838,** 1451–1466 (2014).

3.	Hancock, J. F. Lipid rafts: contentious only from simplistic standpoints. *Nat. Rev. Mol. Cell Biol.* **7,** 456–62 (2006).

4.	Lingwood, D. & Simons, K. Lipid rafts as a membrane-organizing principle. *Science* **327,** 46–50 (2010).

5.	Kraft, M. L. Plasma membrane organization and function: moving past lipid rafts. *Mol. Biol. Cell* **24,** 2765–8 (2013).

6.	Goychuk, I., Kharchenko, V. O. & Metzler, R. How Molecular Motors Work in the Crowded Environment of Living Cells: Coexistence and Efficiency of Normal and Anomalous Transport. *PLoS One* **9,** e91700 (2014).

7.	Missner, A. & Pohl, P. 110 years of the Meyer-Overton rule: Predicting membrane permeability of gases and other small compounds. *Chem. Phys. Chem.* **10,** 1405–1414 (2009).

8.	Al-Awqati, Q. One hundred years of membrane permeability: does Overton still rule? *Nat. Cell Biol.* **1,** E201–E202 (1999).

9.	Korlach, J., Schwille, P., Webb, W. W. & Feigenson, G. W. Characterization of lipid bilayer phases by confocal microscopy and fluorescence correlation spectroscopy. *Proc. Natl. Acad. Sci. U. S. A.* **96,** 8461–8466 (1999).

10.	Truong-Quang, B.-A. & Lenne, P.-F. Membrane microdomains: from seeing to understanding. *Front. Plant Sci.* **5,** 18 (2014).

11.	Eeman, M. & Deleu, M. From biological membranes to biomimetic model membranes. *Biotechnol. Agron. Soc. Environ.* **14,** 719–736 (2010).

12.	Pabst, G., Kucerka, N., Nieh, M.-P., Rheinstädter, M. C. & Katsaras, J. Applications of neutron and X-ray scattering to the study of biologically relevant model membranes. *Chem. Phys. Lipids* **163,** 460–79 (2010).

13. Pignatello, R., Musumeci, T., Basile, L., Carbone, C. & Puglisi, G. Biomembrane models and drug-biomembrane interaction studies: Involvement in drug design and development. *J. Pharm. Bioallied Sci.* **3,** 4–14 (2011).

14. Janshoff, A. & Steinem, C. Mechanics of lipid bilayers: What do we learn from pore-spanning membranes? *Biochim. Biophys. Acta - Mol. Cell Res.* **1853,** 2977–2983 (2015).

15. Lee, D. W. *et al.* Relating domain size distribution to line tension and molecular dipole density in model cytoplasmic myelin lipid monolayers. *Proc. Natl. Acad. Sci. U. S. A.* **108,** 9425–9430 (2011).

16. Zumbuehl, A., Dobner, B. & Brezesinski, G. Phase behavior of selected artificial lipids. *Curr. Opin. Colloid Interface Sci.* **19,** 17–24 (2014).

17. Krafft, M. P. Fluorocarbons and fluorinated amphiphiles in drug delivery and biomedical research. *Adv. Drug Deliv. Rev.* **47,** 209–228 (2001).

18. Malanovic, N. *et al.* Phospholipid-driven Differences Determine the Action of the Synthetic Antimicrobial Peptide OP-145 on Gram-positive Bacterial and Mammalian Membrane Model Systems. *Biochim. Biophys. Acta* **1848,** 2437–2447 (2015).

19. Yu, H. *et al.* A New PAMPA Model Proposed on the Basis of a Synthetic Phospholipid Membrane. *PLoS One* **10,** e0116502 (2015).

20. Hardy, M. D. *et al.* Self-reproducing catalyst drives repeated phospholipid synthesis and membrane growth. *Proc. Natl. Acad. Sci.* **112,** 8187–8192 (2015).

21. Holme, M. N. *et al.* Shear-stress sensitive lenticular vesicles for targeted drug delivery. *Nat. Nanotechnol.* **7,** 536–543 (2012).

22. Mahrhauser, D.-S. *et al.* Simultaneous determination of active component and vehicle penetration from F-DPPC liposomes into porcine skin layers. *Eur. J. Pharm. Biopharm.* **97,** 90–95 (2015).

23. Händel, C. *et al.* Cell membrane softening in human breast and cervical cancer cells. *New J. Phys.* **17,** 83008 (2015).

24. Mai, Y. & Eisenberg, A. Self-assembly of block copolymers. *Chem. Soc. Rev.* **41,** 5969 (2012).

25. Liu, G., Dupont, J., Dou, H., Njikang, G. & Hu, J. Morphologies of Micelles of ABC Linear and Miktostar Triblock Copolymers. *Polym. Prepr.* **51,** 1–6 (2010).

26. Kowal, J., Zhang, X., Dinu, I. A., Palivan, C. G. & Meier, W. Planar biomimetic membranes based on amphiphilic block copolymers. *ACS Macro Lett.* **3,** 59–63 (2014).

27.   Zhao, L. & Lin, Z. Self-assembly of non-linear polymers at the air/water interface: the effect of molecular architecture. *Soft Matter* **7,** 10520 (2011).

28.   Amado, E., Kerth, A., Blume, A. & Kressler, J. Infrared reflection absorption spectroscopy coupled with brewster angle microscopy for studying interactions of amphiphilic triblock copolymers with phospholipid monolayers. *Langmuir* **24,** 10041–10053 (2008).

29.   Riess, G. Micellization of block copolymers. *Prog. Polym. Sci.* **28,** 1107–1170 (2003).

30.   Mecozzi, Sandro. Kwon, G. S. Semi-fluorinated block copolymers for delivery of therapeutic agents. *US Pat. 8,900,562 B2* (2014).

31.   Decato, S., Bemis, T., Madsen, E. & Mecozzi, S. Synthesis and characterization of perfluoro-tert-butyl semifluorinated amphiphilic polymers and their potential application in hydrophobic drug delivery. *Polym. Chem.* **5,** 6461–6471 (2014).

32.   Kita-Tokarczyk, K., Grumelard, J., Haefele, T. & Meier, W. Block copolymer vesicles - Using concepts from polymer chemistry to mimic biomembranes. *Polymer (Guildf).* **46,** 3540–3563 (2005).

33.   Binder, W. H. Polymer-Induced Transient Pores in Lipid Membranes. *Angew. Chemie Int. Ed.* **47,** 3092–3095 (2008).

34.   Shelat, P. B., Plant, L. D., Wang, J. C., Lee, E. & Marks, J. D. The Membrane-Active Tri-Block Copolymer Pluronic F-68 Profoundly Rescues Rat Hippocampal Neurons from Oxygen-Glucose Deprivation-Induced Death through Early Inhibition of Apoptosis. *J. Neurosci.* **33,** 12287–12299 (2013).

35.   Fakhrullin, R. F., Zamaleeva, A. I., Minullina, R. T., Konnova, S. a. & Paunov, V. N. Cyborg cells: functionalisation of living cells with polymers and nanomaterials. *Chem. Soc. Rev.* **41,** 4189 (2012).

36.   Amado, E., Kerth, A., Blume, A. & Kressler, J. Phospholipid crystalline clusters induced by adsorption of novel amphiphilic triblock copolymers to monolayers. *Soft Matter* **5,** 669 (2009).

37.   Wang, R. et al. Generation of toxic degradation products by sonication of Pluronic dispersants: implications for nanotoxicity testing. *Nanotoxicology* **7,** 1272–1281 (2013).

38.   Gerebtzoff, G., Li-Blatter, X., Fischer, H., Frentzel, A. & Seelig, A. Halogenation of drugs enhances membrane binding and permeation. *Chem. Biochem.* **5,** 676–684 (2004).

39. Scholtysek, P., Li, Z., Kressler, J. & Blume, A. Interactions of DPPC with semitelechelic poly(glycerol methacrylate)s with perfluoroalkyl end groups. *Langmuir* **28,** 15651–15662 (2012).

40. Kyeremateng, S. O., Henze, T., Busse, K. & Kressler, J. Effect of hydrophilic block-A length tuning on the aggregation behavior of α,ω-perfluoroalkyl end-capped ABA triblock copolymers in water. *Macromolecules* **43,** 2502–2511 (2010).

41. Parlato, M. C., Jee, J. P., Teshite, M. & Mecozzi, S. Synthesis, characterization, and applications of hemifluorinated dibranched amphiphiles. *J. Org. Chem.* **76,** 6584–6591 (2011).

42. Krafft, M. P. & Riess, J. G. Chemistry, physical chemistry, and uses of molecular fluorocarbon- hydrocarbon diblocks, triblocks, and related compounds-unique 'apolar' components for self-assembled colloid and interface engineering. *Chem. Rev.* **109,** 1714–1792 (2009).

43. Lombeck, F., Komber, H., Sepe, A., Friend, R. H. & Sommer, M. Enhancing Phase Separation and Photovoltaic Performance of All-Conjugated Donor–Acceptor Block Copolymers with Semifluorinated Alkyl Side Chains. *Macromolecules* **48,** 7851–7860 (2015).

44. Amado, E. & Kressler, J. Triphilic block copolymers with perfluorocarbon moieties in aqueous systems and their biochemical perspectives. *Soft Matter* **7,** 7144 (2011).

45. Marsat, J. N. *et al.* Self-assembly into multicompartment micelles and selective solubilization by hydrophilic-lipophilic-fluorophilic block copolymers. *Macromolecules* **44,** 2092–2105 (2011).

46. Schwieger, C. *et al.* Binding of Amphiphilic and Triphilic Block Copolymers to Lipid Model Membranes: The Role of Perfluorinated Moieties. *Soft Matter* **10,** (2014).

47. Hädicke, A. & Blume, A. Interactions of Pluronic block copolymers with lipid vescles depend on lipid phase and pluronic aggregation state. *Colloid Polym. Sci.* **293,** 267–276 (2015).

48. Schulz, M., Werner, S., Bacia, K. & Binder, W. H. Controlling molecular recognition with lipid/polymer domains in vesicle membranes. *Angew. Chemie - Int. Ed.* **52,** 1829–1833 (2013).

49. Li, Z. *et al.* Enantiopure chiral poly(glycerol methacrylate) self-assembled monolayers knock down protein adsorption and cell adhesion. *Adv. Healthc. Mater.* **2,** 1377–1387 (2013).

50. Heimburg, T. in *Handbook of Molecular Biophysics* (ed. Bohr, H. G.) 593–616 (Wiley-VCH, 2009).

51. C. Peetla, A. Stine, V. L. Biophysical interactions with model lipid membranes: applications in drug discovery and drug delivery. *Mol Pharm.* **6,** 1264–1276 (2009).

52. Schubert, T. & Römer, W. How synthetic membrane systems contribute to the understanding of lipid-driven endocytosis. *Biochim. Biophys. Acta - Mol. Cell Res.* **1853,** 2992–3005 (2015).

53. Giner-Casares, J. J., Brezesinski, G. & Möhwald, H. Langmuir monolayers as unique physical models. *Curr. Opin. Colloid Interface Sci.* **19,** 176–182 (2014).

54. Stefaniu, C., Brezesinski, G. & Möhwald, H. Langmuir monolayers as models to study processes at membrane surfaces. *Adv. Colloid Interface Sci.* **208,** 197–213 (2014).

55. Stefaniu, C. & Brezesinski, G. X-ray investigation of monolayers formed at the soft air/water interface. *Curr. Opin. Colloid Interface Sci.* **19,** 216–227 (2014).

56. Brockman, H. Lipid monolayers: Why use half a membrane to characterize protein-membrane interactions? *Curr. Opin. Struct. Biol.* **9,** 438–443 (1999).

57. Mary T. Le, J. K. L. & Prenner, E. J. Biomimetic Model Membrane Systems Serve as Increasingly Valuable in Vitro Tools. *Advances in Biomimetics Prof. Marko Cavrak (Ed.)* 252–269 (2011). doi:10.5772/574

58. Stigter, D., Mingins, J. & Dill, K. a. Phospholipid interactions in model membrane systems. I. Experiments on monolayers. *Biophys. J.* **61,** 1616–29 (1992).

59. Stigter, D., Mingins, J. & Dill, K. Phospholipid interactions in model membrane systems. II. Theory. *Biophys. J.* **61,** (1992).

60. Akbarzadeh, A. *et al.* Liposome: classification, preparation, and applications. *Nanoscale Res. Lett.* **8,** 102 (2013).

61. Wesołowska, O., Michalak, K., Maniewska, J. & Hendrich, A. B. Giant unilamellar vesicles - a perfect tool to visualize phase separation and lipid rafts in model systems. *Acta Biochim. Pol.* **56,** 33–39 (2009).

62. Fenz, S. F. & Sengupta, K. Giant vesicles as cell models. *Integr. Biol.* **4,** 982 (2012).

63. Richter, R. P., Him, J. L. K. & Brisson, A. Supported lipid membranes. *Mater. Today* **6,** 32–37 (2003).

64. González, C. M., Pizarro-Guerra, G., Droguett, F. & Sarabia, M. Artificial biomembrane based on DPPC — Investigation into phase transition and thermal behavior through ellipsometric techniques. *Biochim. Biophys. Acta - Biomembr.* **1848,** 2295–2307 (2015).

65.   Kaganer, V., Möhwald, H. & Dutta, P. Structure and phase transitions in Langmuir monolayers. *Rev. Mod. Phys.* **71,** 779–819 (1999).

66.   Baoukina, S., Monticelli, L., Marrink, S. J. & Tieleman, D. P. Pressure-area isotherm of a lipid monolayer from molecular dynamics simulations. *Langmuir* **23,** 12617–23 (2007).

67.   Vollhardt, D. & Fainerman, V. B. Progress in characterization of Langmuir monolayers by consideration of compressibility. *Adv. Colloid Interface Sci.* **127,** 83–97 (2006).

68.   Moy, V. T., Keller, D. J., Gaub, H. E. & McConnell, H. M. Long-Range Molecular Orientational Order in Monolayer Solid Domains of Phospholipid. *J. Phys. Chem.* **90,** 3198–3202 (1986).

69.   Vysotsky, Y. B. *et al.* Quantization of the Molecular Tilt Angle of Amphiphile Monolayers at the Air/Water Interface. *J. Phys. Chem. C* **119,** 5523–5533 (2015).

70.   Baoukina, S., Monticelli, L., Risselada, H. J., Marrink, S. J. & Tieleman, D. P. The molecular mechanism of lipid monolayer collapse. *Proc. Natl. Acad. Sci. U. S. A.* **105,** 10803–10808 (2008).

71.   Goto, T. E. & Caseli, L. Understanding the Collapse Mechanism in Langmuir Monolayers through Polarization Modulation-Infrared Reflection Absorption Spectroscopy. *Langmuir* **29,** 9063–9071 (2013).

72.   Kosterlitz, J. M. & Thouless, D. J. Ordering, metastability and phase transitions in two-dimensional systems. *J. Phys. C Solid State Phys.* **6,** 1181–1203 (1973).

73.   Blume, A. A comparative study of the phase transitions of phospholipid bilayers and monolayers. *Biochim. Biophys. Acta - Biomembr.* **557,** 32–44 (1979).

74.   Cullis, P. R. & de Kruijff, B. Lipid polymorphism and the functional roles of lipids in biological membranes. *Biochim. Biophys. Acta* **559,** 399–420 (1979).

75.   De Kruijff, B. Lipid polymorphism and biomembrane function. *Curr. Opin. Chem. Biol.* **1,** 564–569 (1997).

76.   Cullis, P. R., de Kruijff, B., Verkleij, a J. & Hope, M. J. Lipid polymorphism and membrane fusion. *Biochem. Soc. Trans.* **14,** 242–245 (1986).

77.   Kodama, M., Kuwabara, M. & Seki, S. Successive phase-transition phenomena and phase diagram of the phosphatidylcholine-water system as revealed by differential scanning calorimetry. *Biochim. Biophys. Acta - Biomembr.* **689,** 567–570 (1982).

78.   Matsuki, H., Goto, M., Tada, K. & Tamai, N. Thermotropic and barotropic phase behavior of phosphatidylcholine bilayers. *Int. J. Mol. Sci.* **14,** 2282–2302 (2013).

79.   Koynova, R. & Caffrey, M. An index of lipid phase diagrams. *Chem. Phys. Lipids* **115,** 107–219 (2002).

80.   Jadidi, T., Seyyed-Allaei, H., Tabar, M. R. R. & Mashaghi, A. Poisson's Ratio and Young's Modulus of Lipid Bilayers in Different Phases. *Front. Bioeng. Biotechnol.* **2,** 8 (2014).

81.   Blume, A. Biological calorimetry: membranes. *Thermochim. Acta* **193,** 299–347 (1991).

82.   Koynova, R. & Caffrey, M. Phases and phase transitions of the phosphatidylcholines. *Biochim. Biophys. Acta - Rev. Biomembr.* **1376,** 91–145 (1998).

83.   Wolf, C., Chachaty, C., Takahashi, H., Hatta, I. & Quinn, P. J. Phase transition sequence between fluid liquid-crystalline and interdigitated lamellar gel phases in mixed-chain diacyl phosphatidylcholine. **87,** 111–124 (1997).

84.   Rowe, E. S. & Campion, J. M. Alcohol induction of interdigitation in distearoylphosphatidylcholine: fluorescence studies of alcohol chain length requirements. *Biophys. J.* **67,** 1888–1895 (1994).

85.   Kurniawan, Y., Venkataramanan, K. P., Scholz, C. & Bothun, G. D. n-Butanol Partitioning and Phase Behavior in DPPC/DOPC Membranes. *J. Phys. Chem. B* **116,** 5919–5924 (2012).

86.   Weinberger, A. *et al.* Bilayer Properties of 1,3-Diamidophospholipids. *Langmuir* **31,** 1879–1884 (2015).

87.   Serrallach, E. N. Dikkman, R. de Hass, G. H. Shipley, G. G. Structure and Thermotropic Properties of 1.3-Dipalmitoyl-glycerol-2-phosphocholine. *J. Mol. Biol.* **170,** 155–174 (1983).

88.   Ngo, A. T. *et al.* Membrane order parameters for interdigitated lipid bilayers measured via polarized total-internal-reflection fluorescence microscopy. *Biochim. Biophys. Acta* **1838,** 2861–9 (2014).

89.   Slater, J. L. & Huang, C. H. Interdigitated bilayer membranes. *Prog. Lipid Res.* **27,** 325–359 (1988).

90.   Nagle, J. F. Theory of the Main Lipid Bilayer Phase Transition. *Annu. Rev. Phys. Chem.* **31,** 157–195 (1980).

91.   Smith, E. a. & Dea, P. K. Differential scanning calorimetry studies of phospholipid membranes: the interdigitated gel phase. *Applications of Calorimetry in a Wide Context - Differential Scanning Calorimetry, Isothermal Titration Calorimetry and Microcalorimetry In: Elkordy, D.A.A. (Ed.), INTECH Open.* 407–444 (2013). doi:10.5772/2898

92. Simon, S. & McIntosh, T. J. Interdigitated hydrocarbon chain packing causes the biphasic transition behavior in lipid/alcohol suspensions. *Biochim. Biophys. Acta* **773,** 169–172 (1984).

93. Winter, R. & Jeworrek, C. Effect of pressure on membranes. *Soft Matter* **5,** 3157 (2009).

94. Laggner, P., Lohner, K., Degovics, G., Mijller, K. & Schuster, A. Structure and thermodynamics of the dihexadecylphosphatidylcholine-water system. *Chem. Phys. Lipids* **44,** 31–60 (1987).

95. Hirsh, D. J. *et al.* A New Monofluorinated Phosphatidylcholine Forms Interdigitated Bilayers. *Biophys. J.* **75,** 1858–1868 (1998).

96. Winter, I., Pabst, G., Rappolt, M. & Lohner, K. Refined structure of 1 , 2-diacyl-P-O-ethylphosphatidylcholine bilayer membranes. *Chem. Phys. Lipids* **112,** 137–150 (2001).

97. Gagnon, M.-C. *et al.* Evaluation of the effect of fluorination on the property of monofluorinated dimyristoylphosphatidylcholines. *Org. Biomol. Chem.* **12,** 5126–35 (2014).

98. Koynova, R. & Tenchov, B. Transitions between lamellar and non-lamellar phases in membrane lipids and their physiological roles. *OA Biochem.* **1,** 1–9 (2013).

99. Edidin, M. Lipids on the frontier: a century of cell-membrane bilayers. *Nat. Rev. Mol. Cell Biol.* **4,** 414–418 (2003).

100. Van Meer, G., Voelker, D. R. & Feigenson, G. W. Membrane lipids: where they are and how they behave. *Nat. Rev. Mol. Cell Biol.* **9,** 112–124 (2008).

101. Elbert, R., Laschewsky, A. & Ringsdorf, H. Hydrophilic spacer groups in polymerizable lipids: formation of biomembrane models from bulk polymerized lipids. *J. Am. Chem. Soc.* **107,** 4134–4141 (1985).

102. Tremblay, P.-A. Chemical and physical studies of phosphatidyl sulfocholine, a sulfonium alalogue of phsophatidyl choline. PhD Dissertation. (University of Ottawa, Canada, 1982).

103. Joseph, J. & Lai, C.-S. Synthesis of spin-labeled phospholipid for studying membrane dynamics in intact mammalian cells. *J. Lipid Res.* **29,** 1101–1104 (1988).

104. Post, J. F. M., Cook, B. W., Dowd, S. R., Lowe, I. J. & Ho, C. Fluorine-19 Nuclear Magnetic Resonance Investigation of Fluorine-19-Labeled Phospholipids. 1. A Multiple-Pulse Study. *Biochemistry* **23,** 6138–6141 (1984).

105. Samuel, N. K. P. *et al.* Polymerized-depolymerized vesicles. Reversible thiol-disulfide-based phosphatidylcholine membranes. *J. Am. Chem. Soc* **107,** 42–47 (1985).

106. Rosseto, R. & Hajdu, J. A rapid and efficient method for migration-free acylation of lysophospholipids : synthesis of phosphatidylcholines with sn -2-chain-terminal reporter groups. *Tetrahedron Lett.* **46,** 2941–2944 (2005).

107. Rose, T. M. Fluorogenic phospholipid and metabolically stabalized inositol analogues as signal transduction probes. PhD Dissertation. (The University of Utah, USA, 2006). doi:10.1017/CBO9781107415324.004

108. Van Hoogevest, P. & Wendel, A. The use of natural and synthetic phospholipids as pharmaceutical excipients. *Eur. J. Lipid Sci. Technol.* **116,** 1088–1107 (2014).

109. Vad, B. S., Balakrishnan, V. S., Nielsen, S. B. & Otzen, D. E. Phospholipid Ether Linkages Significantly Modulate the Membrane Affinity of the Antimicrobial Peptide Novicidin. *J. Membr. Biol.* **248,** 487–496 (2015).

110. MacDonald, R. C. *et al.* Physical and biological properties of cationic triesters of phosphatidylcholine. *Biophys. J.* **77,** 2612–2629 (1999).

111. Marie, E., Sagan, S., Cribier, S. & Tribet, C. Amphiphilic Macromolecules on Cell Membranes: From Protective Layers to Controlled Permeabilization. *J. Membr. Biol.* **247,** 861–881 (2014).

112. Torcello-Gómez, A. *et al.* Block copolymers at interfaces: Interactions with physiological media. *Adv. Colloid Interface Sci.* **206,** 414–427 (2014).

113. Devi, D. R., Sandhya, P. & Hari, B. N. V. Poloxamer: A novel functional molecule for drug delivery and gene therapy. *J. Pharm. Sci. Res.* **5,** 159–165 (2013).

114. Zhao, J. *et al.* Biomimetic and bioinspired membranes: Preparation and application. *Prog. Polym. Sci.* **39,** 1668–1720 (2014).

115. Batrakova, E. V. & Kabanov, A. V. Pluronic block copolymers: Evolution of drug delivery concept from inert nanocarriers to biological response modifiers. *J. Control. Release* **130,** 98–106 (2008).

116. Amado, E. & Kressler, J. Interactions of amphiphilic block copolymers with lipid model membranes. *Curr. Opin. Colloid Interface Sci.* **16,** 491–498 (2011).

117. Scholtysek, P. *et al.* Unusual triskelion patterns and dye-labelled GUVs: consequences of the interaction of cholesterol-containing linear-hyperbranched block copolymers with phospholipids. *Soft Matter* **11,** 6106–6117 (2015).

118. Watschinger, K. & Werner, E. R. Orphan enzymes in ether lipid metabolism. *Biochimie* **95,** 59–65 (2013).

119. Komatsu, H. & Okada, S. Increased permeability of phase-separated liposomal membranes with mixtures of ethanol-induced interdigitated and non-interdigitated structures. *Biochim. Biophys. Acta* **1237,** 169–175 (1995).

120. *Handbook of Surface and Colloid Chemistry*. (CRC Press, Taylor and Francis, 2003). doi:10.1201/9781420007206

121. Smith, E., van Gorkum, C. M. & Dea, P. K. Properties of phosphatidylcholine in the presence of its monofluorinated analogue. *Biophys. Chem.* **147,** 20–27 (2010).

122. Smith, E. a. & Dea, P. K. Influence of the interdigitated gel phase in mixtures of ether-linked and monofluorinated ester-linked phospholipids. *Chem. Phys. Lipids* **165,** 818–825 (2012).

123. Smith, E., Smith, C., Tanksley, B. & Dea, P. K. Effects of cis- and trans-unsaturated lipids on an interdigitated membrane. *Biophys. Chem.* **190-191,** 1–7 (2014).

124. Smith, E. . & Dea, P. K. The interdigitated gel phase in mixtures of cationic and zwitterionic phospholipids. *Biophys. Chem.* **196,** 86–91 (2015).

125. Toimil, P., Prieto, G., Miñones, J. & Sarmiento, F. A comparative study of F-DPPC/DPPC mixed monolayers. Influence of subphase temperature on F-DPPC and DPPC monolayers. *Phys. Chem. Chem. Phys.* **12,** 13323–13332 (2010).

126. Toimil, P., Prieto, G., Jr., J. M., Trillo, J. M. & Sarmiento, F. Interaction of human serum albumin with monofluorinated phospholipid monolayers. *J. Colloid Interface Sci.* **388,** 162–169 (2012).

127. Mattjus, P., Bittman, R. & Slotte, J. P. Molecular Interaction and Lateral Domain Formation in Monolayers containing cholesterol and Phosphatidylcholines with acyl-Linked or alkyl-Linked c16 chains. *Langmuir* **12,** 1284–1290 (1996).

128. Smaby, J. M., Hermetter, A., Schmid, P. C., Paltauf, F. & Brockman, H. L. Packing of ether and ester phospholipids in monolayers. Evidence for hydrogen-bonded water at the sn-1 acyl group of phosphatidylcholines. *Biochemistry* **22,** 5808–5813 (1983).

129. Wilhelm, M. J., Sharifian Gh., M. & Dai, H.-L. Chemically Induced Changes to Membrane Permeability in Living Cells Probed with Nonlinear Light Scattering. *Biochemistry* **54,** 4427–4430 (2015).

130. Toke, O., Maloy, W. L., Kim, S. J., Blazyk, J. & Schaefer, J. Secondary structure and lipid contact of a peptide antibiotic in phospholipid bilayers by REDOR. *Biophys. J.* **87,** 662–674 (2004).

131. Toimil, P., Daviña, R., Prieto, G. & Sarmiento, F. The Influence of Calcium Ions and the Interdigitated Bilayer on the Colloidal Stability of DPPC and F-DPPC Liposomes. *J. Colloid Sci. Biotechnol.* **3,** 194–200 (2014).

132. Guimond-Tremblay, J. *et al.* Synthesis and properties of monofluorinated dimyristoylphosphatidylcholine derivatives: Potential fluorinated probes for the study of membrane topology. *Org. Biomol. Chem.* **10,** 1145 (2012).

133. Sturtevant, J. M., Ho, C. & Reimann, A. Thermotropic behavior of some fluorodimyristoylphosphatidylcholines. *Proc. Natl. Acad. Sci. U. S. A.* **76,** 2239–2243 (1979).

134. Lewis, R. N., Winter, I., Kriechbaum, M., Lohner, K. & McElhaney, R. N. Studies of the structure and organization of cationic lipid bilayer membranes: calorimetric, spectroscopic, and x-ray diffraction studies of linear saturated P-O-ethyl phosphatidylcholines. *Biophys. J.* **80,** 1329–1342 (2001).

135. Koynova, R. Cationic O-ethylphosphatidylcholines and their lipoplexes: phase behavior aspects, structural organization and morphology. *Biochim. Biophys. Acta - Biomembr.* **1613,** 39–48 (2003).

136. Koynova, R. & MacDonald, R. C. Lipid transfer between cationic vesicles and lipid-DNA lipoplexes: Effect of serum. *Biochim. Biophys. Acta - Biomembr.* **1714,** 63–70 (2005).

137. Koyonova-Tenchova, Rumiana. Wang, L. & Cerrito, E. Composition and methods for nucleic acid delivery systems, US Patent 2009/0048198 A1. **1,** (2009).

138. MacDonald, R. C., Rakhmanova, V. a, Choi, K. L., Rosenzweig, H. S. & Lahiri, M. K. O-ethylphosphatidylcholine: A metabolizable cationic phospholipid which is a serum-compatible DNA transfection agent. *J. Pharm. Sci.* **88,** 896–904 (1999).

139. Zabner, J., Fasbender, a. J., Moninger, T., Poellinger, K. a. & Welsh, M. J. Cellular and molecular barriers to gene transfer by a cationic lipid. *J Biol Chem* **270,** 18997–19007 (1995).

140. Cárdenas, M., Nylander, T., Jönsson, B. & Lindman, B. The interaction between DNA and cationic lipid films at the air–water interface. *J. Colloid Interface Sci.* **286,** 166–175 (2005).

141. Symietz, C., Schneider, M., Brezesinski, G. & Möhwald, H. DNA Alignment at Cationic Lipid Monolayers at the Air/Water Interface. *Macromolecules* **37,** 3865–3873 (2004).

142. Gomes, P. J. P. Characterization of Molecular Damage Induced by UV Photons and Carbon Ions on Biomimetic Heterostructures. PhD Dissertation. (Universidade Nova de Lisboa, Portugal, 2014).

143. Woese, C. R., Kandler, O. & Wheelis, M. L. Towards a natural system of organisms: proposal for the domains Archaea, Bacteria, and Eucarya. *Proc. Natl. Acad. Sci. U. S. A.* **87,** 4576–4579 (1990).

144. Matsuki, H., Miyazaki, E., Sakano, F., Tamai, N. & Kaneshina, S. Thermotropic and barotropic phase transitions in bilayer membranes of ether-linked phospholipids with varying alkyl chain lengths. *Biochim. Biophys. Acta - Biomembr.* **1768,** 479–489 (2007).

145. Ruocco, M. J. Siminovitch, D.J. and Griffin, R. G. Comparative study of the gel phases of ether- and ester-linked phosphatidylcholines. *Biochemistry* **24,** 2406–2411 (1985).

146. Lohner, K., Schuster, A., Muller, K. & Laggner, P. Thermal phase behaviour and structure of hydrated mixtures between dipalmitoyl- and dihexadecylphosphatidylcholine. *Chem. Phys. Lipids* **44,** 61–70 (1987).

147. Laggner, P., Lohner, K., Koynova, R. & Tenchov, B. The influence of low amounts of cholesterol on the interdigitated gel phase of hydrated dihexadecylphosphatidylcholine. *Chem. Phys. Lipids* **60,** 153–161 (1991).

148. Paltauf, F. Hauser, H. Phillipis, M. C. Monolayer characterisitcs of some 1,2-diacyl, 1-alkyl-2-acyl and 1,2-dialkyl phospholipids at the air-water interface. *Biochim. Biophys. Acta* **249,** 539–547 (1971).

149. Kato, Michiko and Hayashi, R. Effects of High Pressure on Lipids and Biomembranes for Understanding High-Pressure-Induced Biological Phenomena. *Biosci. Biotechnol. Biochem.* **63,** 1321–1328 (1999).

150. Kyeremateng, S. O., Amado, E., Blume, a & Kressler, J. Synthesis of ABC and CABAC triphilic block copolymers by ATRP combined with 'Click' chemistry. *Macromol. Rapid Commun.* **29,** 1140–1146 (2008).

151. Jang, S. S., Blanco, M., Goddard, W. a., Caldwell, G. & Ross, R. B. The source of helicity in perfluorniated n-alkanes. *Macromolecules* **36,** 5331–5341 (2003).

152. Li, Z., Amado, E. & Kressler, J. Self-assembly behavior of fluorocarbon-end-capped poly(glycerol methacrylate) in aqueous solution. *Colloid Polym. Sci.* **291,** 867–877 (2013).

153. Kyeremateng, S. O. unpublished results.

154. Szcześ, a., Jurak, M. & Chibowski, E. Stability of binary model membranes-Prediction of the liposome stability by the Langmuir monolayer study. *J. Colloid Interface Sci.* **372,** 212–216 (2012).

155. Smith, E., Wang, W. & Dea, P. K. Effects of cholesterol on phospholipid membranes: Inhibition of the interdigitated gel phase of F-DPPC and F-DPPC/DPPC. *Chem. Phys. Lipids* **165,** 151–159 (2012).

156. Peng, X., Hofmann, A. M., Reuter, S., Frey, H. & Kressler, J. Mixed layers of DPPC and a linear poly(ethylene glycol)-b-hyperbranched poly(glycerol) block

copolymer having a cholesteryl end group. *Colloid Polym. Sci.* **290,** 579–588 (2012).

157. Klymchenko, A. S. & Kreder, R. Fluorescent Probes for Lipid Rafts: From Model Membranes to Living Cells. *Chem. Biol.* **21,** 97–113 (2014).

158. Tsukanova, V., Grainger, D. W. & Salesse, C. Monolayer behavior of NBD-labeled phospholipids at the air/water interface. *Langmuir* **18,** 5539–5550 (2002).

159. Lyklema, J. in *Fundamentals of Interface and Colloid Science* **3,** (Academic Press, 2000).

160. Albrecht, O., Gruler, H. & Sackmann, E. Polymorphism of phospholipid monolayers. *J. Phys.* **39,** 301–313 (1978).

161. Möhwald, H. in *Handbook of Biological Physics* (eds. Lipowsky, R. & Sackman, E.) **1,** 161–211 (1995).

162. Israelachvili, J. N. *Intermolecular and Surface Forces*. (Academic Press, 2011).

163. Pallas, N. & Pethica, B. Liquid-Expanded to Liquid-Condensed Transitions Monolayers at the Air/Water Interface. *Langmuir* **1,** 509–513 (1985).

164. Gibbs, I. & Langmuir, U. 4 Gibbs monolayers. *Fundam. Interface Colloid Sci.* **3,** 1–101 (2000).

165. Shibata, O., Nakahara, H. & Moroi, Y. New Adsorption Model ―Theory, Phenomena and New Concept. *J. Oleo Sci.* **64,** 1–8 (2015).

166. Biscan & Moroi, Y. Air/Solution Interface and Adsorption - Solution for the Gibbs Paradox. *Croat. Chem. Acta* **80,** 357–365 (2007).

167. Melzer, V., Vollhardt, D., Brezesinski, G. & Mohwald, H. Similarities in the phase properties of Gibbs and Langmuir monolayers. *J. Phys. Chem. B* **102,** 591–597 (1998).

168. Sauer, M., Hofkens, J. & Enderlein, J. *Basic Principles of Fluorescence Spectroscopy. Handbook of Fluorescence Spectroscopy and Imaging: From Single Molecules to Ensembles* (Wiley-VCH, 2011). doi:10.1002/9783527633500.ch1

169. Florida State University. (http://micro.magnet.fsu.edu/primer/techniques/fluorescence/fluorescenceintro.html).

170. Stine, K. J. Investigations of monolayers by fluorescence microscopy. *Microsc. Res. Tech.* **27,** 439–450 (1994).

171. Weis, R. M. & McConnell, H. M. Two-dimensional chiral crystals of phospholipid. *Nature* **310,** 47–49 (1984).

172. Webb, D. J. & Brown, C. M. Epi-fluorsecence Microscopy. *Methods Mol. Biol.* **931,** 29–59 (2013).

173. Weis, R. M. Fluorescence microscopy of phospholipid monolayer phase transitions. *Chem. Phys. Lipids* **57,** 227–239 (1991).

174. Krüger, P. & Lösche, M. Molecular chirality and domain shapes in lipid monolayers on aqueous surfaces. *Phys. Rev. E* **62,** 7031–7043 (2000).

175. Leiske, D. L. *et al.* Insertion mechanism of a poly(ethylene oxide)-poly(butylene oxide) block copolymer into a DPPC monolayer. *Langmuir* **27,** 11444–50 (2011).

176. Chaires, J. B. *et al.* Biocalorimetry. *Methods* **76,** 1–2 (2015).

177. Bruylants, G., Wouters, J. & Michaux, C. Differential scanning calorimetry in life science: thermodynamics, stability, molecular recognition and application in drug design. *Curr. Med. Chem.* **12,** 2011–2020 (2005).

178. McElhaney, R. N. The use of differential scanning calorimetry and differential thermal analysis in studies of model and biological membranes. *Chem. Phys. Lipids* **30,** 229–259 (1982).

179. Menczel, J. & Judovits, L. Differential scanning calorimetry (DSC). *Nat. Protoc. Exch.* (2009). doi:10.1038/nprot.2009.18

180. Cooper, A., Nutley, M. a. & Wadood, A. in *Protein-Ligand Interactions: hydrodynamics and calorimetry* (eds. Harding, S. E. & Chowdhry, B. Z.) 287–318 (Oxford University Press, Oxford New York, 2000). doi:10.1016/j.bpc.2005.06.012

181. Heerklotz, H. The microcalorimetry of lipid membranes. *J. Phys. Condens. Matter* **16,** R441–R467 (2004).

182. Robertson, A. D. & Murphy, K. P. Protein Structure and the Energetics of Protein Stability. *Chem. Rev.* **97,** 1251–1267 (1997).

183. Chowdhry, B. Z. & Cole, S. C. Differential scanning calorimetry: applications in biotechnology. *TIBTECH* **7,** 11–18 (1989).

184. Mabrey, S. & Sturtevant, J. M. Investigation of phase transitions of lipids and lipid mixtures by sensitivity differential scanning calorimetry. *Proc. Natl. Acad. Sci. U. S. A.* **73,** 3862–3866 (1976).

185. Toimil, P., Daviña, R., Sabín, J., Prieto, G. & Sarmiento, F. Influence of temperature on the colloidal stability of the F-DPPC and DPPC liposomes induced by lanthanum ions. *J. Colloid Interface Sci.* **367,** 193–198 (2012).

186. Sanii, B., Szmodis, A. W., Bricarello, D., Oliver, A. E. & Parikh, A. N. Frustrated phase transformations in supported, interdigitating lipid bilayers. *J. Phys. Chem. B* **114,** 215–219 (2010).

187. Tegze, G., Tóth, G. I. & Gránásy, L. Faceting and Branching in 2D Crystal Growth. *Phys. Rev. Lett.* **106,** 195502 (2011).

188. Vanderlick, T. K. & Möhwald, H. Mode selection and shape transition of phospholipid monolayer domains. *J. Phys. Chem. B* **94,** 886–890 (1990).

189. Miller, A. & Mohwald, H. Diffusion limited growth of crystalline domains in phospholipid monolayers. *J. Chem. Phys.* **86,** 4258–4265 (1987).

190. Weidemann, G. & Vollhardt, D. Long-range tilt orientational order in phospholipid monolayers: a comparative study. *Biophys. J.* **70,** 2758–2766 (1996).

191. Weidemann, G. & Vollhardt, D. Nonequilibrium domain growth in fatty acid ethyl ester monolayers. *Langmuir* **13,** 1623–1628 (1997).

192. Gehlert, U. & Vollhardt, D. Nonequilibrium structures in 1-monopalmitoyl-rac-glycerol monolayers. *Langmuir* **13,** 277–282 (1997).

193. Gutierrez-campos, A., Diaz-leines, G. & Castillo, R. Domain Growth , Pattern Formation , and Morphology Transitions in Langmuir Monolayers . A New Growth Instability. *J Phys. Chem. B* **114,** 5034–5046 (2010).

194. Lehn, J.-M. Perspectives in Chemistry-Aspects of Adaptive Chemistry and Materials. *Angew. Chemie Int. Ed.* **54,** 3276–3289 (2015).

195. Povibavsek, Luka. Dellsy, Robert, Kern, Andrew, Johnson, Sebastian, Lin, Binhua. Lee, K. Y. C. & Cerda, E. Stress and Fold Localization in Thin Elastic Membranes. *Science* **320,** 912 – 916 (2008).

196. Oppenheimer, N., Diamant, H. & Witten, T. a. Anomalously fast kinetics of lipid monolayer buckling. *Phys. Rev. E* **88,** 2–7 (2013).

197. Gopal, a., Belyi, V. a., Diamant, H., Witten, T. a. & Lee, K. Y. C. Microscopic folds and macroscopic jerks in compressed lipid monolayers. *J. Phys. Chem. B* **110,** 10220–10223 (2006).

198. Raghuraman, H., Shrivastava, S. & Chattopadhyay, A. Monitoring the looping up of acyl chain labeled NBD lipids in membranes as a function of membrane phase state. *Biochim. Biophys. Acta - Biomembr.* **1768,** 1258–1267 (2007).

199. Kane, S. A., Compton, M. & Wilder, N. Interactions determining the growth of chiral domains in phospholipid monolayers: Experimental results and comparison with theory. *Langmuir* **16,** 8447–8455 (2000).

_____

200. Lin, L., Liu, A. & Guo, Y. Heterochiral domain formation in homochiral α-Dipalmitoylphosphatidylcholine (DPPC) Langmuir monolayers at the air/water interface. *J. Phys. Chem. C* **116,** 14863–14872 (2012).

201. Yamamoto, T., Aida, T., Manaka, T. & Iwamoto, M. Chiral phase separation of a monolayer domain comprised of racemic mixture of chiral phospholipids due to the electrostatic energy. *Colloids Surf. A* **321,** 151–157 (2008).

202. Moy, V. T., Keller, D. J. & McConnell, H. M. Molecular order in finite two-dimensional crystals of lipid at the air-water interface. *J. Phys. Chem.* **92,** 5233–5238 (1988).

203. Liu, H. & Kao, W. W. Y. A novel protocol of whole mount electro-immunofluorescence staining. *Mol. Vis.* **15,** 505–517 (2009).

204. Amado, E., Blume, A. & Kressler, J. Novel non-ionic block copolymers tailored for interactions with phospholipids. *React. Funct. Polym.* **69,** 450–456 (2009).

205. Ruger, J. Fluoreszenzspektroskopische Untersuchung der Wechselwirkungen von Polyphilen mit Lipidmodellmembransystemen. M.Sc. Thesis. (Martin-Luther University, Halle-Wittenberg, Germany, 2012).

206. Anwar, J., Khan, S. & Lindfors, L. Secondary Crystal Nucleation: Nuclei Breeding Factory Uncovered. *Angew. Chemie Int. Ed.* **127,** 14894–14897 (2015).

207. Henderson, M. J. & Richards, R. Organization of Poly(ethylene oxide) Monolayers. *Macromolecules* **26,** 4591–4600 (1993).

208. Kjellander, R. & Florin, E. Water structure and changes in thermal stability of the system poly (ethylene oxide)–water. *J. Chem. Soc. Faraday Trans.* **77,** 2053–2077 (1981).

209. Lee, W. Strcuture and dynamics of polyhedral oligomeric silsequioxane (POSS) and poly(ethyleneglycol) based amphiphiles as langmuir monolars at the air/water interface. PhD Dissertation. (Virginia Polytechnic Institute and State University, USA, 2008).

210. Hädicke, A. & Blume, A. Interactions of Pluronic block copolymers with lipid monolayers studied by epi-fluorescence microscopy and by adsorption experiments. *J. Colloid Interface Sci.* **407,** 327–338 (2013).

211. McMullen, T. P. W., Lewis, R. N. a H. & McElhaney, R. N. Cholesterol-phospholipid interactions, the liquid-ordered phase and lipid rafts in model and biological membranes. *Curr. Opin. Colloid Interface Sci.* **8,** 459–468 (2004).

212. Vist, M. R. & Davis, J. H. Phase equilibria of cholesterol/dipalmitoylphosphatidyl-choline mixtures: 2H nuclear magnetic resonance and differential scanning calorimetry. *Biochemistry* **29,** 451–464 (1990).

213. Pandit, S., Bostick, D. & Berkowitz, M. L. Complexation of phosphatidylcholine lipids with cholesterol. *Biophys. J.* **86,** 1345–1356 (2004).

214. Tabaei, S. R., Jackman, J. a, Liedberg, B., Parikh, A. N. & Cho, N. Observation of Stripe Superstructure in the β - Two-Phase Coexistence Region of Cholesterol – Phospholipid Mixtures in Supported Membranes. *J. Am. Chem. Soc* **136,** 16962–16965 (2014).

215. Chang, L. C., Chang, Y. Y. & Gau, C. S. Interfacial properties of Pluronics and the interactions between Pluronics and cholesterol/DPPC mixed monolayers. *J. Colloid Interface Sci.* **322,** 263–273 (2008).

216. Weis, R. & McConnell, H. Cholesterol stabilizes the crystal-liquid interface in phospholipid monolayers. *J. Phys. Chem.* **89,** 4453–4459 (1985).

217. Nakamura, S., Nakahara, H., Krafft, M. P. & Shibata, O. Two-component langmuir monolayers of single-chain partially fluorinated amphiphiles with dipalmitoylphosphatidylcholine (DPPC). *Langmuir* **23,** 12634–12644 (2007).

218. *Liposomes : A Practical Approach*. (Oxford University Press, Oxford New York, 1997).

219. Koynova, R., Brankov, J. & Tenchov, B. Modulation of lipid phase behavior by kosmotropic and chaotropic solutes. Experiment and thermodynamic theory. *Eur. Biophys. J.* **25,** 261–274 (1997).

220. Clejan, S., Bittman, R., Deroo, P. W., Isaacson, Y. a & Rosenthal, a F. Permeability properties of sterol-containing liposomes from analogues of phosphatidylcholine lacking acyl groups. *Biochemistry* **18,** 2118–2125 (1979).

221. Yamazaki, M., Kashiwagi, N., Miyazu, M. & Asano, T. Effect of oligomers Of ethylene glycol on thermotropic phase transition of dipalmitoylphosphatidylcholine multilamellar vesicles. **1109,** 43–47 (1992).

222. Yamazaki, M., Ohshika, M., Kashiwagi, N. & Asano, T. Phase transitions of phospholipid vesicles under osmotic stress and in the presence of ethylene glycol. *Biophys. Chem.* **43,** 29–37 (1992).

223. Papahadjopoulos, D., Moscarello, M., Eylar, E. H. & Isac, T. Effects of proteins on thermotropic phase transitions of phospholipid membranes. *Biochim. Biophys. Acta* **401,** 317–335 (1975).

224. Gawrisch, K. *et al.* Membrane dipole potentials, hydration forces, and the ordering of water at membrane surfaces. *Biophys. J.* **61,** 1213–1223 (1992).

225. Brezesinski, G. *et al.* Influence of ether linkages on the structure of double-chain phospholipid monolayers. *Chem. Phys. Lipids* **76,** 145–157 (1995).

226. Wang, M. *et al.* Dynamic behaviors of fractal-like domains in monolayers. **53,** 6121–6125 (1996).

227. Vaughan, D. J. & Keough, K. M. Changes in phase transitions of phosphatidylethanolamine- and phosphatidylcholine-water dispersions induced by small modifications in the headgroup and backbone regions. *FEBS Lett.* **47,** 158–161 (1974).

228. Fuchs, C., Hussain, H., Amado, E., Busse, K. & Kressler, J. Self-Organization of Poly (ethylene oxide) on the Surface of Aqueous Salt Solutions. 211–218

229. Hafez, I. M., Maurer, N. & Cullis, P. R. On the mechanism whereby cationic lipids promote intracellular delivery of polynucleic acids. *Gene Ther.* **8,** 1188–1196 (2001).

230. Koynova, R. & MacDonald, R. C. Mixtures of cationic lipid O-ethylphosphatidylcholine with membrane lipids and DNA: phase diagrams. *Biophys. J.* **85,** 2449–2465 (2003).

231. Ahl, P. L. *et al.* Interdigitation-fusion: a new method for producing lipid vesicles of high internal volume. *Biechimica Biophys. Acta* **1195,** 237–244 (1994).

232. Schneider, M. F., Marsh, D., Jahn, W., Kloesgen, B. & Heimburg, T. Network formation of lipid membranes: triggering structural transitions by chain melting. *Proc. Natl. Acad. Sci. U. S. A.* **96,** 14312–14317 (1999).

233. Jacobson, K. & Papahadjopoulos, D. Phase transitions and phase separations in phospholipid membranes induced by changes in temperature, pH, and concentration of bivalent cations. *Biochemistry* **14,** 152–161 (1975).

234. Kinnunen, P. K. J. & Chemistry, M. Monovalent cation dependent phase behaviour of dipalmitoylphosphatidylglycerol. **50,** 71–78 (1989).

235. Wilkinson, D.A., Tirrell, D.A., Turek, A.B., and McIntosh, T. J. Tris buffer causes acyl chain interdigitation in phosphatidylglycerol. *Biochim. Biophys. Acta* **905,** 447–453 (1987).

Curriculum Vitae

Syed Waqar Hussain Shah
Born: 28.02.1972
Rawalpindi, Pakistan.

Education and Work Experience

Since 2013   Doctoral study at Institute of Chemistry, Martin-Luther University, Halle-Wittenberg under the supervision of Prof. Alfred Blume *(Faculty Development Program, Higher Education Commission, Pakistan)*

2009-2011   Studied for *M.Phil (Organic Chemistry)* at Hazara University, Mansehra, Pakistan

M.Phil Thesis Title: Synthesis of novel corticosteroid derivatives as anticonvulsant prodrugs and potential inhibitors of prostatic cancer

Since 2008   Lecturer in Chemistry, Hazara University, Mansehra, Pakistan

1995 – 2008   Lecturer in Chemistry, Higher Education Department, Punjab/ Federal Govt.(Pakistan)

1992 – 1994   Studied for *M.Sc (Chemistry)* at Quaid-i-Azam University, Islamabad, Pakistan

M.Sc Thesis Title: Synthesis of hemicyanine dyes as probes of micellar solubilization sites

1989 – 1991   Studied for *B.Sc* at Govt. Postgraduate College Asghar Mall, Rawalpindi/Punjab University, Lahore, Pakistan

Publications

"Unusual triskelion patterns and dye-labelled GUVs: Consequences of the interaction of cholesterol-containing linear-hyperbranched block copolymers with phospholipids" Peggy Scholtysek, Syed Waqar Hussain Shah, Sophie Müller, Regina Schöps, Holger Frey, Alfred Blume, Jörg Kressler, *Soft Matter*, 11, 6106 (2015).

"Interaction of short chain phenyl alkanoic acids within cationic and anionic surfactants" Kashif Naeem, Syed Waqar Hussain Shah, Bushra Naseem, Syed Sakhawat Shah, *Arabian J. Sci. Eng.*, 37, 1339 (2012).

"Interaction of short chain phenyl alkanoic acids within ionic surfactant micelles in aqueous media" Kashif Naeem, Syed Waqar Hussain Shah, Bushra Naseem, Syed Sakhawat Shah, *J. Serb. Chem. Soc.*, 77, 201 (2012).

"Triorganotin (IV) complexes with biologically potent Schiff bases: Infrared, ^{119}Sn spectral characteristics and antimicrobial applications" Wajid Rehman, Jamil Khan" Bakhtiar Muhammad, Javed Iqbal, Syed Waqar Hussain Shah, *Mini Rev. Med. Chem.,* 12, 426 (2012).

"Investigation of 1-alkanols in organised solutions" Syed Waqar Hussain Shah, Bushra Naseem, Wajid Rehman, Nadia Bashir, Syed Sakhawat Shah, *Bull. Chem. Soc. Ethiop.,* 25, 469 (2011).

"A novel spectrophotometric determination of atenolol using sodium nitroprusside" Nadia Bashir, Syed Waqar Hussain Shah, Masroor Bangesh, Riazullah, *J. Sci. Ind. Res.,* 70, 51 (2011).

"A comparative study of various grains from different cities of Pakistan" Wajid Rehman, Syed Waqar Hussain Shah, Kamran Younis, Mohsan Nawaz, Musa Kaleem Baloch, Gulzar Hameed, *Environ. Monit. Assess.,* 175, 151 (2011).

"Synthesis, spectral characterization and antibacterial activity of some Schiff base metal complexes" Wajid Rehman, Irum Shehzadi, Bakhtiar Muhammad, Zonera Hassan, Syed Waqar Hussain Shah, *Rev. Inorg. Chem.,* 30, 175 (2010).

"Role of micellar media in radical scavenging ability of flavonoids: A review" Syed Sakhawat Shah, Syed Waqar Hussain Shah, *J. Surf. Sci. Technol.,* 26, 159 (2010).

"Science from Literature: An easy way to learn complex phenomena of the site-specific drug delivery using liposomes" Syed Waqar Hussain Shah, Wajid Rehman, *Chemistry/Bulgarian J. Sci. Educ., 19, E45 (2010).*

"Interaction of flavonoids, the naturally occurring antioxidants with different media: A UV-visible Spectroscopic Study" Bushra Naseem, Syed Waqar Hussain Shah, Aurangzeb Hasan, Syed Sakhawat Shah *Spectrochim. Acta, Part A,* 75, 1341 (2010).

"Spectroscopic analysis of naphtholazobenzimidazole in organised solution" Syed Waqar Hussain Shah, Bushra Naseem, Kashif Naeem, Mashooda Hassan, Syed Sakhawat Shah, *Phys. Chem. Liq.,* 48, 316 (2010).

"Complex formation study of hemicyanine dyes with sodium dodecyl sulphate by differential spectroscopy" Syed Waqar Hussain Shah, Bushra Naseem, Kashif Naeem, Syed Sakhawat Shah, *Colloids Surf., A,* 331, 227 (2008).

"Surfactant-Dye Aggregates" Syed Sakhawat Shah, Syed Waqar Hussain Shah, Kashif Naeem, *Encyclopedia of Surface and Colloid Science*, 2nd Ed, Taylor and Francis, NY, 6082, (2006).

"Surfactant-Dye Aggregates" Syed Sakhawat Shah, Syed Waqar Hussain Shah, Kashif Naeem, *Encyclopedia of Surface and Colloid Science*, 1st Ed, Marcel Dekker, NY, 5205 (2002).

"Spectroscopic study of cationic hemicyanine dyes in lithium dodecyl sulfate solution" Syed Waqar Hussain Shah, Kashif Naeem, Khan Muhammad Asif, Syed Sakhawat Shah, *Pak. J. Sci. Ind. Res.,* 44, 340 (2001).

"Incorporation of aromatic acids into sodium dodecyl sulfate micelles: A UV Spectroscopic Analysis" Syed Waqar Hussain Shah, Bushra Naseem, Kashif Naeem, Qaiser M. Malik, Syed Sakhawat Shah, *J. Surf. Sci. Technol.,* 49, 17 (2001).

"Solubilization of cationic hemicyanine dyes in anionic surfactant micelles, a partitioning study" Kashif Naeem, Syed Sakhawat Shah, Syed Waqar Hussain Shah, *Monatsh. Chem.,* 131, 761 (2000).

"Differential absorbance measurements of amphiphilic hemicyanine dyes, solubilization study in anionic surfactant" Syed Sakhawat Shah, K. Naeem, Syed Waqar Hussain Shah, Gul Mohammad Laghari, *Colloids Surf., A,* 168, 77 (2000).

"Solubilization of short chain phenyl alkanoic acids by a cationic surfactant, cetyltrimethyl-ammonium bromide" Syed Sakhawat Shah, Kashif Naeem, Syed Waqar Hussain Shah, Hazrat Hussain, *Colloids Surf., A,* 148, 299 (1999).

"Partition Coefficient of amphiphilic hemicyanine dyes between aqueous and micellar phase of sodium dodecyl sulfate by differential absorbance spectroscopy" Syed Sakhawat Shah, Gul Muhammad Laghari, Kashif Naeem, Syed Waqar Hussain Shah, *Colloids Surf., A,* 143, 111 (1998).

"Synthesis of cationic hemicyanine dyes and their interactions with ionic surfactants" Syed Sakhawat Shah, Roshan Ahmad, Syed Waqar Hussain Shah, Khan Muhammad Asif, Kashif Naeem, *Colloids Surf., A,* 137, 301 (1998).

_____

DECLARATION

This is hereby confirmed that this thesis is entirely my own work and has been written without any help of others. I only used the mentioned sources and indicated all kind of citations correctly.

<div align="right">

Syed Waqar Hussain Shah
Feb 17, 2016
Halle (Germany)

</div>